Distribution System Analysis Tools for Studying High Penetration of PV with Grid Support Features

Final Project Report

Power Systems Engineering Research Center

Empowering Minds to Engineer
the Future Electric Energy System

Distribution System Analysis Tools for Studying High Penetration of PV with Grid Support Features

Final Project Report

Project Team

Raja Ayyanar
Adarsh Nagarajan, Ph.D. Student
Arizona State University

Tom Overbye
Rajesh Bhana, Ph.D. Student
University of Illinois at Urbana-Champaign

PSERC Publication 13-45

September 2013

For information about the report, contact:

Raja Ayyanar
Associate Professor
School of Electrical, Computer and Energy Engineering
Arizona State University
551 E. Tyler Mall
Tempe, AZ 85287
Tel: (480)727-7307
Fax: (480)965-0745
Email: rayyanar@asu.edu

Power Systems Engineering Research Center

The Power Systems Engineering Research Center (PSERC) is a multi-university Center conducting research on challenges facing the electric power industry and educating the next generation of power engineers. More information about PSERC can be found at the Center's website: http://www.PSERC.org.

For additional information, contact:

Power Systems Engineering Research Center
Arizona State University
527 Engineering Research Center
Tempe, Arizona 85287-5706
Phone: 480-965-1643
Fax: 480-965-0745

Notice Concerning Copyright Material

Acknowledgements

This is the final report for the Power Systems Engineering Research Center (PSERC) research project titled “Distribution System Analysis Tools for Studying High Penetration of PV with Grid Support Features” (project T-44). We express our appreciation for the support provided by PSERC’s industry members and by the National Science Foundation under the Industry / University Cooperative Research Center program. We also express our appreciation for the support provided by the Illinois Center for a Smarter Electric Grid (at the University of Illinois at Urbana-Champaign) and the U.S. Department of Energy for the project “High Penetration of Photovoltaic Generation Study – Flagstaff Community Power - DE-EE0004679”.

The authors would also like to convey special acknowledgement to the PSERC member companies who provided direct assistance with this project: Arizona Public Service Corp. and PowerWorld Corporation.

Executive Summary

Large penetration levels of distributed renewable resources in power distribution systems, especially photovoltaic generators, can potentially impose a paradigm shift in the design, operation, protection and control of the distribution systems. Large scale implementation of distributed generators may lead to a gradual transition of feeders fed from large centralized generators to a system with a large number of small to medium sized distributed generators interfaced through power electronic converters. In order to understand and analyze the impact of high penetration of inverter-interfaced PV with sophisticated grid support features, it is essential to have a distribution system analysis tool capable of modeling the complex static and dynamic behavior of these devices and the distribution system under a wide range of time scales. The objective of this project is to develop new features and enhance the capabilities of distribution systems analysis tools so as to fully capture the static, quasi-static and dynamic impact of distributed photovoltaic generators at high penetration levels.

The major tasks of the project include development of models of varying complexity for inverter controlled generators, algorithms for incorporating voltage regulation features of PV generators, algorithms for dynamic analysis including voltage flicker and interaction with other control devices, and automation of feeder model development directly from GIS data, AMI load data and solar insolation data in the analysis tools.

As part of a related project funded by the Department of Energy and in collaboration with Arizona Public Service, Arizona State University is modeling and studying extensively the impact of an actual, large scale, field implementation of distributed PV. Many of the modeling methods and algorithms developed as part of this PSERC project have been implemented and validated on the feeder studied as part of the above DOE project.

Part 1 - Distribution System Analysis Tools for Studying High Penetration of PV with Grid Support Features

Part 1 of the project aims to develop the required new features and enhance the capabilities of distribution systems analysis tools to study the impact, including the dynamic effects, of large scale penetration of PV. As a first step, a survey of existing distribution system analysis tools has been conducted and three of the tools are compared extensively. CYMDIST as a representative of state-of-the-art commercially available distribution level tools, and OpenDSS and GridLab-D as popularly employed open source modeling tools have been included in the detailed comparison. The results of the comparison, and the identified gaps in terms of the features needed to analyze high PV penetration and supported models are presented in Chapter 2.

Most utilities now have extensive geographic information system (GIS) data and load data from AMI. In this work, a detailed procedure and scripts for its implementation have been developed to facilitate the automated development of the complete feeder network and equipment model from the GIS data, and incorporation of AMI load data and PV

data, if available. These methods and their implementation for a specific feeder in OpenDSS are detailed in Chapter 3. Results of quasi-static or time-series analysis using the models developed in OpenDSS, and their validation through comparison with measured field data are also presented.

A major part of this research project focuses on the use of the concept of dynamic phasors for analyzing distribution systems with large number of inverter-interfaced PV generators. The analysis of fast electromagnetic transients normally involves the computation of instantaneous values of voltages and currents. However, in dynamic phasor analysis the transient quantities – voltages and currents, are obtained not by their instantaneous values but by their time-varying Fourier coefficients. In comparison with the conventional time domain analysis, the dynamic phasor formulation has the advantage that the properties of the transients can be directly interpreted in terms of the envelop variation, giving it the benefit of significantly smaller simulation times. The application of the dynamic phasors in the context of high PV penetration distribution system analysis is fully developed including detailed phasor models of single-phase PV inverters. Methods and models for executing dynamic phasor analysis in general purpose simulation tools with a defined ordinary differential equation solver have been developed and are presented in Chapter 4 along with the phasor model of PV inverters.

The dynamic phasor approach greatly reduces the simulation times for dynamic analysis compared to other methods. However, modeling every single branch and load of a feeder together with the detailed model of each inverter with its different controllers is both quite time intensive even with dynamic phasor approach and unnecessary for most study objectives. Hence, network reduction techniques involving graph search algorithms based on minimum spanning tree have been used to obtain a feeder model that has significantly lower overall model complexity in terms of number of nodes and loads, while still retaining the required details of relevant parts of the feeder and PV systems. With this reduced network it becomes practical to conduct various analyses such as impact of change in PV insolation at high ramp rates or capacitor bank operations over relatively long time intervals. The network reduction algorithm is explained in detail in Chapter 5. In addition, a non-heuristic network flow technique to automate the implementation of the model of a large distribution feeder in a transient analysis tool such as Simulink/SimPowerSystems has also been developed and described in detail in Chapter 5. Several case studies involving sudden changes in PV insolation, load shedding and voltage control by PV inverters have been studied in the transient analysis tool using the dynamic phasor approach. In combination, the developed techniques, algorithms and models enable a detailed study of realistic distribution feeders under different levels of PV penetration and under many different grid conditions.

Part 2 - The Modeling of Distributed Photovoltaic Generation for the Transient Stability Assessment of Power Grids.

In recent times, there has been a rapid increase in small-scale, grid-connected, photovoltaic (PV) generation systems and that increase is expected to continue. As a result, system planners and regulators require transient analysis models for the stability

assessment of systems with a high penetration of distributed PV resources. The response of PV generation to system events is typically dictated by the control scheme employed by the inverter. The power-electronic inverter interface of PV generation with the grid and the lack of energy storage results in a generation source with no natural inertia. However, given the correct economic incentive, the curtailment of PV together with the appropriate inverter control can allow a PV generator to provide synthetic inertia.

Transient analysis models of distributed PV of varying complexity have been developed. Analysis of these models and a number of load models are presented in this report with the results highlighting the importance of more complex load models. The generator speed response analysis showed the very similar performance of three of the PV models on the analyzed test systems.

Simulations were also performed to assess the rotor angle stability of test systems under increasing PV penetration. As expected, the results show decreased inertial response with increased PV penetration. As PV generation is immune to rotor angle instability, however, it should be noted that increased PV penetration also results in a lower number of conventional generators at risk of instability.

Large-system analysis was also performed to investigate localized PV penetration. It is shown that decreased inertia in one area of a weakly connected system can give rise to instabilities. The combination of both locational and temporal variability of renewable resources like PV can result in dramatic changes in power flow. Such changes warrant an investigation into the benefits of employing adaptive control techniques in order to maintain system security.

Project Publications

1. A. Nagarajan and R. Ayyanar, "Dynamic Phasor Model of Single-Phase PV Inverters for Analysis and Simulation of Large Power Distribution Systems", *IEEE 4th International Symposium on Power Electronics for Distributed Generation System,* July 2013.

2. A. Nagarajan and R. Ayyanar, "Application of Minimum Spanning Tree Algorithm for Network Reduction of Distribution Systems," *IEEE 50th PES T&D Conference and Exposition*, Chicago, April 14, 2014 (Submitted)

Students Theses

1. A. Nagarajan, " Model Development and Analysis of Large Distribution Feeders with High Penetration of PV Generators," Ph.D. Dissertation, Expected - May 2014

Part 1

Distribution System Analysis Tools for Studying High Penetration of PV with Grid Support Features

Authors

Raja Ayyanar
Adarsh Nagarajan, Ph.D. Student
Arizona State University

For information about Part 1, contact:

Raja Ayyanar
Associate Professor
School of Electrical, Computer and Energy Engineering
Arizona State University
551 E. Tyler Mall
Tempe, AZ 85287
Tel: (480)727-7307
Fax: (480)727-7307
Email: rayyanar@asu.edu

Power Systems Engineering Research Center

The Power Systems Engineering Research Center (PSERC) is a multi-university Center conducting research on challenges facing the electric power industry and educating the next generation of power engineers. More information about PSERC can be found at the Center's website: http://www.PSERC.org.

For additional information, contact:

Power Systems Engineering Research Center
Arizona State University
527 Engineering Research Center
Tempe, Arizona 85287-5706
Phone: 480-965-1643
Fax: 480-965-0745

Notice Concerning Copyright Material

Table of Contents

Table of Contents . . . . . **i**
List of Figures . . . . . **iii**
List of Tables . . . . . **v**
1 Introduction **1**
1.1 Introduction 1
1.1.1 Requirements of a distribution system analysis tool 1
1.2 Existing distribution system analysis tools 2
1.3 Gaps in the existing distribution system analysis tool 3
1.4 Research objectives 4
2 Comparison of Distribution System Analysis Tools **6**
2.1 Introduction 6
2.2 Comparison of the features of the tools 6
2.3 Special module in the tools 6
3 Model Development in OpenDSS from GIS and Quasi-static Analysis **11**
3.1 Introduction 11
3.2 Overview of model development in distribution system tools 11
3.2.1 CYMDIST 11
3.2.2 OpenDSS 11
3.2.3 GridLab-D 12
3.3 Detailed model development in OpenDSS 12
3.4 Developed feeder model 15
4 Dynamic Phasor Models of PV Generators **21**
4.1 Introduction 21
4.2 Reduced order models for tools with inbuilt phasor solvers 21
4.3 Generalized phasor model of power converter 22
4.4 Dynamic phasor problem formulation 24
4.4.1 Analogy between the state-space averaging and the dynamic phasor approach 25
4.4.2 Properties of the Fourier coefficients 25
4.5 Generalized dynamic phasor model of a single-phase inverter 27
4.6 Results 30
5 Model Reduction and Dynamic Analysis using Transient Analysis Tool **33**
5.1 Introduction 33
5.1.1 Literature search on network reduction of distribution feeders 35
5.1.2 Analogy between trees and distribution feeders 36
5.1.3 Differences between modeling in distribution system analysis tool and transient analysis tool 36
5.2 Proposed approach for dynamic analysis 37
5.2.1 Algorithm for network reduction 37
5.2.2 Algorithm for modeling in transient analysis tool 40
5.2.3 Model development in Simulink 41

5.3 Results and validation 42
5.3.1 Results pertaining to network reduction 43
5.3.2 Results from Dynamic Analysis using Reduced Model pertaining to dynamic model 46
6 Conclusions **54**
References **56**

List of Figures

Figure 1.1 Comparison of timeframes of the events in power systems 2
Figure 1.2 Generalized block diagram for modeling the distribution feeders in quasi-static and transient analysis tools 5
Figure 3.1 Generalized block diagram for modeling the distribution feeders in quasi-static and transient analysis tools 13
Figure 3.2 Modeling process flowchart specific to OpenDSS 14
Figure 3.3 Example for a case with phase conflict 16
Figure 3.4 Feeder view of the extended-model from OpenDSS 17
Figure 3.5 Feeder view of the base-model from OpenDSS 18
Figure 3.6 Measured and simulated substation kW at one-minute-interval of phase A for one day 19
Figure 3.7 Measured and simulated voltage plot at midway from the substation at one-minute-interval of phase A for one day 20
Figure 4.1 Block diagram of the simplified average model of power converter 22
Figure 4.2 Block diagram of the phasor model of the PV converter 22
Figure 4.3 Full switching model of the single-phase full bridge inverter and its control strategy 27
Figure 4.4 Combined transformer equivalent circuit of a full bridge single-phase inverter 27
Figure 4.5 Reduced transformer equivalent circuit of the single-phase full bridge inverter and its control strategy 28
Figure 4.6 Waveforms of the inductor current presenting multiple types of dynamic phasors along with the average model for a step change in the current reference signal 30
Figure 4.7 Waveforms of grid voltage, current through filter inductor, and active power during a voltage sag with active power set point 31
Figure 5.1 Generalized block diagram for modeling the distribution feeders in quasi-static and transient analysis tools 34
Figure 5.2 View of the distribution feeder in Simulink 42
Figure 5.3 Feeder diagram of the original feeder 43
Figure 5.4 Feeder diagram after applying the network reduction 44
Figure 5.5 Voltage profile for the original network 45
Figure 5.6 Voltage profile for the reduced network 45
Figure 5.7 View of the test feeder from a quasi-static analysis tool (CYMDIST) . . 47
Figure 5.8 Waveforms of voltages and currents for each phase at the feeder head. . . 48
Figure 5.9 Waveforms of voltages for each phase at DAS near capacitor banks. . . . 49
Figure 5.10 Waveforms of voltages and currents for each phase at the DAS 5 50
Figure 5.11 Solar irradiance as a random signal between 1 and 0.4 (p.u.) 50
Figure 5.12 Voltages at the feeder head with solar irradiance varying as a random signal 51

Figure 5.13 Voltages near the capacitor banks with the solar irradiance varying as a random signal 51
Figure 5.14 Effect on capacitor bank operation without voltage control feature of two three-phase PV generators 52
Figure 5.15 Effect on capacitor bank voltage without voltage control feature of two three-phase PV generators 52
Figure 5.16 Effect on capacitor bank operation with voltage control feature of two three-phase PV generators 53
Figure 5.17 Effect on capacitor bank voltage with voltage control feature of two three-phase PV generators 53

List of Tables

Table 1.1 Count of the power system components present in the models built in OpenDSS 3
Table 2.1 Comparison of the basic features for distribution system analysis tools . 8
Table 2.2 Comparison of the available equipment models in the distribution system analysis tools 9
Table 2.3 Comparison of the on-screen design and editing capability in the selected distribution system analysis tools 10
Table 2.4 Comparison of the display and reporting feature in the selected distribution system analysis tools 10
Table 2.5 Comparison of the miscellaneous feature of the distribution system analysis tools 10
Table 4.1 Simulation speed comparison between full switching model, average, and dynamic phasor model 32
Table 5.1 Effect on network reduction aspects of the distribution feeder 43
Table 5.2 Performance details of network reduction on the distribution feeder . . . 44
Table 5.3 Comparison of measured power system quantities (voltage and current) from CYMDIST and MATLAB/Simulink 46

1. Introduction

1.1 Introduction

The penetration levels of distributed renewable resources in power distribution systems are increasing at a rapid rate, from presently negligible values, to levels significant enough to warrant a paradigm shift in the design, operation, protection, and control of distribution systems. The increase in penetration levels of photovoltaics is driven by the renewable energy standards (RES) of most of the states which have specific requirements on the distributed generation component, for example, AZ mandates 30% of its RES requirement (which itself is 15% of the total generation) to be met through distributed generation with half of that derived from residential generators.

In addition to the intermittent behavior and uncertainty issues, the inverter controlled PV generators have very different static and dynamic characteristics (compared to conventional generation) as these are determined to a large extent by the inverter control. Present distribution infrastructure that is designed mainly for unidirectional power flow poses challenges, to the to the integration of large scale PV, in terms of voltage profile, reverse power flow and protection. In addition, recent emphasis on smart grid features, where the PV generator is required to offer several grid support functionalities based on system-wide measurements adds another significant layer of complexity.

To analyze the impact of high penetration of the inverter-interfaced PV generators with sophisticated grid support features, it is critical to have a distribution system analysis tool capable of modeling the complex quasi-static and dynamic behavior of these devices under a wide range of time-scales. This work concentrates on the identifying the necessary features which do not exist is the contemporary distribution tools and developing them.

1.1.1 Requirements of a distribution system analysis tool

The basic features required from a distribution system analysis tool with specific reference to the PV inverters include:

- Power flow analysis for radial/looped networks.
- Balanced and unbalanced (single phase loads) power flow analysis.
- Shunt capacitors with the associated control.
- Capability to generate feeder configuration and equipment model directly from the GIS data.
- Time series solution.
- Models of PV generators.
- Predefined control blocks for PV inverters.

- Capable of accepting and processing geographical PV insolation data.
- Capability for transient analysis for specific analysis.

1.2 Existing distribution system analysis tools

Figure 1.1 enlists the timeframes of the typical events observed in power systems. This project aims at extending the ability of the quasi-static tools to perform the dynamic analysis. Commenting on the features required in the quasi-static domain requires the understanding of the existing tools. Since none of the distribution system analysis tools are capable of dynamic analysis comparison cannot be performed. The feeder models developed for quasi-static analysis will be used to validate the dynamic models. Dynamic analysis will be used to study the effects of dynamics such as voltage flicker and interaction of different control devices.

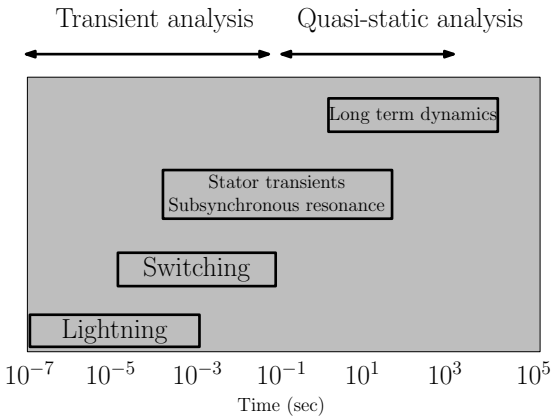

Figure 1.1 Comparison of timeframes of the events in power systems

A list of the existing distribution system analysis tools typically used for studying the effect of distributed energy resources are mentioned below. Some of the tools are, PSS Adept by Power Technologies, WindMil by Milsoft Integrated Solutions, CYMDIST by CYME International, Technical 2000 by EDSA Micro Corporation, SynerGEE Electric by Advantica Stoner, Dapper Demand Load Analysis by SKM Systems Analysis, OpenDSS by EPRI, GridLab-D by PNNL, Power System Toolbox (PST) & MATLAB by Cherry Tree Scientific Software, ABB Feederall by ABB, Power Tools for Windows from SKM Systems Analysis, Inc., PowerWorld Simulator by PowerWorld Corporation, EuroStag by Tractebel, DigSilent PowerFactory by DigSILENT and NEPLAN by BCP-Suiza [1].

For the purpose of detailed comparison, CYMDIST, OpenDSS, and GridLab-D are chosen. CYMDIST is representative of the state-of-the-art tool commercially available, whereas OpenDSS and GridLab-D represents a set of open-source tools. Recognizing the new features to enhance the capabilities of the distribution system analysis tools demands a close understanding of the operation and features provided by the existing tools. For the detailed

comparison and understanding of the capabilities of these tools, two feeder models representing urban area are chosen as a test bed. The two feeders are referred to as base-model and extended-model. The composition of these two models are shown in Table 1.1.

Table 1.1 Count of the power system components present in the models built in OpenDSS

Model	**Nodes**	**Transformers**	**Capacitor banks**	**PV Generators**	**Loads**
Base-model	4000	929	3	111	1002
extended-model	9299	929	3	111	2618

Additionally the base model will be modeled in a transient analysis tool. The overall load connected to the base-model and the extended-model is approximately 6 MW, and the magnitude of PV generation is 1298 kW. 398 kW out of 1298 kW comes from roof-top single-phase PV generators. 900 kW is generated from two large three-phase PV generators. A complete model of the feeder is developed in the tools such as CYMDIST, OpenDSS, and MATLAB/Simulink. The typical components of a distribution feeder include the lumped line/cable impedances throughout the length of the feeder, distribution transformers, voltage regulators, and loads. A survey of the existing state-of-the-art analysis tools reveals several required features in the capabilities, features, and the supported models that are discussed in the later part of this chapter.

1.3 Gaps in the existing distribution system analysis tool

This work is motivated by the limitations of the existing distribution system analysis tools. This work aims to develop new features for the distribution system analysis tools to enhance the capabilities to study the impact of large scale penetration of PV. The required features include:

- Development of various models of PV generators for different study objectives.
- Automated development of static, quasi-static, and dynamic model for analysis including voltage flicker and interaction with other control devices from GIS.

Most utilities have a complete GIS database on the equipment and conductor segments for the feeders. Large scale deployments of data acquisition systems and smart meters are leading to the availability of high resolution load and PV insolation data. Hence, major objective of this work is to have automated transfer of GIS data, load data and solar irradiation data directly, such that very large distribution systems can be easily studied for impact of PV generation.

1.4 Research objectives

Section 1.3 presents in detail the expectations from the updated distribution system analysis tool. The major work presented includes:

- Understanding the structure, features, algorithms, and models of the distribution system analysis tools.
  - Selecting a prototypical feeder model, representing a heavily populated urban area, as a test-bed.
  - Identifying the state-of-the-art distribution system analysis tools for analysis of the existing features.
  - Survey and detailed understanding of the capabilities of the operation and features, and the supported models.
  - Recognizing the new features to enhance the capabilities of the distribution system analysis tools.
- Development of various models of inverter controlled generators for different study objectives.
  - Simplified average model.
  - Models for dynamic phasor analysis.
- Static, quasi-static, and dynamic model for analysis including voltage flicker and interaction with other control devices from GIS.
  - Distribution feeder models in CYMDIST and OpenDSS from GIS.
  - Automated model construction in Simulink from GIS.

Understanding the structure, features, algorithms, and models of the distribution system analysis tools

Recognizing new features to enhance the capabilities of the distribution system analysis tools demands a close understanding of the operation and features provided by the existing tools. For the purpose of detailed comparison, CYMDIST, OpenDSS, and GridLab-D are chosen. CYMDIST is representative of the state-of-the-art distribution system analysis tool, commercially available, whereas OpenDSS and GridLab-D represents a set of open-source tools. Among the selected distribution system analysis tools, the prototypical feeders are modeled in CYMDIST and OpenDSS, whereas the comparison of the features is performed among the three tools. Details will be provided in Chapter 2.

Development of various models of inverter controlled generators for different study objectives

Considering the distribution feeders as passive might not be valid with large penetration of distributed generators. Grid-interfaced roof-top photovoltaic systems are predominantly used as sources of energy in a distribution feeder. The development of a power electronic circuit involves the design of the power stage, as well as the control algorithms.

Power stage includes all the semiconductor switches in different configurations, transformers, and filters. Control algorithms include control of the grid injected currents, dc link control, maximum power point tracking and grid synchronization. The controller of state-of-the-art inverters contains multiple stages of inner and outer control loops with widely different control bandwidth. Controllers with high bandwidth limit the time-step for solving the differential equation. A major part of the computation in power electronic converter simulations involves in modeling the equations governing the operation of a typical switch.

Quasi-static and dynamic model for analysis including voltage flicker and interaction with other control devices from GIS

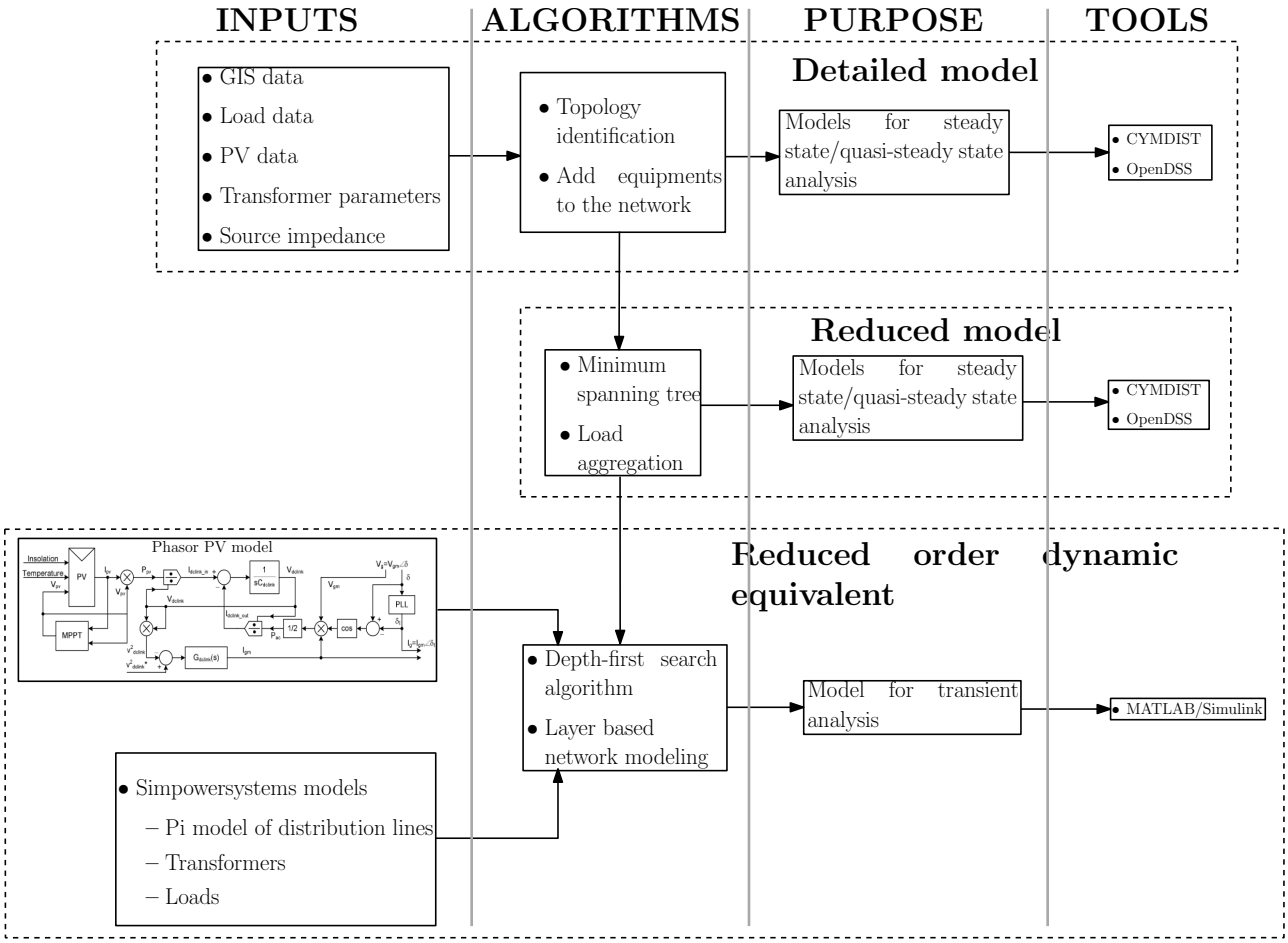

Figure 1.2 Generalized block diagram for modeling the distribution feeders in quasi-static and transient analysis tools

General framework for the modeling of distribution feeders in quasi-static and dynamic analysis tools is displayed in the Figure 1.2. The procedure presented diagrammatically in Figure 1.2 is capable of modeling the feeder starting from the GIS database.

2. Comparison of Distribution System Analysis Tools

2.1 Introduction

Recognizing new features to enhance the capabilities of the distribution system analysis tools demands a close understanding of the operation and features provided by the existing tools. There are numerous distribution system analysis tools supporting quasi-static analysis. For the purpose of detailed comparison; CYMDIST, OpenDSS, and GridLab-D are chosen. CYMDIST is representative of the state-of-the-art distribution system analysis tool, commercially available, whereas OpenDSS and GridLab-D represents a set of open-source tools. Among the selected distribution system analysis tools, the prototypical feeders are modeled in CYMDIST and OpenDSS, whereas the comparison of the features is performed among the three tools.

2.2 Comparison of the features of the tools

Tables 2.1 through 2.5 present the comparison of the features of the selected distribution system analysis tools. The comparison has been divided into five domains, namely:

- Basic features.
- Available equipment models.
- On-screen design and editing.
- Display and reporting.
- Miscellaneous and additional features.

2.3 Special module in the tools

Features available in the key modules, such as PV generator modules and residential end-use load module are discussed in detail below. The list provides the fields which can be used for precise modeling.

- PV generator modules
  - CYMDIST -active power (watts), power factor, and fault contribution.
  - OpenDSS - active power (watts for $1kW/m^2$ irradiation), irradiance (yearly, daily), inverter efficiency, ambient temperature, nominal voltage (kV), phases, power factor, connection (wye, delta, line-neutral, line-line), kVA rating of inverter, cut-in %, cut-out %
  - GridLab-D - In addition to the fields mentioned for OpenDSS; shading factor (pu), tilt angle in degrees, orientation azimuth in degrees.

- Residential end-use load modules
  - CYMDIST - Available as spot loads - fields available include active power (kW) and power factor.
  - OpenDSS - Available as spot loads - fields available include active power (kW) and power factor.
  - GridLab-D - Implicit end-uses : lights, plugs, occupancy, dishwasher, microwave, freezer, refrigerator, range, ev charger, water heater, clothes washer, dryer, default outdoor temperature, default humidity, house low temperature warning, house high temperature warning, ZIP load.
- Voltage regulating transformer module
  - CYMDIST - none.
  - OpenDSS - none.
  - GridLab-D - connection type (wye-wye, open-delta), band center (voltage calibration at the center of the tap), band width (voltage range available for regulation), time delay (mechanical time delay), dwell time (wait time), raise taps and lower taps (upper and lower tap limits), control (self, remote node, manual),tap position for phases A,B and C (initial tap position)

Table 2.1 Comparison of the basic features for distribution system analysis tools

Basic Features			
Features	**CYMDIST**	**OpenDSS**	**GridLab-D**
Power flow analysis for radial/looped networks	yes	yes	yes
Power flow analysis for system with unbalanced loads	yes	yes	yes
Source unbalance for slack bus	no	no	yes
Three-phase/single-phase power flow analysis	yes	yes	yes
Available power flow study techniques	unknown	Newton-Raphson	Forward-backward sweep Newton-Raphson Gauss-Seidel
Choosing type of power flow technique	n/a	n/a	yes
PV voltage regulation support in power flow study	no	yes	yes
Short-circuit analysis	yes	yes	no
Open conductor fault analysis	no	yes	no
Capacitor bank control	yes	yes	yes
Capacitor bank control modes	voltage current - -	voltage current kVAr time	voltage current kVAr VArvolt
Level of control of the capacitor bank (individual/bank)	no	no	yes
Capacitor bank control based on remote node sensing	no	no	yes
Makes use of GIS	no	no	no

Table 2.2 Comparison of the available equipment models in the distribution system analysis tools

Equipment models			
Features	**CYMDIST**	**OpenDSS**	**GridLab-D**
Pi-equivalent of transmission line or cables	yes	yes	yes
Generators (synchronous)	yes	yes	yes
Transformer configurations			
3 winding	delta/grounded wye ungrounded wye/ delta grounded wye/grounded wye delta/delta	delta/grounded wye ungrounded wye/delta grounded wye/grounded wye delta/delta	delta/grounded wye ungrounded wye/delta grounded wye/grounded wye delta/delta
single phase	single phase - - -	single phase single phase center-tapped - -	single phase single phase center-tapped open-wye open-delta
Voltage regulating transformers	no	no	yes
Models of PV generators	no	yes	yes
Reduced order PV models for study of high penetration of PV	no	no	no
Preloaded geographical PV insolation data	no	no	yes
Residential end-use models	no	no	yes

Table 2.3 Comparison of the on-screen design and editing capability in the selected distribution system analysis tools

On-screen design and editing			
Features	**CYMDIST**	**OpenDSS**	**GridLab-D**
On-line editing and zooming (buses, nodes, branches)	yes	no	no
Panning of diagram	yes	yes	no
Drag and drop shapes quickly with automatic snap and align into position	yes	no	no

Table 2.4 Comparison of the display and reporting feature in the selected distribution system analysis tools

Display and reporting			
Features	**CYMDIST**	**OpenDSS**	**GridLab-D**
Power flow displays (arrows indicating direction)	yes	no	no
Color displays (overloads, different feeders)	yes	yes	no
Abnormal conditions flagging	no	yes	no
Display selected number of phases or selected equipment	yes	no	no
Display control (e.g., zoom, pan, size labels and end points)	yes	yes	no
Graphical displays of result boxes or entire report	yes	yes	no
Distribution system profiles	yes	yes	no

Table 2.5 Comparison of the miscellaneous feature of the distribution system analysis tools

Other features			
Features	**CYMDIST**	**OpenDSS**	**GridLab-D**
Import/export from other database	yes	no	no
Help utility	no	online help	online help

3. Model Development in OpenDSS from GIS and Quasi-static Analysis

3.1 Introduction

An approach for modeling distribution feeder starting from GIS data in the OpenDSS is presented in this chapter. The GIS coordinates of the nodes, equipment rating, conductor details, PV insolation data, and load data will be used for the automated modeling of the feeder in the OpenDSS. Two feeders will be modeled using the described procedure. The two feeders, which will be modeled, will be referred to as base-model and extended-model all through in the report. This chapter details the modeling procedure used and a comparison of results are carried out.

3.2 Overview of model development in distribution system tools

3.2.1 CYMDIST

In CYMDIST, a distribution system model consists of three parts: equipment library, network model, and load model. The equipment library contains the definitions of all the equipments (including conductors) that may be used in the network model. The network model contains physical model of the system, containing detailed information about the equipment devices that are present in the system and their interconnection.

Each equipment in the network model is a reference to its type defined in the equipment library; although it may have extra parameters that are not defined in the library, or have some parameters values changed from their standard values. The load model defines the loads, including the load locations and the load data to be used for the power flow study. All the processed data are combined, entered or imported into CYMDIST to build the distribution system model, with the one-line diagram automatically generated.

CYMDIST supports unbalanced power flow analysis, which is required for a distribution system. The CYMDIST also generates multiple chart profiles; for example, kVA profile, kVAr profile, voltage profile, fault current profile, either for the selected part of the distribution system or for the tracing the source from the current selection. Models of PV are not supported mandating the use of an electronically coupled generator for simulating the PV.

3.2.2 OpenDSS

In OpenDSS, a distribution system model consists of multiple parts depending upon the detail expected from the system. Some of the important parts include: X-Y coordinates

of all the nodes, line codes, line data, distributed generation data, transformer data, capacitor data along with associated control, and the load model. The line codes contain the definitions of all the conductors that may be used in the line data. The line data is the physical model of the distribution lines, containing detailed information about the from-nodes and the to-nodes The transformer data will have all the parameters related to the distribution transformers along with the data of the nodes between which these transformers are connected. The load model defines the load, including the load locations and the load data to be used for the power flow study. All the processed data are combined and imported into OpenDSS to build the distribution system model, with the one-line diagram generated.

OpenDSS supports unbalanced power flow analysis, which is current injection based Newton-Raphson technique, for solving the distribution system. The OpenDSS also generates voltage profile by tracing the whole system from the chosen head node. Different models of PV generators are supported for static analysis. OpenDSS comes with a component object model (COM), which makes the OpenDSS accessible from MATLAB, Python and C++ programming languages.

3.2.3 GridLab-D

In GridLab-D, a distribution system model consists of a single file containing all the data related to the system. GridLab-D is not specific to hierarchy; for example, it is not mandatory to define conductor specific data prior to the corresponding overhead/underground line. Also, GridLab-D cannot generate one-line diagram specific to the system. GridLab-D supports several types of unbalanced power flow techniques, Gauss-Seidel, forward-backward sweep, and Newton-Raphson for solving the distribution system. Moreover GridLab-D is not capable of generating a voltage profile. Models of PV are supported for static analysis. GridLab-D comes with a component object model (COM), which makes the GridLab-D accessible from MATLAB and C++.

3.3 Detailed model development in OpenDSS

This section presents in detail the procedure for modeling the base-model and the extended-model. Modeling involves acquiring all the input data required. The inputs, from shape files (GIS data), are processed using MATLAB programming tool. This work concentrates on modeling in OpenDSS. Finally, all the processed data are combined and imported into CYMDIST and OpenDSS, to build the distribution system model. Figure 3.1 shows a general structure of the modeling process followed. Reference [2] presents a detailed explanation of the modeling procedure specific to CYMDIST. The results presented in this chapter from CYME were taken from the reference report [3]. This chapter provides a detailed procedure for modeling in OpenDSS.

The initial step for modeling the feeder is to identify the topology from the GIS data. Topology identification is the process of finding the electrical connections of the line

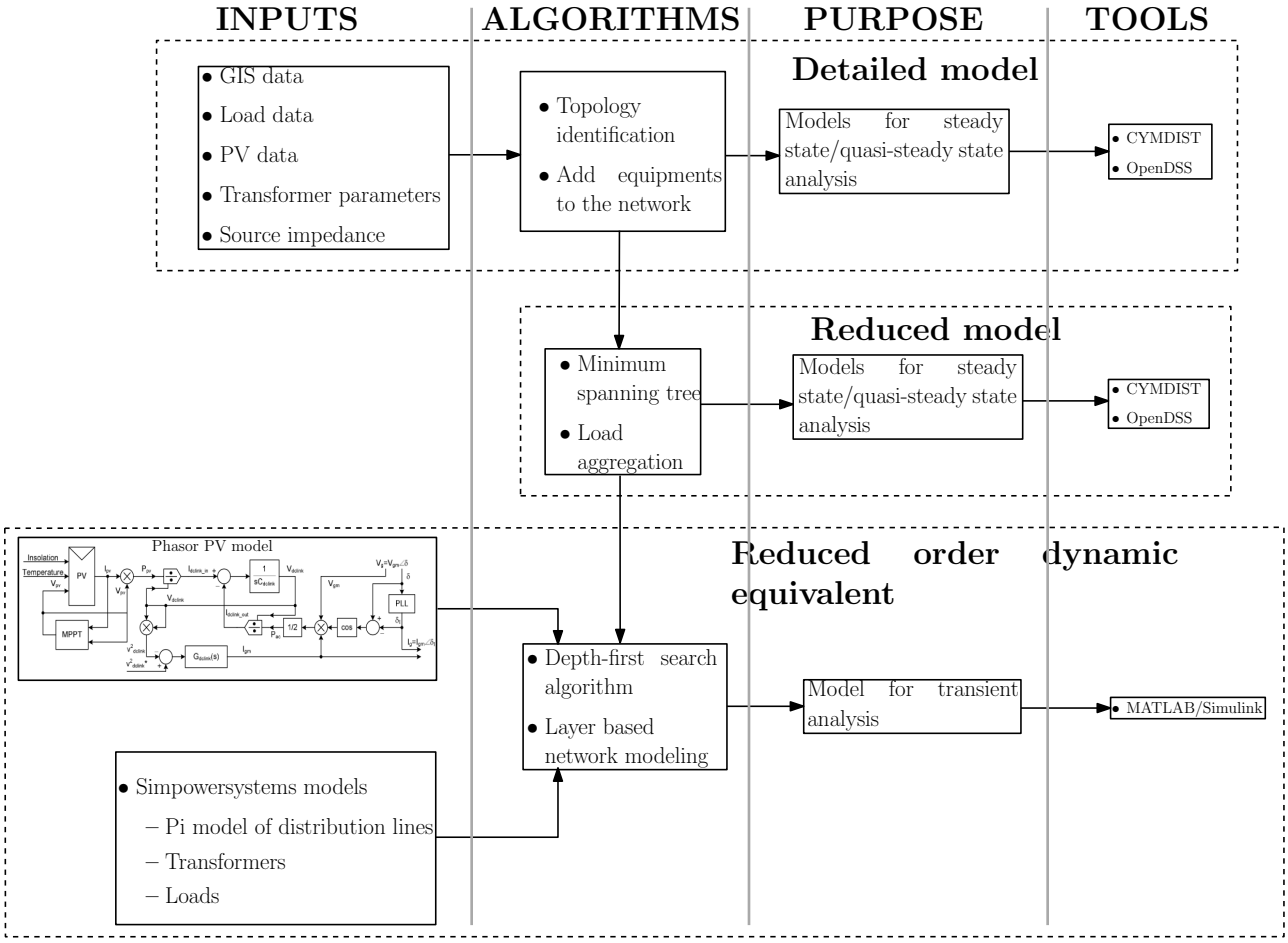

Figure 3.1 Generalized block diagram for modeling the distribution feeders in quasi-static and transient analysis tools

segments and the equipments. Although the GIS data indicates the locations of all the lines and the equipment devices, it does not contain the explicit information about the electrical connectivity. The output of the topology identification is a set of data as shown below:

- Section configuration - Section ID, from node id, to node id, phase
- Line configuration - Section ID, device number, line cable ID, length, overhead, number of cables in parallel
- Distributed generation configuration - Section ID, device number, phase, kW, power factor
- Capacitor data and control configuration - Section ID, device number, connection type (Y), phase, three-phase kVAr, nominal kV, control type, on-setting, off-setting
- Transformer configuration - Section ID, kVA rating, Voltage (secondary), device ID, type (Y-Y), phase

- Load configuration - Section ID, device number, connection status, load phase, kVA rating, power factor
- Bus coordinates - Node ID, coordinate X, coordinate Y

The set of data listed above will be again used for modeling the data in a transient analysis tool. Hence these extracted data set is a reordered data which will be used for modeling for rest of the report. The modeling process specific to OpenDSS from the data set listed above is presented in Figure 3.2. The complete model for a typical distribution system implemented in OpenDSS involves a total count of 8 files, containing details specific to the model adhering to the syntax specifications for OpenDSS.

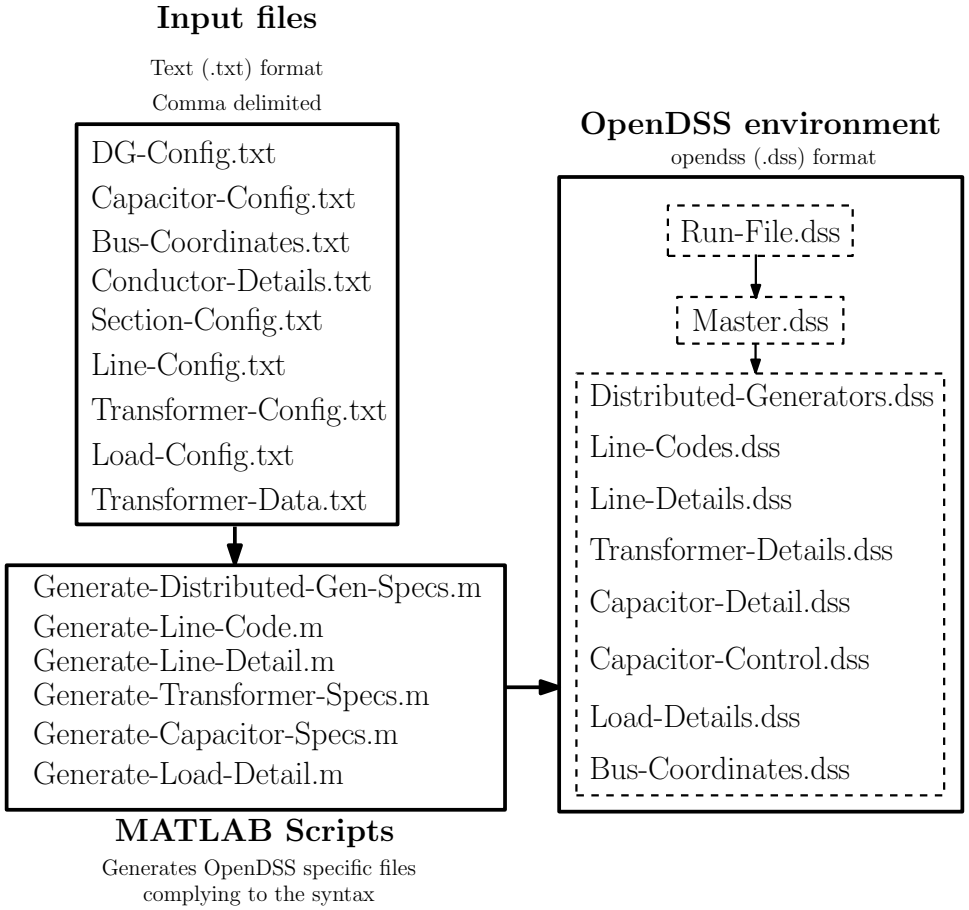

Figure 3.2 Modeling process flowchart specific to OpenDSS

Details of fuse and recloser configuration are not considered at this stage, because the scope of this work does not involve fault studies. The mentioned input files (*.txt* or *.mat* format) are read using a MATLAB script (*.m* format) and the files specific to OpenDSS (*.dss* format) are generated. The approach for compiling, in OpenDSS, involves creating a *run.dss* file. The *run.dss* file includes the path for *master.dss* and also it is recommended to mention all the output requirements. For example, the output involves line-to-neutral/line-to-line voltages for each node, currents in each section, power through each section, voltage profiles,

and a summary report. As the typical distribution feeder includes thousands of nodes and feeder spanning for multiple miles, a summary report is necessary to assess the validity of the model.

The *master.dss* creates a new circuit at the very beginning and starts building the feeder model by including the path for *.dss* files consisting the feeder data. The *master.dss* also includes the details of the source node along with its source impedance and the nominal voltage. The overall process is also represented in the Figure 3.2.

In addition to the data extracted from the shape files (*.shp*) files, the OpenDSS needs phase for each node. CYMDIST needs phases specific to each section, whereas the OpenDSS requires phases for each node. An algorithm is developed for identification of the phases of each node from the data available. The nodes with the incoming and the outgoing sections having identical phase, are simple to conclude upon, whereas, if the phases of all the incoming and the outgoing sections are not the same, identification of the correct phase needs specific analysis.

As an example Figure 3.3 shows a case with a typical phase conflict, where node 239 has three sections connected, of which, section from node 238 to node 239 has three-phase lines, whereas section between nodes 239 and 599 contains phase C. An algorithm was developed to detect phase conflicts and assign a proper phase. The developed algorithm will assign the phase of node 239 to be ABC and node 599 as phase C. The presence of repeating phase conflicts and similar complex scenarios make it necessary to develop a robust algorithm for the same.

3.4 Developed feeder model

The modeling procedure presented in the previous section pertains for steady state analysis. The same model needs to be updated for performing time-series simulations. In the time series solution mode, each load/PV generator follows the daily or yearly profiles. The yearly curve magnitudes (normalized) and the growth multiplier determine the value of the load and the PV generator that finally logs to the power flow. The time step can be tuned to any value of interest. Meters and monitors are reset at the beginning of solution and sampled after each solution. Several monitors are set near data acquisition systems (DAS) locations of the model to capture temporary results of voltages and power at those points. Results of the monitor can be compared with the DAS measurements and thus the system model can be validated. In OpenDSS the base model is used for time series simulation.

The profiles of the loads and the PV generators are inputed to the OpenDSS through shape files. Shape file name is defined as the same with the transformer ID to simplify the process. Figure 3.5 presents the feeder view from the OpenDSS. The results of a time-series analysis for the base-model is presented in Figure3.6 and Figure 3.7. The generation at the feeder head and the voltage measurement at the center of the base feeder is field tested and the results are presented. Figure 3.4 presents the feeder view of the extended-model.

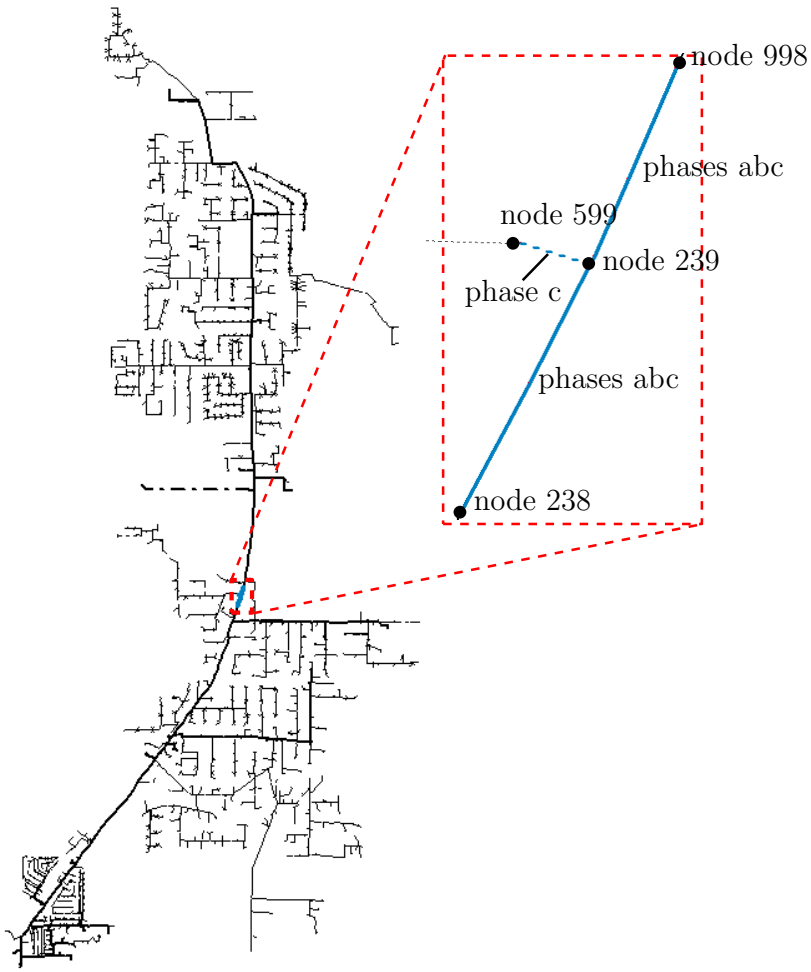

Figure 3.3 Example for a case with phase conflict

Figure 3.6 shows the comparison between the measured and simulated one-minute-interval kW plot of phase A at the substation in one day. As seen from Figure 3.6, the modeled kW values are following the DAS kW measurement closely. Figure 3.7 show the comparison between the measured and the simulated kVLN plot of phase A at DAS 5, which is at the middle of the feeder. As seen from Figure 3.7, the simulated voltage values are matching closely to the measured data throughout the feeder.

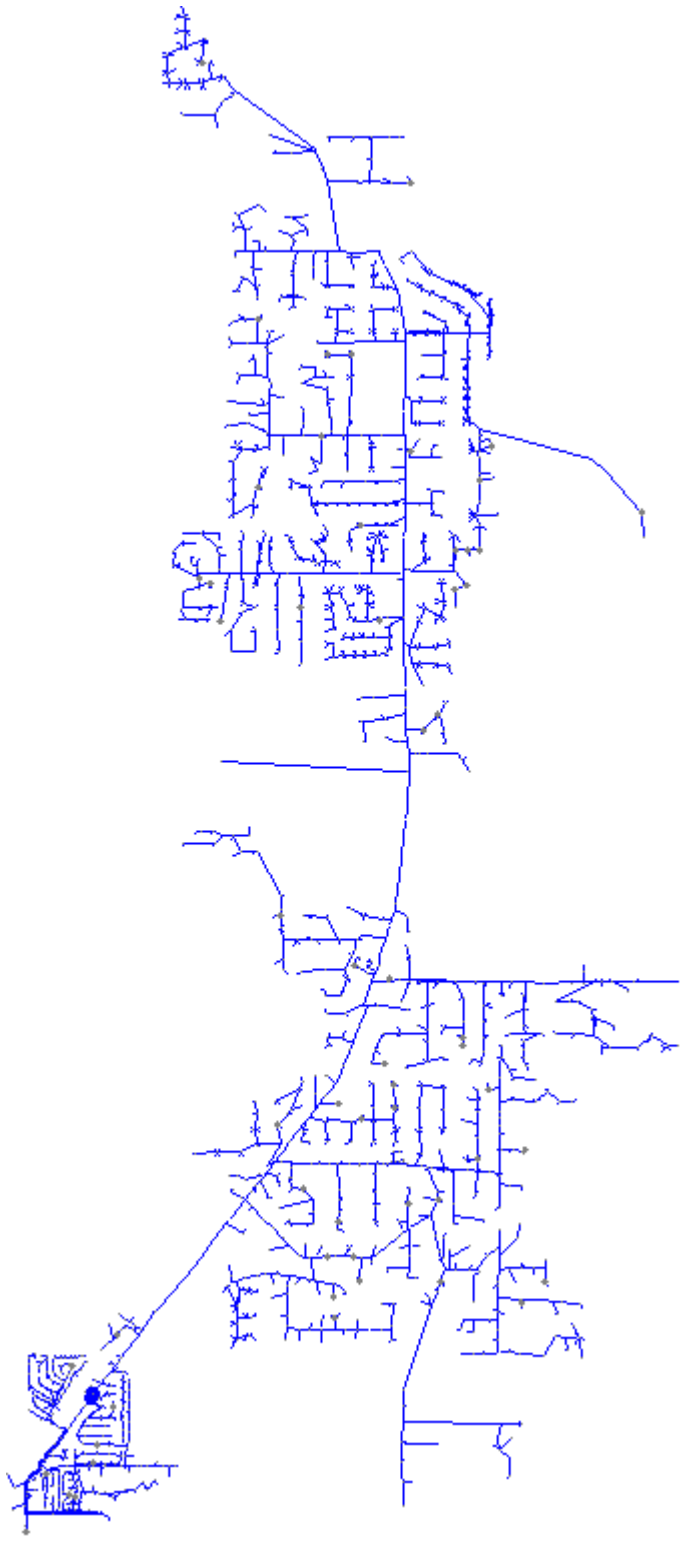

Figure 3.4 Feeder view of the extended-model from OpenDSS

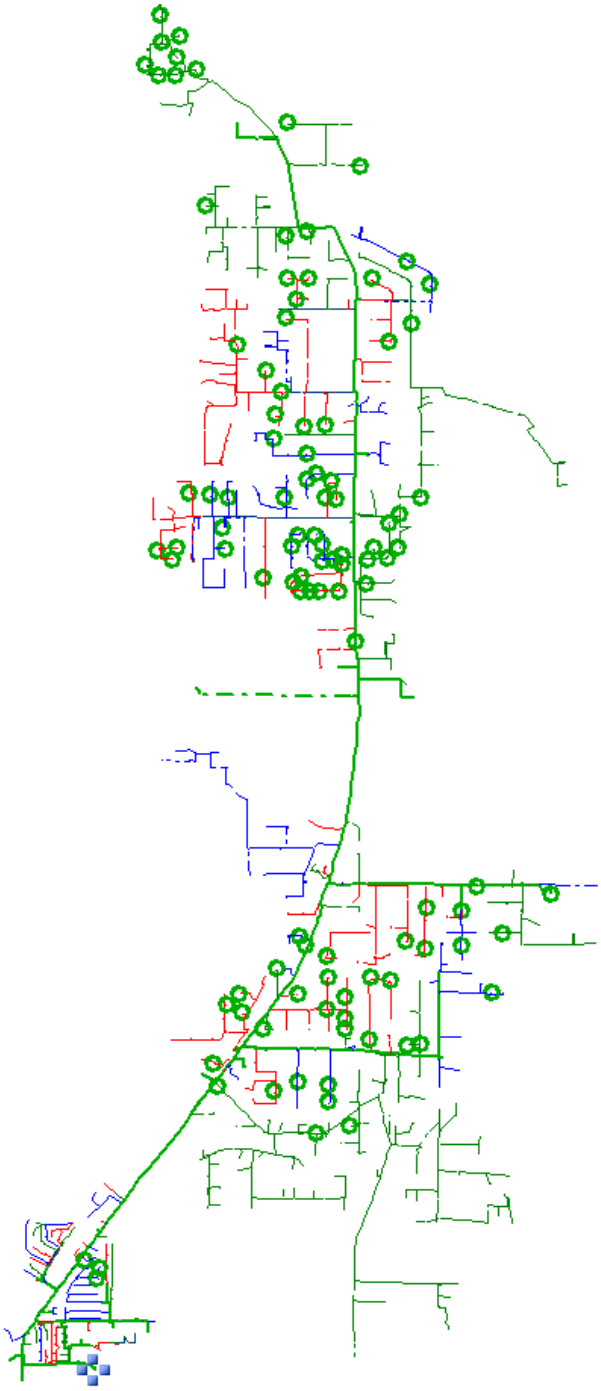

Figure 3.5 Feeder view of the base-model from OpenDSS

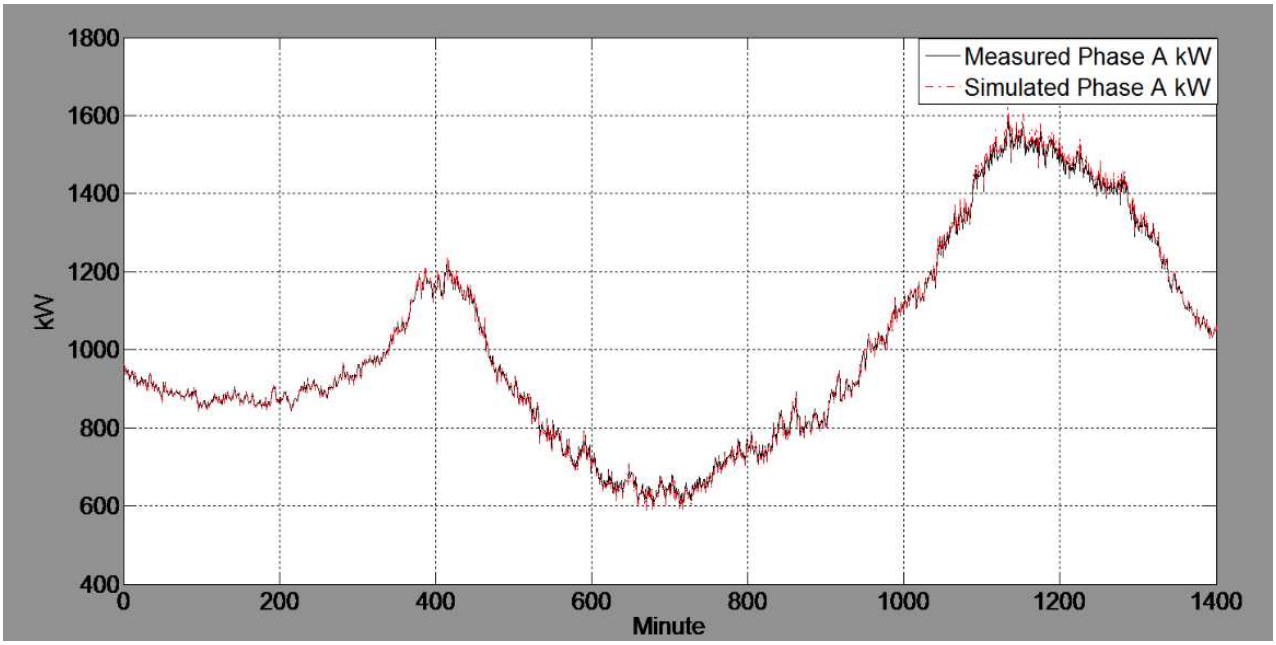

Figure 3.6 Measured and simulated substation kW at one-minute-interval of phase A for one day

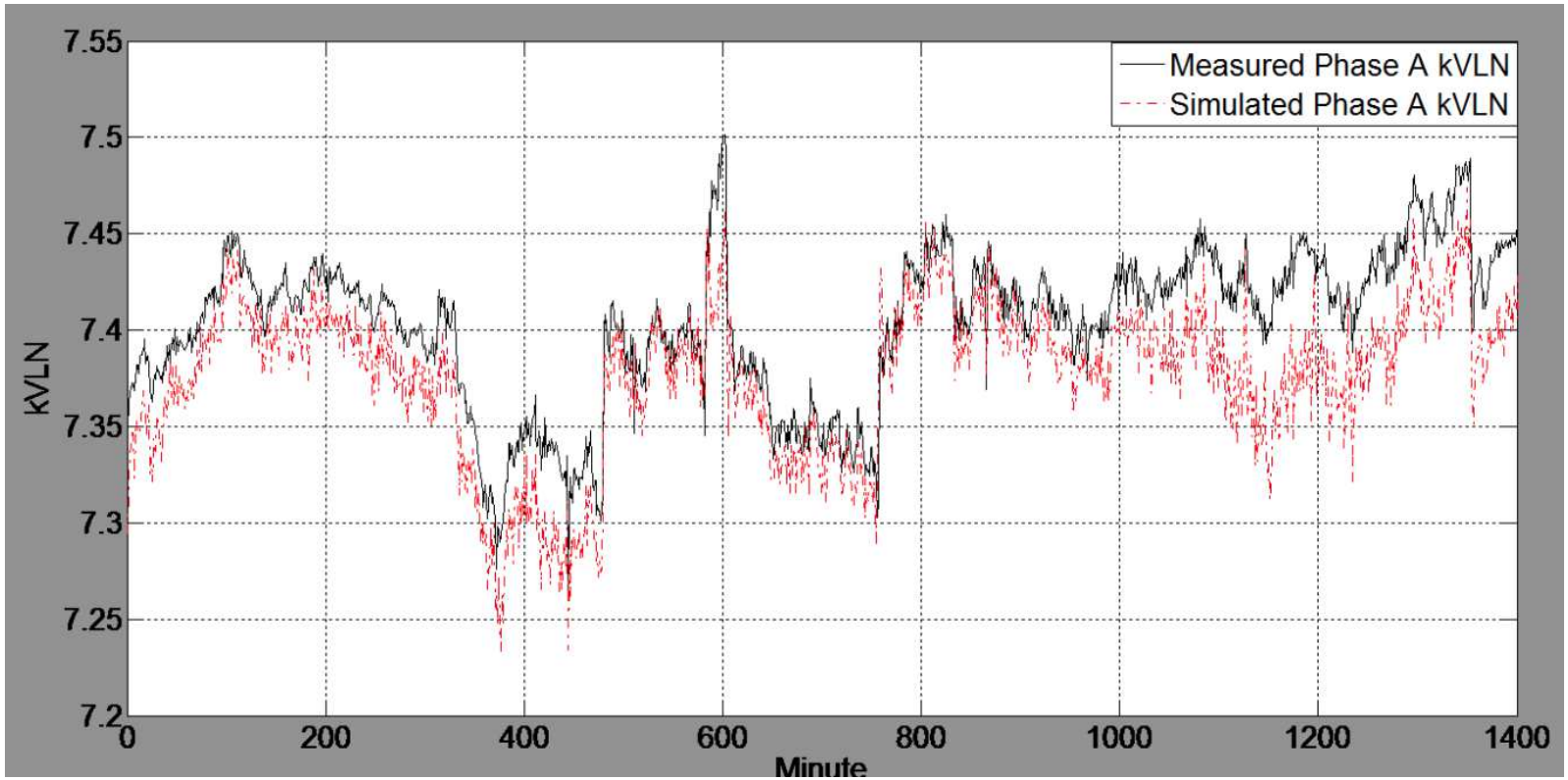

Figure 3.7 Measured and simulated voltage plot at midway from the substation at one-minute-interval of phase A for one day

4. Dynamic Phasor Models of PV Generators

4.1 Introduction

High penetration of PV generators in distribution feeders have considerable impact on the system behavior. For a good understanding of these impacts redevelopment and fine-tuning of the existing power system and power converter models in the simulation environments are essential. In particular dynamic models for the various components and various stages for fast computation of large distribution systems are essential. This chapter presents the dynamic models of Pulse Width Modulated (PWM) power converters that are capable of capturing the transients of interest with significant reduction in computation thereby making the detailed dynamic analysis of large distribution systems possible.

4.2 Reduced order models for tools with inbuilt phasor solvers

This section develops reduced order models of the single-phase and three-phase inverter for transient analysis tools with inbuilt phasor solvers. Phasor solvers exist in MATLAB/Simulink and OPAL-RT. Detailed models are not required for solving large distribution systems. This section provides the structure of the following models:

- Simplified average model.
- Phasor model.

Simplified average model

The detailed switching model of the PV converter suffers from slow simulation, due to the complexity of the model as well as the small time steps that the simulator has to choose. Thus, a simplified model is necessary for simulating a system with many PV generators. Along with replacing the switches with its cycle-by-cycle average the high bandwidth controller will be assumed with ideal operation. The block diagram of the simplified average model is as shown in the Figure 4.1. Details of the circuit is proposed in the reference [4].

Phasor model

The simplified average model has been further customized specifically for the inbuilt phasor solvers in the SimPowerSystems toolbox in MATLAB/Simulink. The phase locked loop (PLL) has been redesigned specifically for the phasor mode. The block diagram of the phasor model is as shown in the Figure 4.2. Using the phasor method, the fast oscillation modes associated with the network R, L, and C elements are ignored by replacing the network's differential equations by a set of algebraic equations. The state-space model of the network is therefore replaced by a transfer function evaluated at the fundamental frequency and relating inputs (current phasors injected by generators into the network) and outputs

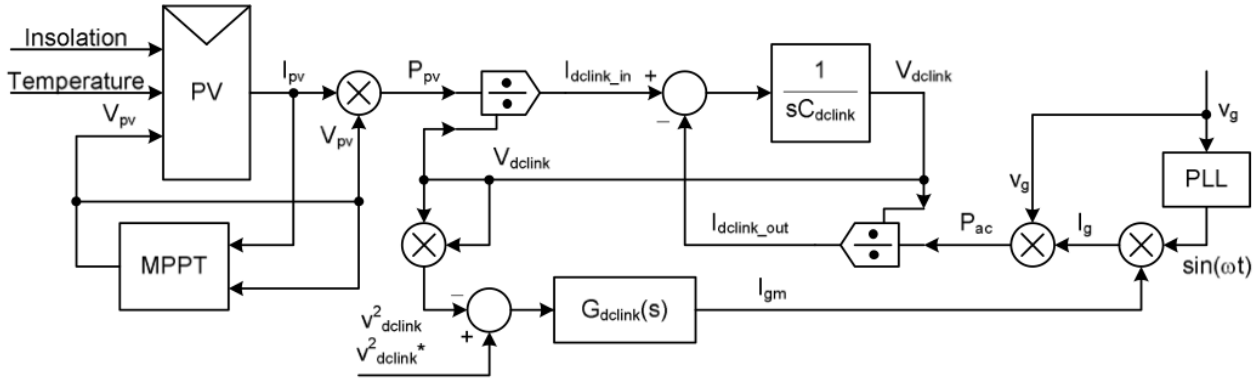

Figure 4.1 Block diagram of the simplified average model of power converter

(voltage phasors at generator terminals). Thus, the phasor method uses a significantly reduced state-space model consisting of slow states of machines and controllers, dramatically reducing the required simulation time. The details of the model can be obtained from reference [4].

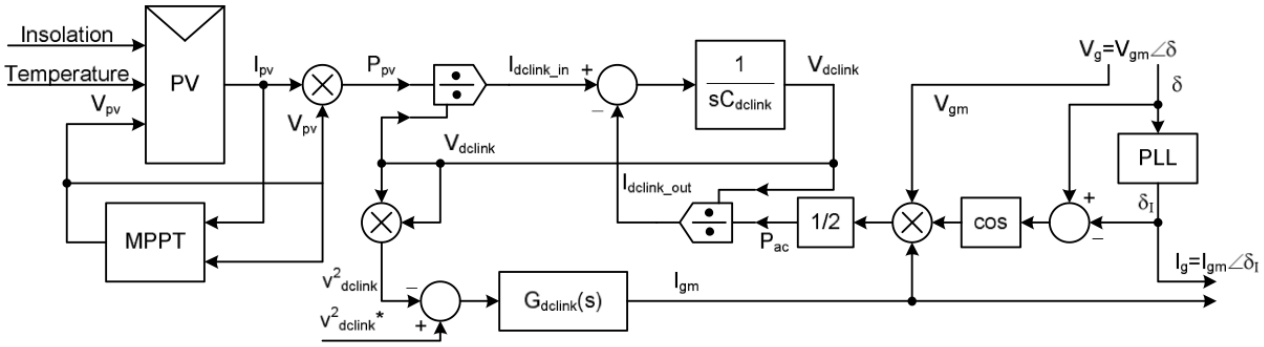

Figure 4.2 Block diagram of the phasor model of the PV converter

4.3 Generalized phasor model of power converter

This section provides the generalized dynamic phasor model for the single phase PV converter. The model proposed in this section can be implemented in any tool with a defined ordinary differential equation solver. The dependency on the tool to have inbuilt phasor solver is completely exempted. The methodical mathematical transformation of an ordinary differential equation in the time domain to frequency domain is defined the following section. Since the work related to development of the phasor models of general purpose power system equipments (conductors, generators, capacitor banks) are pre-existing [5] this work only develops the phasor model for the single-phase inverter. The existing literature work is initially explored.

The development of a power electronic circuit involves the design of the power stage, as well as the control algorithms. Power stage includes all the semiconductor switches in different configurations, transformers, and filters. Control algorithms include control of the grid injected currents, dc link control, maximum power point tracking and grid synchronization. The controller of state-of-the-art inverters contains multiple stages of inner and outer control loops with widely different control bandwidth. Controllers with high bandwidth limit the time-step for solving the differential equation. A major part of the computation in power electronic converter simulations involves in modeling the equations governing the operation of a typical switch. State-space averaging methods developed in [6] is an effective tool for modeling switch-mode converters and aiding in the controller design. Another important contribution in this area is the development of the average model of the PWM switch (combination of the controlled switch and the diode) by its equivalent average model [7, 8]. Numerous authors have refined the state-space averaging method in various ways [4, 7, 9–11].

State-space averaging involves the application of one-cycle averaging operator for a periodically switched circuit with a period T. This method is also referred as in-place circuit averaging or cycle-by-cycle averaging. Averaging the state-space models over each cycle drastically reduces the computation time otherwise. Another approach to the state-space averaging is through a circuit-oriented approach. Circuit-oriented approach relies on the identification of a three-terminal nonlinear device - the PWM switch, and replacing by an average equivalent circuit model.

The strength of the state-space averaging is in permitting direct analysis on a given circuit rather than on the state-space equation. State-space averaging technique is principally refined with large number of publications. For the purpose of validation and comparison this work develops a state-space average model of an inverter and compares it with the dynamic phasor model. Even though state-space averaging technique was a major step towards fast simulation, it has certain limitations as follows:

- State-space averaging cannot be applied to switched circuits that do not satisfy small ripple condition.
- The gain in computation time fades as the number of PWM power converters increases in the simulation.

It has been well noted in the literature that the class of converters that the state-space averaging method can be applied to is limited. Conditions for justification of state-space averaging has been characterized by linear ripple approximation [12]. The small ripple condition confirms that a Fourier series expansion of the waveform for a finite length of time should be dominated by the DC component. The linear ripple approximation requires that the circuit waveform should be linear functions of time when examined over a time interval in-between switching instances. Detailed explanation of the condition is provided in the reference [13]. Resonant type converters cannot be modeled using state-space averaging.

Although a full bridge sine PWM power converter satisfies the linear ripple approximation, the gain in computation time fades with the increase in the number of PWM

converters in the simulation. Additionally the computation time drastically increases with the magnitude of of distribution feeder under study. This work presents a more general averaging procedure that encompasses state-space averaging and is potentially applicable to a much broader class of circuits and systems. Furthermore dynamic phasor formulation supports fast computations for systems with large number of switched converters including a large distribution feeder. The dynamic phasor circuit models can be modeled directly into circuit simulators such as MATLAB, PSCAD, MODELICA, or any other ordinary differential equation solver.

The averaging technique considered in this work is based on the Fourier series averaging method initially proposed in reference [14]. The averaging technique is referred to as the dynamic phasor apporach. Dynamic phasor modeling approach has been applied to various aspects of power systems. Some of the key references in the application of dynamic phasors include [5, 15–18]. This averaging method is based on demodulating the circuit waveform, $x(\bullet)$, to its components over the interval $(t-T, t]$ with Fourier series representation. This generalized averaging method will be referred as dynamic phasor for rest of the work. Dynamic phasor method is also referred to as time-varying phasors in some of the publications.

4.4 Dynamic phasor problem formulation

Phasor representation of a sinusoidal signal is a powerful tool for analyzing the steady state behavior of voltages and currents. Phasors has always been used for the analysis of the power systems in the stationary sense. Phasor representation is a class of mathematical transformation to eliminate the fundamental frequency component in the calculation. In the stationary case/steady-state there will be only one frequency component. A single-phase signal can be represented as

$$x(t) = X(t)cos(\omega t + \delta(t)), \tag{4.1}$$

where $x(t)$ is a time varying signal which is periodic with at frequency ω. The phasor representation links $\hat{x}(t)$

$$\hat{x}(t) = X(t)\ e^{j\delta(t)} = X(t)\angle\delta(t), \tag{4.2}$$

with the modulated signal $x(t)$. In other words, the original signal $x(t)$ is related to its phasor $\hat{x}(t)$ by

$$x(t) = Re(\hat{x}(t)e^{j\omega t}). \tag{4.3}$$

With these fundamentals the dynamic phasor method is based on the fact that the waveform $x(\bullet)$ can be decomposed into its individual frequency components on the time interval $(t-T, t]$ to arbitrary accuracy with a Fourier series representation of the form

$$x(t-T+\tau) = \sum_k \langle x \rangle_k (t)\, e^{jk\omega(t-T+\tau)} \tag{4.4}$$

where the sum is over all integer values of k, $\tau \in (0, T]$, $\omega = 2\pi/T$, and the $\langle x \rangle_k (t)$ are the complex Fourier coefficients. These Fourier coefficients are functions of time. The interval under consideration for the Fourier coefficient slides as a function of time. The k-th coefficient is calculated using

$$\langle x \rangle_k (t) = \frac{1}{T} \int_0^T x(t - T + \tau)\, e^{-jk\omega(t-T+\tau)}\, d\tau. \tag{4.5}$$

The analysis computes the time-evolution of the Fourier series coefficients as the window of length T slides over the actual waveform. Hence to summarize at this juncture the study should determine appropriate dynamic phasor model in which the coefficients, defined in (4.5), are the state variables. The kth Fourier coefficient of a time-domain signal $x(t)$ is represented as $\langle x \rangle_k (t)$. For the purpose of convenience (t) is dropped for rest of the work. As the $\langle x \rangle_k$ is a complex quantity, except the dc-coefficient ($\langle x \rangle_0$), a typical kth Fourier coefficient can be rewritten in terms of real and imaginary parts as

$$\langle x \rangle_k = \langle x \rangle_k^R + j\ \langle x \rangle_k^I \tag{4.6}$$

where the superscripts R and the I represent the real and the imaginary components of a Fourier coefficient.

4.4.1 Analogy between the state-space averaging and the dynamic phasor approach

One possible way of deriving the theory of state-space averaging is to consider the one-cycle average

$$\bar{x}(t) = \frac{1}{T} \int_{t-T}^{t} x(\tau)\, d\tau \tag{4.7}$$

for the state $x(t)$ of a switching converter operating at a frequency of $1/T$. The connection with the dynamic phasor scheme is that $\bar{x}(t) = \langle x \rangle_0 (t)$ corresponds to the dc coefficient of the Fourier series representation.

4.4.2 Properties of the Fourier coefficients

Differentiation with respect to time

The time derivative of the first order for the kth coefficient is computed to be

$$\frac{d}{dt} \langle x \rangle_k = \left\langle \frac{d}{dt} x \right\rangle_k - jk\omega \langle x \rangle_k . \tag{4.8}$$

This chapter uses the dynamic phasor model with a second order derivative. The time derivative of the second order for the kth coefficient is computed as

$$\frac{d^2}{dt^2} \langle x \rangle_k = \left\langle \frac{d^2}{dt^2} x \right\rangle_k - k^2\omega^2 \langle x \rangle_k . \tag{4.9}$$

In case the ω is time varying the varying nature of the frequency should be accommodated into the equations.

Product of Fourier coefficients

The procedure is based on convolution

$$\langle x\, y\rangle_k = \sum_l \langle x\rangle_{k-l}\, \langle y\rangle_l \tag{4.10}$$

Linear elements

The branch variables for a linear resistive element are related by Ohm's law. The Ohm's law for the k-th coefficient will be

$$\langle e\rangle_k = R\ \langle i\rangle_k \tag{4.11}$$

where e represents voltage applied across the resistor, R is the resistance and the i is the current flowing through the resistor.

The dynamic phasor equations for capacitor voltage and inductor current

The current i_C flowing through a capacitor C with a terminal voltage e can be represented by

$$\langle i_C\rangle_k = C\ \frac{d}{dt}\langle e\rangle_k + j\ \omega\ C\ \langle e\rangle_k \tag{4.12}$$

Similarly with the voltage $e(t)$ across an inductor, L, a current of $i_L(t)$ is flowing through can be represented by

$$\langle e\rangle_k = L\ \frac{d}{dt}\langle i_L\rangle_k + j\ \omega\ L\ \langle i_L\rangle_k \tag{4.13}$$

Model of a switch

Variables associated with a typical switch are duty cycle d and switching period T_s. Let 1 represent a closed position and 0 represent an open position.

$$u(t) = \begin{cases} 1, & 0\ < t <\ dT_s \\ 0, & dT_s\ < t < T_s \end{cases} \tag{4.14}$$

$$\langle u(t)\rangle_0 = d \tag{4.15}$$

$$\langle u(t)\rangle_1 = \frac{sin2\pi d\ +\ j\ (cos2\pi d\ -\ 1)}{2\pi} \tag{4.16}$$

The differential equations which include the time-varying sinusoidal carrier signal can be rewritten as a set of time-invariant differential equations by replacing all the derivatives using the differentiation rule. The new set of equations being in the complex phasor domain are of twice the original dimension of the system. The trajectory of the transients can be directly interpreted in terms of the envelop variation using the dynamic phasor formulation.

4.5 Generalized dynamic phasor model of a single-phase inverter

A full bridge single-phase inverter with its current control loop is as shown in Figure 4.3. To develop a dynamic phasor model of a single-phase inverter a transformer equivalent circuit as shown in Figure 4.4 is used. The purpose to develop a transformer equivalent circuit is to avoid the modeling of high frequency switching transients. Since the variation of the voltage at the DC link is not considered the transformer equivalent can be further reduced to Figure 4.5. This work initially develops a state-space model for the system shown in Figure 4.5 and further establishes the dynamic phasor equivalent for the same.

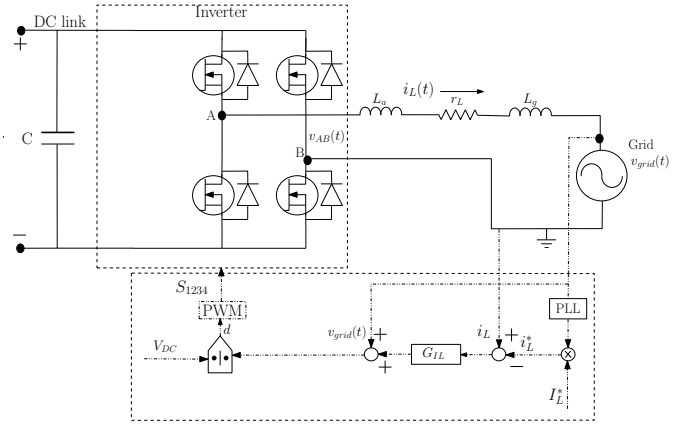

Figure 4.3 Full switching model of the single-phase full bridge inverter and its control strategy

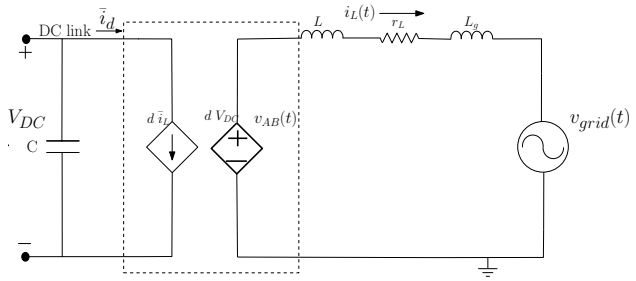

Figure 4.4 Combined transformer equivalent circuit of a full bridge single-phase inverter

With reference to Figure 4.5 a single-phase inverter with a r_L and L filter, V_{DC} as the dc input voltage, $v_{grid}(t) = V_{gm}sin(\omega t)$ as the output voltage, $v_c(t)$ as the control voltage at the output of the controller is considered in this study. The spate-space model of the inverter, as in Figure 4.5, can be realized as

$$L\,\frac{di_L}{dt}\;+\;r_L\;i_L(t)\;+\;v_{grid}(t) =\;v_c(t)\;V_{DC}, \tag{4.17}$$

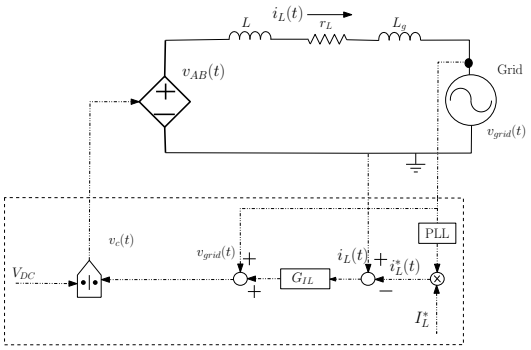

Figure 4.5 Reduced transformer equivalent circuit of the single-phase full bridge inverter and its control strategy

where $v_c(t) = x_1 \ \frac{v_{grid}(t)}{V_{DC}}$ and x_1 is the state obtained from the current control loop $G_{IL}(s)$ with a form

$$\frac{x_1}{\epsilon} = \frac{K(1+\frac{s}{\omega_z})}{s\ (1+\frac{s}{\omega_p})}, \tag{4.18}$$

$$\frac{d^2x_1}{dt^2} = K\ \omega_p\ \epsilon + K\ \frac{d\epsilon}{dt}\frac{\omega_p}{\omega_z} - \frac{dx_1}{dt}\omega_p, \tag{4.19}$$

where $\epsilon = i_L^* sin(\omega t) - i_L(t)$. Based on the properties of the Fourier coefficients in Section 4.4 the state-space model of the inverter is converted to the dynamic phasor model as

$$\frac{d\langle i_L\rangle_1^R}{dt} = \omega\ \langle i_L\rangle_1^I + \frac{1}{L}\ \left(-r_L\ \langle i_L\rangle_1^R\ -\ \langle x_1\rangle_1^R\ V_{DC}\right), \tag{4.20}$$

$$\frac{d\langle i_L\rangle_1^I}{dt} = -\ \omega\ \langle i_L\rangle_1^R + \frac{1}{L}\ \left(-r_L\ \langle i_L\rangle_1^I\ -\ \frac{\langle V_{gm}\rangle_1^I}{2} - \langle x_1\rangle_1^I\ V_{DC}\right). \tag{4.21}$$

Each ordinary differential equation in time domain generates two equations in the dynamic phasor form (real and imaginary). Equation (4.20) and (4.21) represent the dynamic phasor equivalent of the spate-space equation (4.17). Equations (4.22) and (4.23) present the dynamic phasor equivalent of the second order current controller for the spate-space

equation (4.19)

$$\begin{aligned}\frac{d^2\langle x_1\rangle_1^R}{dt^2} =& -\langle i_L\rangle_1^R K\omega_p + \frac{K\omega_p\omega}{2\omega_z} i_L^* - \frac{d\langle i_L\rangle_1^R}{dt}\frac{K\omega_p}{\omega_z} \\ &+ \frac{K\omega_p\omega}{\omega_z}\langle i_L\rangle_1^I - \omega_p\frac{d\langle x_1\rangle_1^R}{dt} + \omega\omega_p\langle x_1\rangle_1^I \\ &- \omega^2\langle x_1\rangle_1^R \end{aligned} \tag{4.22}$$

$$\begin{aligned}\frac{d^2\langle x_1\rangle_1^I}{dt^2} =& -\frac{K\omega_p\omega}{2} i_L^* - K\omega_p\langle i_L\rangle_1^I - \frac{K\omega_p}{\omega_z}\frac{d\langle i_L\rangle_1^I}{dt} \\ &- \frac{K\omega_p\omega}{\omega_z}\langle i_L\rangle_1^R - \omega_p\frac{d\langle x_1\rangle_1^I}{dt} - \omega_p\omega\langle x_1\rangle_1^R \\ &- \omega^2\langle x_1\rangle_1^I \end{aligned} \tag{4.23}$$

Combined equations (4.20), (4.21), (4.22), and (4.23) present the dynamic phasor equivalent for the reduced transformer equivalent of the single-phase inverter (Figure 4.5) along with the controller. The dynamic phasor model (equations (4.20), (4.21), (4.22), and (4.23)) is modeled in the transient analysis tool. Numerical differential equation solvers are used to solve the dynamic phasor equations.

The superscripts R and I represent the real and the imaginary components of a Fourier coefficient and the subscript 1 refers to the harmonic. The dynamic phasor equivalent being in the complex phasor domain are twice the original dimension of the original system. The absence of the 60 Hz component in dynamic phasor formulation will reduce the computation time drastically. Large time steps will be sufficient for solving the system of equations.

Dynamic phasor models can be used to capture multiple levels of detail. The dynamic phasor equivalent presented in the equations (4.20), (4.21), (4.22), and (4.23) capture only the first harmonic (fundamental frequency, $k = 1$). The same set of equations can be used to capture additional harmonics of interest by appending the system with additional equations with other values for k (kth harmonic). Each harmonic adds two more equations, one for real part (R) and the other for the imaginary part (I). Additionally the reconstruction of the waveforms obtained from the real and imaginary components can be performed in multiple ways.

$$i_L(t) = 2\ \sum_k \langle i_L\rangle_k^R cos(k\omega t) - \langle i_L\rangle_k^I sin(k\omega t) \tag{4.24}$$

$$\widehat{i}_L(t) = 2\ \sqrt{[\langle i_L\rangle_k^R]^2 + [\langle i_L\rangle_k^I]^2} \tag{4.25}$$

Equations (4.24) and (4.25) are be used to reconstruct the detailed dynamic phasor and the peak dynamic phasor respectively. The detailed dynamic phasor is analogous to the cycle-by-cycle average model whereas the peak dynamic phasor envelops the cycle-by-cycle average waveform. The complete system has been realized in MATLAB/Simulink. For the

purpose of verification the state-space model of the single-phase inverter (equation (4.17)) along with the controller is realized and compared with the dynamic phasor equivalent model.

4.6 Results

This section presents the results of the state-space model and the dynamic phasor equivalent for the transformer equivalent of the single-phase inverter along with the current controller. The models for the state-space form and the dynamic phasor equivalent are developed in MATLAB/Simulink. Equations (4.17) and (4.19) are solved simultaneously for multiple transients to generate results for the spate-space form. Equations (4.20), (4.21), (4.22), and (4.23) are solved simultaneously for similar set of transients to generate results for the dynamic phasor equivalent. The results for both the models are compared for the purpose of validation.

The current controller is capable of operating in two modes - current reference tracking and active power reference tracking. Additionally different types of dynamic phasors are captured and presented in the results. Similarities and advantages of the study performed as a part of this chapter in comparison with the inbuilt dynamic phasor solver available in MATLAB/Simulink is presented.

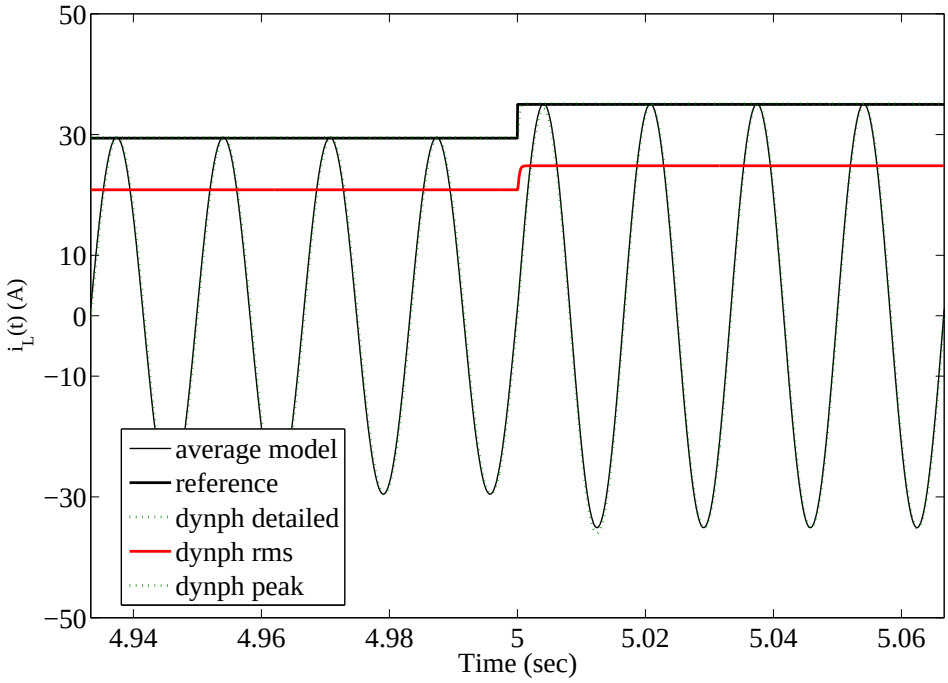

Figure 4.6 Waveforms of the inductor current presenting multiple types of dynamic phasors along with the average model for a step change in the current reference signal

Figure 4.6 presents the waveforms of the current through the filter inductor during a step change in the current reference signal from 29.45 Amps to 35 Amps at fifth second of the

simulation. Current waveforms of the cycle-by-cycle average model, detailed dynamic phasor model, peak dynamic phasor model, and rms dynamic phasor model has been furnished in Figure 4.6.

The SimPowerSystems toolbox of the MATLAB/Simulink contains an inbuilt dynamic phasor solver. The dynamic phasor model for the single-phase inverter is not present in the SimPowerSystems. Additionally the dynamic phasor model presented in this chapter can be used to capture multiple harmonics (various values of k) simultaneously, which is not possible in the inbuilt solver of Simulink. Furthermore the advantage with the model developed in this chapter is that the mathematical formulations of the inverter can be modeled in any other tool such as PSCAD, MODELICA.

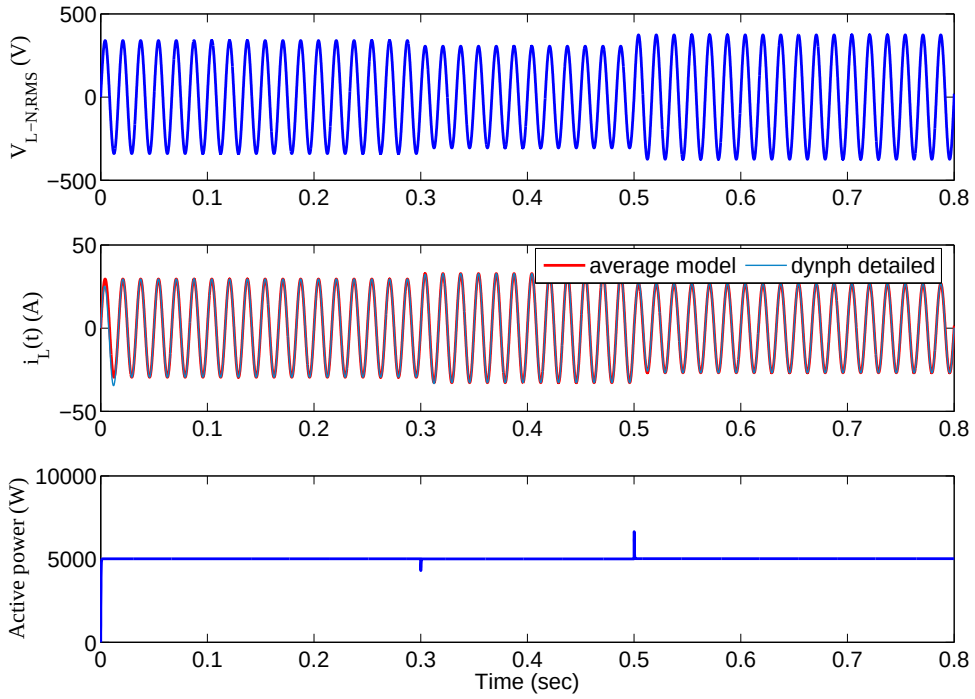

Figure 4.7 Waveforms of grid voltage, current through filter inductor, and active power during a voltage sag with active power set point

The behavior of the system during a sag in the grid voltage with an active power set point is captured in the Figure 4.7. Figure 4.7 compares the waveforms of the current through the filter inductor for the average model and the dynamic phasor model. The active power set point is set to 5 kW. Figure 4.7 clearly shows that the active power remains at the set point.

The simulation time of the dynamic phasor with the average model and the full switching model is also compared. Table 4.1 compares the simulation speed for the three models using various ordinary differential equation (ODE) solvers available in MATLAB/Simulink

Table 4.1 Simulation speed comparison between full switching model, average, and dynamic phasor model

Model	Simulation duration	Solver	Time step	Simulation time
Full switching	10 seconds	ODE45	1μ seconds	210 seconds
	10 seconds	ODE23t	1μ seconds	150 seconds
	10 seconds	ODE23s	1μ seconds	165 seconds
Average	10 seconds	ODE45	1μ seconds	75 seconds
	10 seconds	ODE23t	1μ seconds	40 seconds
	10 seconds	ODE23s	1μ seconds	38 seconds
Dynamic phasor	10 seconds	ODE45	1μ seconds	10 seconds
	10 seconds	ODE23t	1μ seconds	6 seconds
	10 seconds	ODE23s	1μ seconds	5 seconds

[19, 20]. The simulation time presented in the Table 4.1 clearly restates that the dynamic phasor is extremely competent compared to the other two.

The simulation time for the full switching and the average model raises drastically as the number of PV converters increase. For the case of large distribution feeders neither the full switching model nor the average model is practical for solving. The presence of large number of transmission lines and other power system equipments adds to the complexity. Modeling dynamic phasor equivalent for a complete distribution feeder will lead to extreme reduction in the consumption time.

5. Model Reduction and Dynamic Analysis using Transient Analysis Tool

5.1 Introduction

Modeling of distribution feeders in transient analysis tool is dealt in this chapter. Models in transient analysis tools can be used for studies such as - islanding protection, impact of cloud transients and simultaneous action from multiple correction devices. Quasi-static analysis is not capable of capturing all the impacts and the necessary transients. This imposes the need for modeling the large distribution feeders in transient analysis tools such as MATLAB/Simulink, PSCAD.

The quasi-static analysis is explanatory only if either the change in system state is relatively small or sufficient time interval has been chosen for the system to reach a steady state. Hence the accuracy of the study depends on the right choice between quasi-static and transient analysis. Electromagnetic Transient Programs (EMTP) are generally used for a detailed simulation of such fast electromagnetic transients. But with this note, performing a transient analysis on a large distribution system with high penetration of PV generators is extremely time consuming and impracticable.

For this purpose, the concept of dynamic phasors or time-varying phasors approach is used in this work [9, 14, 15]. The main idea behind this method is to represent the periodical or nearly periodical system quantities not by their instantaneous values but by their time varying Fourier coefficients (dynamic phasors). Dynamic phasors is based on a Fourier approximation of the system quantities.

The analysis of fast electromagnetic transients involve the computation of instantaneous values of voltages and currents. In comparison with the classical time domain analysis the dynamic phasor formulation has the advantage that the properties of the transients can be directly interpreted in terms of the envelop variation. The dynamic phasors based modeling technique is suitable for solving the large distribution system with high penetration of PV. The inbuilt phasor solver in MATLAB/Simulink will be used to solve the distribution feeder in Simulink.

Figure 5.1 presents the generalized framework of the modeling process. The modeling process starts from the GIS database. The proposed algorithm will read the GIS database, explore the structure of the feeder, and provide inputs as required for the transient analysis tool. Graph search algorithm will be extensively used for this purpose.

SimPowerSystems toolbox of MATLAB/Simulink has an inbuilt dynamic phasor solver. Hence the final model will be developed in MATLAB/Simulink using the SimPowerSystems toolbox. The main idea behind this work is the development of a non-heuristic network flow technique to model a large distribution system in the transient analysis tool.

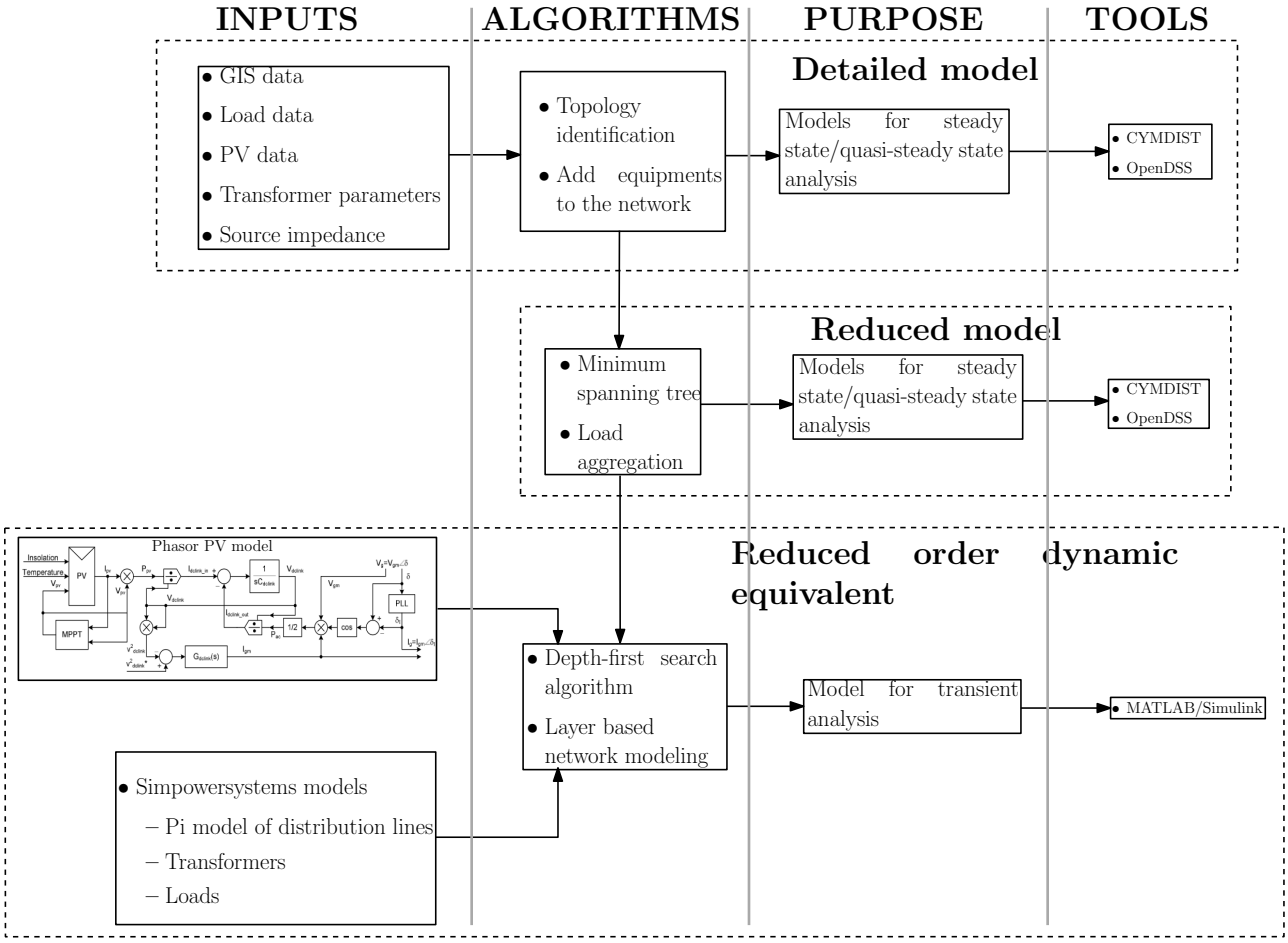

Figure 5.1 Generalized block diagram for modeling the distribution feeders in quasi-static and transient analysis tools

A typical distribution feeder consists of a primary three-phase line which runs through the complete feeder. Numerous single-phase laterals branch out of the primary three-phase line and eventually connects to the load centers. Detailed modeling of the three-phase lateral in a distribution feeder is crucial, whereas modeling of each and every single-phase lateral may be avoided. Detailed modeling of the complete distribution feeder will add to a lot more complexity and time for the electromagnetic transient program. Therefore identifying efficient ways to develop reduced dynamic equivalent of distribution feeder is required. For this purpose graph search algorithm based on minimum spanning tree will be used. The details of the algorithm will be presented in the following sections. A graph search algorithm based on depth-first search will be used to model in reduced distribution feeder in an appropriate transient analysis tool. A detailed literature search specific to modeling in the transient analysis tools is presented.

5.1.1 Literature search on network reduction of distribution feeders

Literature search can be dealt in two separate topics, developing reduced network for the distribution feeder and the modeling the reduced network for dynamic analysis. Very few published material can be even found on the topic of modeling the network for dynamic analysis. Whereas topics on network reduction is an old and frequently visited topic.

Even though a detailed work on the reduction of network was published in 1949 [21], the network reduction has been revisited on regular intervals over time [22–24]. Network-reduction techniques has always been applied for multiple reasons in the area of power systems. Generally, investigation of dynamic behavior of large power systems requires the usage of reduced order systems. Some of the major applications are

- Transmission expansion planning
- Capacitor bank placements for reduced losses
- Reconfiguration of distribution feeders for better performance

Usually, in all the existing techniques, a power system is partitioned into two areas during dynamic reduction - the study area which contains the variables of interest, and therefore it is represented in a detailed manner; and the external area which is represented in reduced form by a linear system. The dynamic reduction of the power system model can also be divided into three stages: coherency identification, generator aggregation, and network reduction [25].

From the description above, most of the reduction techniques which are referred to as classical, are heuristic (experience-based) or semi-heuristic. These methods have been developed for transmission systems with multiple synchronous generators, physically distant. However this work concentrates on the distribution systems and involves modeling of large numbers of distributed PV generators. Use of power electronics based converters makes them impossible to aggregate, as opposed to the synchronous generators. The term, coherency, widely adopted by traditional reduction methods becomes not so meaningful since PV generators have power electronics interfaces. Obviously, these methods might give very rough approximation in case of dynamic analysis of complex power systems with PV. Therefore different techniques should be looked upon for distribution network reduction with PV generators.

Reference [25] provides an approach for dynamic reduction of distribution networks with dispersed generation. This reference presents the usage of Singular Value Decomposition (SVD) with Hankel norm approximation to achieve the same. But, the end application is for a test system with only induction generators (wind systems) as dispersed generators and neglects the PV generators. Similar application of network reduction can be found in the reference [26]. Reference [26] focuses the attention onto synchronous generators and disregards the participation of power electronics interfaced renewable sources for system studies.

A similar intention to the proposed technique in this work, as opposed to previous references, has been mentioned in the reference [27]. Network reduction algorithm based on grouping of nodes is proposed in reference [27]. The distinction is that the grouping in [27] will be decided based on congestion studies. Reference [28] proposes a technique for network reduction but the study is confined to reduction in solving times and the proposed technique is predominantly heuristic and data specific.

5.1.2 Analogy between trees and distribution feeders

Network flow algorithms are extensively used for network reduction and modeling in transient analysis tools. The analysis of the structure of a distribution feeder can be skillfully performed using network-flow algorithms [29]. Basic components of a graph includes edges and vertices. An edge in a tree is equivalent of a section in a feeder and a vertex is analogous to a bus/node in a distribution system. Since data for large distribution systems are shared in the GIS form, application of graph algorithms for understanding the structure of the distribution system is direct and necessary. A typical distribution feeder consists of the following

- Three-phase primary main feeder
- Three-phase, two-phase (V phase), and single-phase laterals
- Step-type voltage regulators or load tap changing transformer (LTC)
- Shunt capacitor banks
- Three-phase, two-phase, and single-phase loads
- Distribution transformers (step-down to customers voltage)
- Distributed PV generators (stand-alone or grid-connected)

After the network reduction all the details as listed above needs to be retained for rebuilding the feeder in the quasi-static analysis tool(CYMDIST). The proposed algorithm and the process of rebuilding the feeder from the reduced adjacency list will be described in the following section.

5.1.3 Differences between modeling in distribution system analysis tool and transient analysis tool

The modeling procedure in a distribution system modeling tool is non-hierarchical. x-y coordinates of each node, incidence list of each edge with additional system specific information such as phase of each section, transmission line codes make the network complete. Well defined network flow techniques such as minimum spanning tree, shortest path algorithms are sufficient to this purpose. Confirming that all the sections and nodes are covered in any random order is sufficient.

In a transient analysis tool the order of connectivity plays an important role. The order of the edges needs to be retained. The network search algorithm capable of retaining the

hierarchy is necessary. For this purpose depth-first search algorithm is used. The terminology used in this chapter is as follows:

- Distribution feeder is referred to as a graph
- Section in a distribution feeder is referred to as an edge in a graph
- Node in a distribution feeder is referred to as vertex in a graph

5.2 Proposed approach for dynamic analysis

This section details out the approach for modeling the distribution feeder in a transient analysis tool. The development of the of the distribution feeder mainly uses three algorithms as follows:

- Topology identification [30].
- Network reduction
- Modeling in transient analysis tool.

The complete procedure has been diagrammatically displayed in Figure 5.1. Algorithm for the identification of the topology has been briefly explained in Section 3.3. The algorithm for topology identification has been principally referred from reference [30]. The algorithms for network reduction and modeling in transient analysis tool is developed from the conception. The following two subsections elucidates on the procedure of network reduction and dynamic model respectively.

5.2.1 Algorithm for network reduction

This subsection proposes an efficient way to develop a reduced dynamic equivalent of the distribution feeder. The purpose behind the network-reduction is to develop a reduced distribution system to facilitate dynamic analysis of the feeders with high penetration of PV generators. For the purpose of validating the proposed network reduction technique a test-bed containing 4000 sections, 921 spot loads, 107 PV inverters is chosen.

Even though, techniques have been developed to reduce the inherent switching complexities in the modeling of single-phase and three-phase PV inverters, the presence of large number of sections, transformers and loads in the distribution feeders still pose an issue. The issue of modeling a large distribution feeder becomes evident while modeling in transient analysis tools; such as MATLAB/Simulink and PSCAD. This study proposes a network-reduction technique by using Minimum Spanning Tree (MST) algorithm by considering the distribution feeder as a rooted free tree. The highlights of the proposed technique is as follows.

- The algorithm identifies the nearest three-phase section for each load and PV generator.
- Aggregates all the loads for each phase and links it to the nearest three-phase section

- Retains all the loads which have PV generators associated. PV generators are retained since the final goal is to study the dynamic impact of PV inverters on the distribution system.

Proposed algorithm

This section describes the proposed technique. A network flow algorithm has been applied for the purpose of network reduction. Minimum Spanning Tree (MST) has been used for this endeavor. The first algorithm for finding a minimum spanning tree was developed by Czech scientist, Otakar Borvka, in 1926. The purpose was finding an efficient electrical coverage of Moravia, Czech Republic. Even now MST is applied by some utilities . MST is typical example for greedy algorithms that run in polynomial time. Even though the content was initially published in 1926 in a non-English journal, the same work was recreated in English and re-published [31, 32].

Fundamental application of the network-flow technique is finding the shortest path between two nodes of interest (with path length measured by number of edges). A distribution feeder is an example of a directed unweighted graph. Searching a graph involves systematically following the edges of the graph so as to visit all the vertices. Graph-search algorithm can discover the structure of the graph.

Trees can also be traversed in multiple ways, but minimum spanning tree is based on level-order; where every node on a level is visited before going to the next level. This work implements Prim's algorithm for minimum-spanning-tree. Even though minimum-spanning-tree algorithm are of multiple kinds, Prim's minimum spanning tree algorithm has been used in the work. Prim's algorithm is a special case of the generic minimum-spanning-tree algorithm based on breadth-first search. Operation of Prim's algorithm has similarity with Dijkstra's algorithm for finding the shortest paths in a graph.

Typically distribution feeders are radial in structure and a single source exists for all the loads. Hence applying the minimum-spanning-tree algorithm to a radial distribution feeder results in identifying the existing single path. The tree starts from an arbitrary load section (edge) and grows until the tree spans all the edges in the lateral. In the process of spanning, all the loads and the PV's are identified and analyzed. Loads without any PV generators will be aggregated whereas the loads with the PV generators will be retained.

During the execution of the algorithm, all the edges which are non-loads and non-PV generators reside in a priority queue. At every iteration the child edges will be enqueued onto the priority queue. The exit condition for the algorithm is when the priority queue lacks new entries. This algorithm uses a first-in, first-out queue. This algorithm operates completely based on the edges (section numbers).

Procedure of the algorithm

Algorithm 1 presents the algorithm implemented in MATLAB script in a concise manner. The procedure of the algorithm are as follows. Lines 1-3 set the parent of every

```
foreach section s do
| π[s] ← NIL
end
Q ← u
while Q ≠ ∅ do
| s ← head[Q]
| foreach v ∈ Adj[s] do
| | if v ∉ Q & v ∉ L & v ∉ P & v ∉ s_three_phase then
| | | π[v] ← s
| | | Enqueue(Q, v)
| | end
| | if v ∈ L then
| | | Enqueue(L_test, v)
| | end
| | if v ∈ P then
| | | Enqueue(P_test, v)
| | end
| end
| foreach v ∈ Adj[s] do
| | if v ∈ s_three_phase then
| | | [v] ∈ s_three_phase
| | end
| | Enqueue(junction_section, s)
| end
| Dequeue(Q)
end
```

Algorithm 1: Algorithm used to implement the minimum-spanning-tree for the distribution feeder

edge to be NIL. Line 4 initializes Q to the queue just containing the edge u; thereafter Q always contains the set of edges to be read in consequent iterations. The main loop of the program is defined in lines 5-26. The loop iterates as long as there remains edges unread, which are discovered edges that have not yet had their adjacency lists fully examined. Line 6 determines edge s at the head of the queue Q. The for loop of lines 7-18 considers each edge v in the adjacency list of s. If v is not a load section, not a PV generator section, and not a three-phase section then it is enqueued at the tail of the queue Q. Then, s will be recorded as its parent. Algorithm 1 acts as the stage I for the complete process. Stage I explores the single-phase laterals and keep track of loads and PV generators. The final outcome of stage I are as follows.

1. value of aggregated single-phase loads of phase A lateral, nearest junction section of the three-phase lateral

2. value of aggregated single-phase loads of phase B lateral, nearest junction section of the three-phase lateral
3. value of aggregated single-phase loads of phase C lateral, nearest junction section of the three-phase lateral
4. section numbers of the PV generators on phase A lateral, nearest junction section of the three-phase lateral
5. section numbers of the PV generators on phase B lateral, nearest junction section of the three-phase lateral
6. section numbers of the PV generators on phase C lateral, nearest junction section of the three-phase lateral

Rebuilding the reduced-order distribution system is identified as Stage II. Since the x-coordinates and the y-coordinates for the aggregated loads are unknown, an algorithm for the calculation of x-coordinates and y-coordinates has been developed. The key steps are as follows

- Retain the details of bus coordinate configuration, section configuration, line configuration for three-phase components.
- For loads without associated PV generators - create a new entry for distribution transformer (entries should appear in bus coordinate configuration, check that from code), create a new entry for the aggregated load.
- For loads with an associated PV generator - update the previously existing x-coordinate, y-coordinate entries for the distribution transformer, load and the PV generator.

5.2.2 Algorithm for modeling in transient analysis tool

This subsection implements a depth-first search algorithm for modeling a distribution feeder in a transient analysis tool. The concept followed by the depth-first search is to search deeper in the graph. The edges are explored out of the most recently discovered edge that still has unexplored edges leaving it. The identified new edge will be placed as the child edge in the adjacency list. Only one edge adjacent to the parent edge will be recorded in the adjacency list. The predecessor subgraph produced by depth first search may be composed of several trees [29]. When all the succeeding edges have been explored, the search backtracks to explore the edges excluding the edge from which the rest was discovered. If any undiscovered edges remain the undiscovered one will be selected as a new source and search is repeated from that source. The entire process is repeated until all the vertices are discovered.

The pseudo code presented in the Algorithm 2 has been implemented in the MATLAB programming language to develop the feeder in the transient analysis tool (Simulink). The procedure is as follows. Lines 2-6 initializes the parent for each section to nil and resets the queues $Q1$ and $Q2$. Lines 7-10 checks each section in the distribution feeder and if the section is not present in the queue $Q1$ calls the subroutine SUB DFS(s). The subroutine SUB DFS(s) is a recursive subroutine.

MAIN DFS
foreach *section* s **do**
  $\pi[s] \leftarrow NIL$
end
$Q1 = \emptyset$
$Q2 = \emptyset$
foreach *section* s **do**
  if $s \notin Q1$ **then**
    SUB DFS(s)
  end
end
SUB DFS(s)
Enqueue($Q1, s$)
foreach $v \in Adj[s]$ **do**
  if $v \notin Q1$ **then**
    $\pi[v] \leftarrow s$
    SUB DFS(v)
  end
  Enqueue($Q2, s$)
end

Algorithm 2: Algorithm used to develop a model in the transient analysis tool

The functionality of the subroutine SUB DFS(s) is as follows. The edges are explored out of the most recently discovered edge that still has unexplored edges leaving it. In the process of exploring all the edges leaving the parent, s, the parent will be enqueued into $Q1$. After all the edges are explored the parent edge will be enqueued into $Q2$. Line 13 enqueues s to the $Q1$. Queuing the section s in the queue $Q1$ avoids reentry of data in the final adjacency list. The connectivity of the original graph is available as an incidence list. An incidence list consists of all the edges storing its incident vertices. The list of adjacent edges will be extracted from the incident list and the subroutine SUB DFS(s) is recursively called for each edge leaving the vertex. After exploring all the edges downstream the section s will be enqueued into the queue $Q2$.

5.2.3 Model development in Simulink

MATLAB scripts have been used to configure the model in Simulink. The procedure for developing the model in Simulink is entirely automated. The pseudo code presented in the algorithm 1 and 2 is seamlessly merged with the configuring tools of Simulink to develop the model from GIS database. SimPowerSystems toolbox has been extensively used for this purpose. Additionally the models of PV inverters presented in Section 4.2 are also included from an external source.

The overall modeling procedure is performed based on a multi-layer approach. The first layer involves the implementation of the distribution lines along with the source. The MATLAB script retains the details of the loads and the PV generators without modeling them in the Simulink model along with the distribution lines at the first layer.

Subsequent to the modeling of the distribution lines, loads will be modeled as a part of the second layer. As a third layer PV generators will be included in the transient model. The model of the PV generator is as shown the Figure 5.1. The model of the PV generator compliant with the phasor simulator is referred from the reference [4]. The model of the PV generator implements the incremental conductance theorem with a voltage controller acting as a maximum power point tracker. The PV generator also contains a low bandwidth voltage controller for the DC link voltage along with a Phase Locked Loop (PLL). The view of the feeder in Simulink at different parts of the feeder is presented in Figure 5.2.

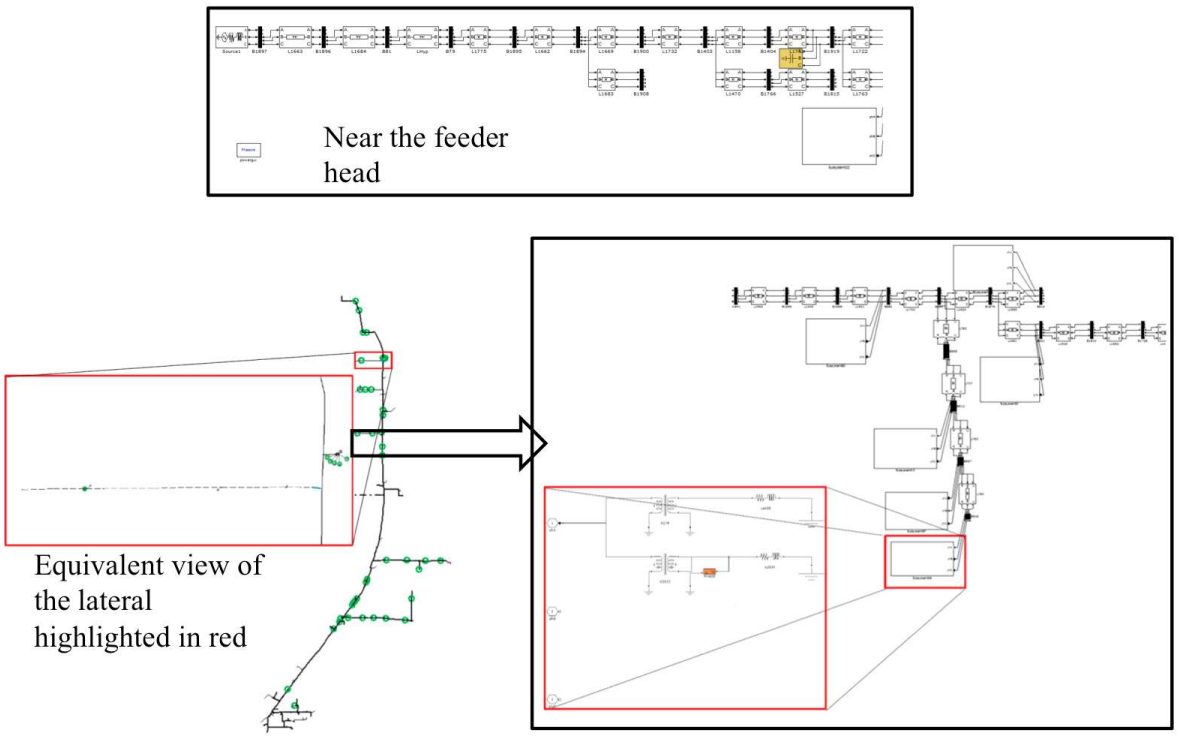

Figure 5.2 View of the distribution feeder in Simulink

5.3 Results and validation

This section presents the necessary results to validate the operation of the previously explained algorithms. The results will be presented in two subsections. The first subsection pertains to the network reduction and the second subsection pertains to the validation of the dynamic model.

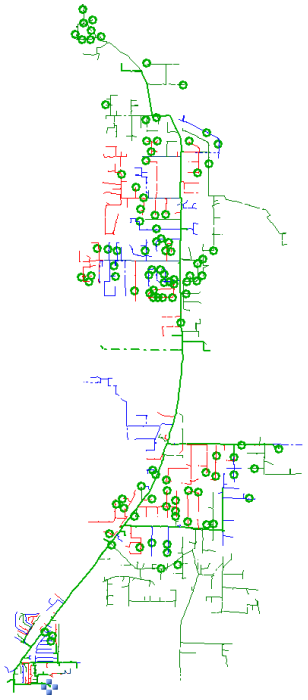

Figure 5.3 Feeder diagram of the original feeder

5.3.1 Results pertaining to network reduction

Table 5.1 compares various details of the test feeder before and after the application of network reduction. From the values in the Table 5.1 significant reduction in the number of nodes, sections, transformers and loads can be observed. As mentioned in the beginning of this chapter, since the goal is to study the impact of the PV generators, all the PV generators are retained. Figures 5.3 and 5.4 furnishes the view of the test feeder in CYMDIST before and after the network reduction respectively. Green circles in the Figure 5.7 depict the PV generators in the feeder.

Table 5.1 Effect on network reduction aspects of the distribution feeder

Feeder details	**Original network**	**After network reduction**
Number of nodes	3032	738
Number of sections	4094	1142
Number of Transformers	929	174
Number of PV generators	107	107
Number of Loads	921	287

Based on the values in the Table 5.2 it can be clearly observed that the network reduction technique has retained majority of the critical feeder details. The test feeder under consideration has large number of the three-phase segments as overhead lines and

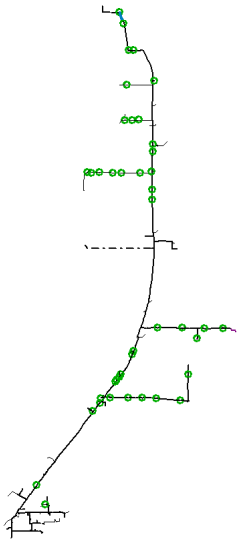

Figure 5.4 Feeder diagram after applying the network reduction

all of the single-phase laterals as underground cables. Since the network reduction largely cuts down the single-phase laterals, i.e. underground cables, the line capacitance decreases in the reduced network. Since the number of distribution transformers are largely reduced the losses due to the transformers are also affected. Figures 5.5 and 5.6 provide the voltage profile of the original and the reduced network respectively.

Table 5.2 Performance details of network reduction on the distribution feeder

Feeder details	**Original network**	**After network reduction**
Current drawn from the substation (Amps)	226.9(Phase A), 284.9(Phase B), 246.1(Phase C)	231.7(Phase A), 281.8(Phase B), 251(Phase C)
Line losses (kW)	119.97	118.07
Cable losses (kW)	4.74	3.27
Transformer losses (kW)	57.29	15.55
Line losses (kVar)	310.66	309.52
Cable losses (kVar)	2.93	2.19
Transformer losses (kVar)	108.18	15.34
Line capacitance (kVar)	16.63	12.80
Cable capacitance (kVar)	340.74	55.27

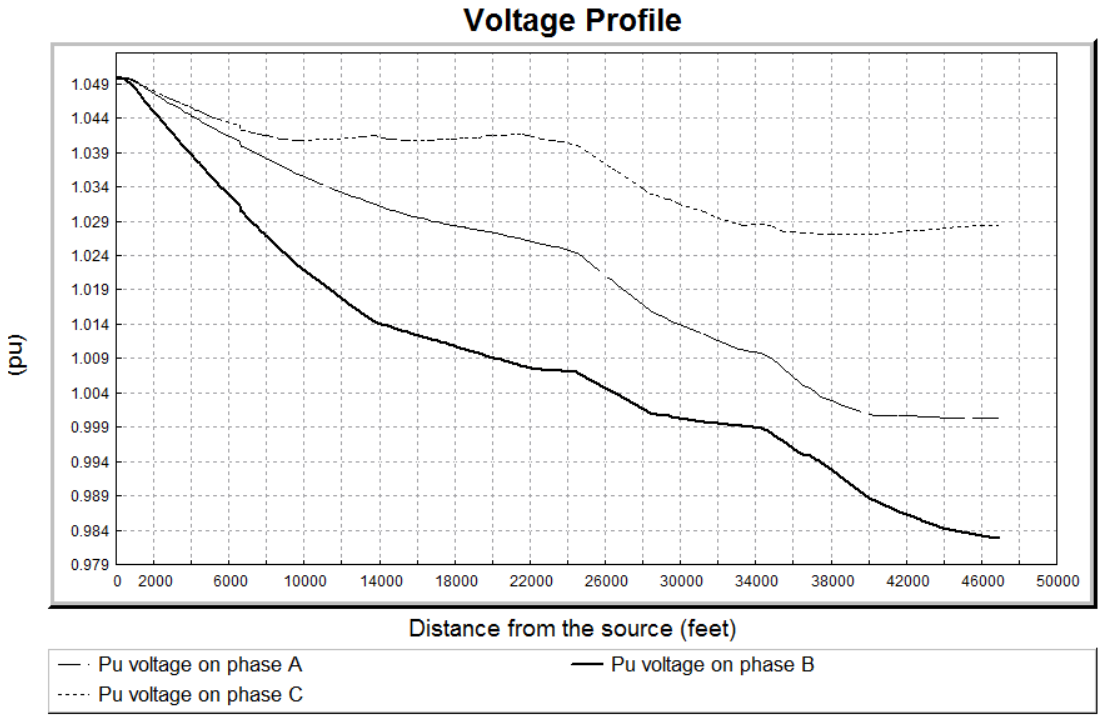

Figure 5.5 Voltage profile for the original network

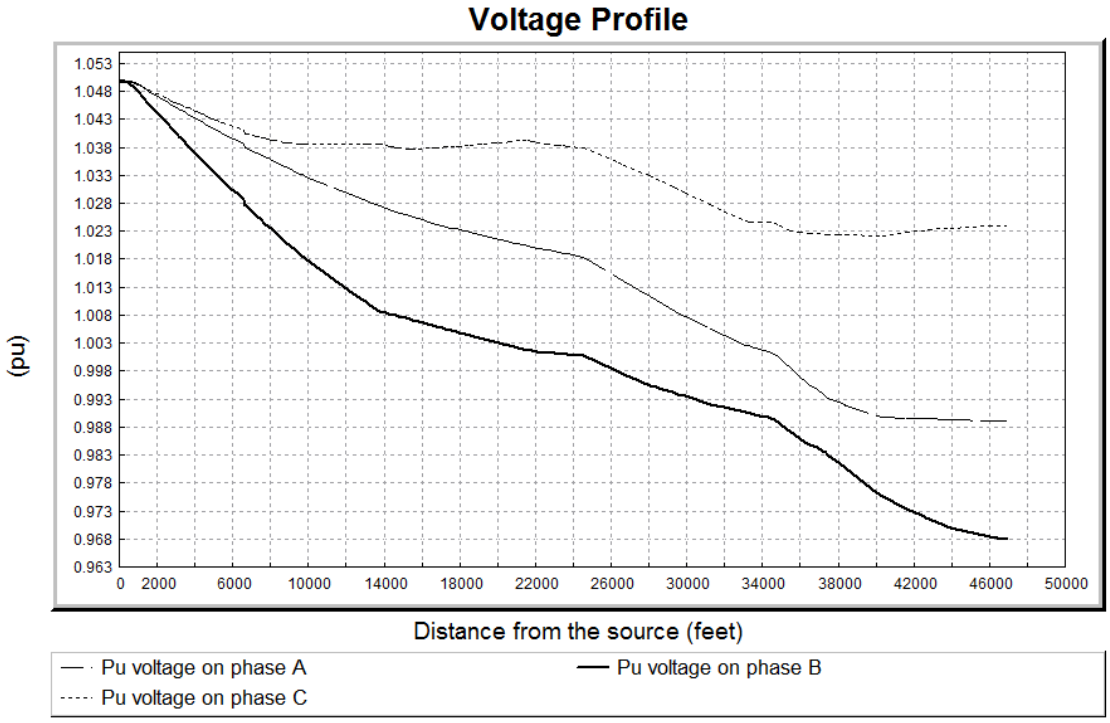

Figure 5.6 Voltage profile for the reduced network

5.3.2 Results from Dynamic Analysis using Reduced Model pertaining to dynamic model

The original feeder (Figure 5.3) after the network reduction (Figure 5.4) will be modeled in the MATLAB/Simulink based on the algorithm defined in the Section 5.2.2. The developed model will be simulated for various scenarios with the results presented in the following sections.

Validation of the transient model

Table 5.3 compares the values of the voltages and the currents for the test feeder model in the transient analysis tool with those of the quasi-static analysis tool. The feeder model in the transient analysis tool will be verified with the results of the quasi-static analysis tool CYMDIST for one of the common cases. The model of the feeder in the transient analysis tool is provided enough time to reach a steady-state and for the same load condition the values of voltages and currents are captured in the quasi-static analysis tool. Table 5.3 compares the values of the currents and voltages at various points of the test feeder. The physical location of the measurement points has been highlighted in the Figure 5.7.

Table 5.3 Comparison of measured power system quantities (voltage and current) from CYMDIST and MATLAB/Simulink

DAS number	CYME						MATLAB/Simulink					
	Voltage (kV)			Current (A)			Voltage (kV)			Current (A)		
	A	B	C	A	B	C	A	B	C	A	B	C
-	7.2	7.2	7.2	189.4	251.5	209.1	7.2	7.2	7.2	187.38	247.5	208.6
DAS 6	7.2	7.1	7.2	172.7	229.2	174.4	7.2	7.16	7.2	167.93	215.2	178.2
DAS 5	7	6.9	7.1	91.4	103.4	58.6	7.04	7	7.15	97.4	110.4	65.3
DAS 4	7	6.9	7.2	9.4	9.4	12.9	6.999	7	7.2	8.48	8.5	8.13
DAS 3	6.9	6.8	7.1	77.7	54.1	72	6.9	6.89	7.1	75	55.05	77.7
DAS 2	6.8	6.7	7	55.6	49.9	19.6	6.8	6.7	7.05	52.32	53.98	21
DAS 1	6.8	6.6	7	1.3	26.2	0.2	6.79	6.6	7	1.414	33.9	0.67

The inbuilt phasor solver as a part of SimPowerSystems toolbox of MATLAB/Simulink will be used for solving the test feeder. The complete time domain simulation for one cycle (20 ms of simulation time) requires 5 days of CPU time whereas phasor simulation needs 15 minutes of CPU time for 70 seconds of simulation time. Phasor solvers are suitable for solution of large systems. The test feeder was solved for a sequence of transients to validate the system. The sequence of events are as follows:

- Simulation of a cloud transient - variation of the solar irradiation from 100% to 40% in a ramp of 1 second for the two large three-phase PV generators at the 35th second.

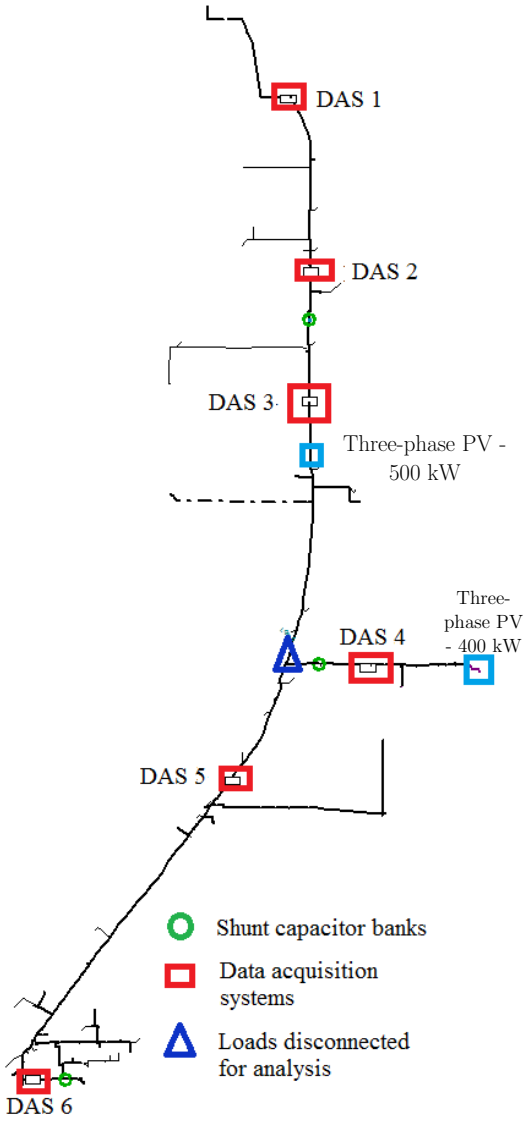

Figure 5.7 View of the test feeder from a quasi-static analysis tool (CYMDIST)

- Simulation of a cloud transient - variation of the solar irradiation from 40% insolation to 70% insolation in a ramp of 3 second for the two large three-phase PV generators at the 45th second.
- Simulation of load shedding - Shedding of 500 kW of loads (120 kW in Phase A, 280 kW in Phase B, and 100 kW in Phase C) at the 55th second.
- Adding back the 500 kW of loads (which were disconnected previously at the 55th second) at the 65th second.

The loads which gets shed at the 55th second of the simulation and get connected back are highlighted in the Figure 5.7. Figures 5.8 through 5.10 present the voltages and currents at various points of the test feeder during the sequence of transients as previously listed. In comparison with the classical time domain analysis the dynamic phasor solution directly

interprets the voltages and currents in terms of the envelop variation. The lines which can be witnessed in Figures 5.8 through 5.10 are the peak values. Figure 5.8 furnishes the waveforms of the voltages and currents at the feeder head. Figure 5.9 present the waveforms of the voltages at the DAS 2 and DAS 4 located near the shunt capacitor banks. Figure 5.10 shows the waveforms of the voltages and currents at the DAS 5.

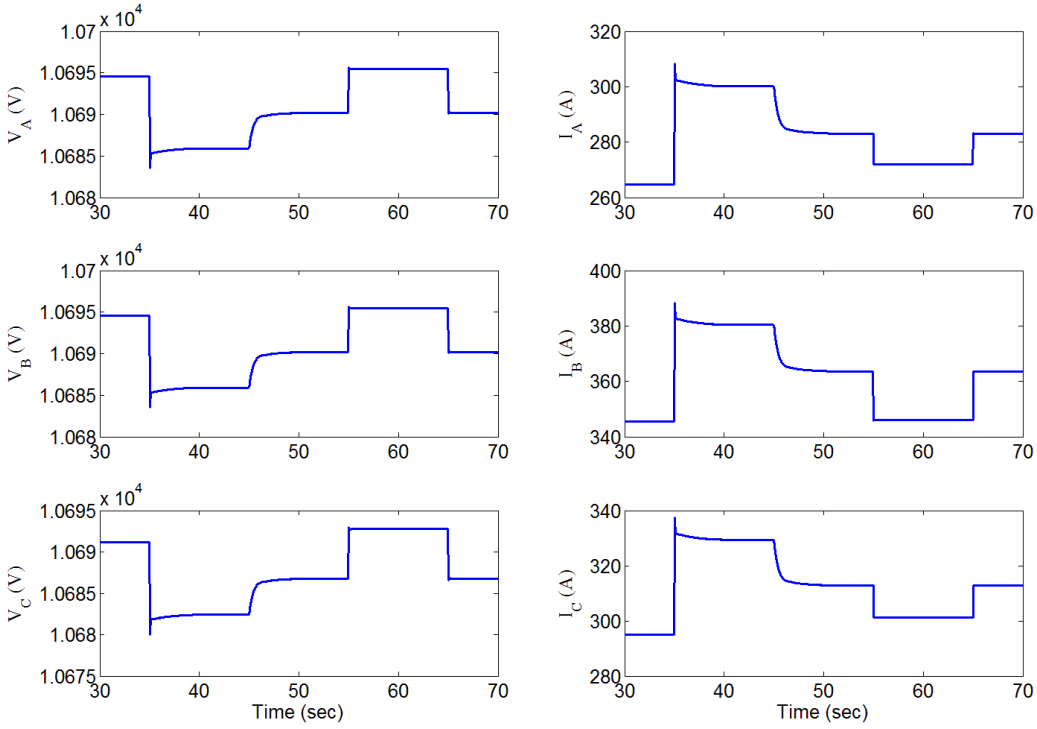

Figure 5.8 Waveforms of voltages and currents for each phase at the feeder head.

Impact of fast changes in solar irradiance

This section presents the results for fast changing cloud transients. This section presents the set of results of the distribution feeder with the solar irradiation varying at regular intervals as a random number. The solar irradiation is generated by a random signal generator as presented in Figure 5.11. The associated variation of the voltages and currents at the feeder head and capacitor banks are furnished in the Figures 5.12 and 5.13 respectively.

Voltage control by three-phase PV generators

The effect of reactive power control by the three-phase PV generators is studied in this section. The effective interaction of the controllers of the PV generator with that of the capacitor banks is studied. The impact of the capacitor bank switching with and without the voltage regulation feature in the PV generator will be presented in the results. Figures 5.14 through 5.17 belong to this section. Figures 5.14 and 5.15 present the capacitor

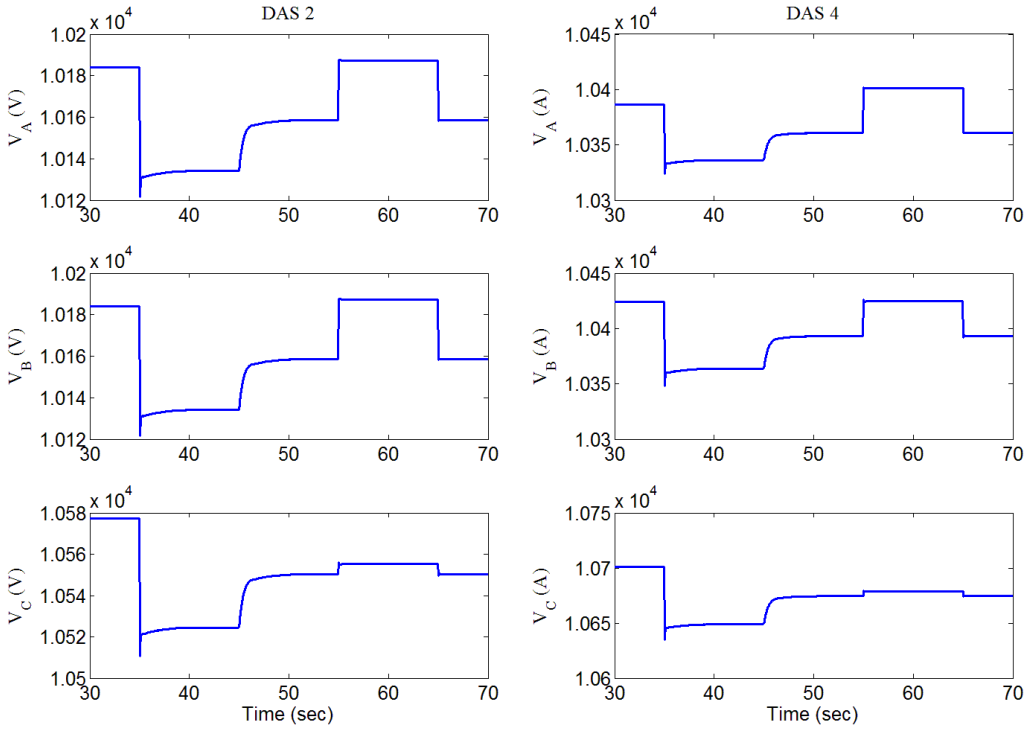

Figure 5.9 Waveforms of voltages for each phase at DAS near capacitor banks.

bank switching and the voltages respectively without voltage regulation from the two large PV generators. Figures 5.16 and 5.17 present the capacitor bank switching and the voltages respectively with voltage regulation from the two large PV generators. The voltage regulation by the large PV generators avoids the switching of the shunt capacitors.

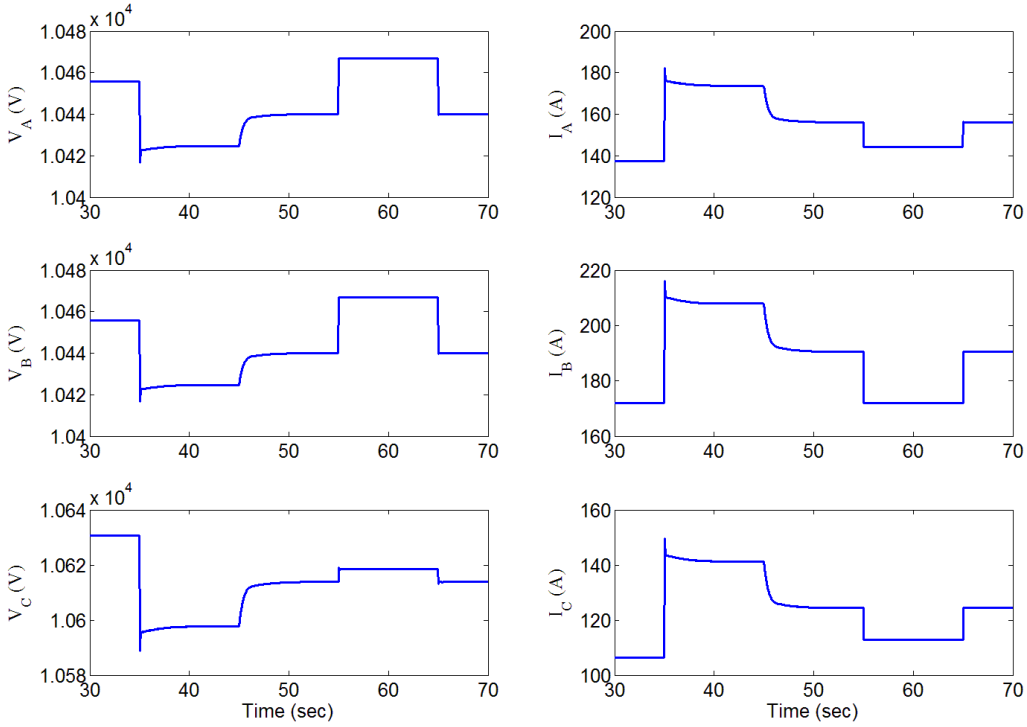

Figure 5.10 Waveforms of voltages and currents for each phase at the DAS 5

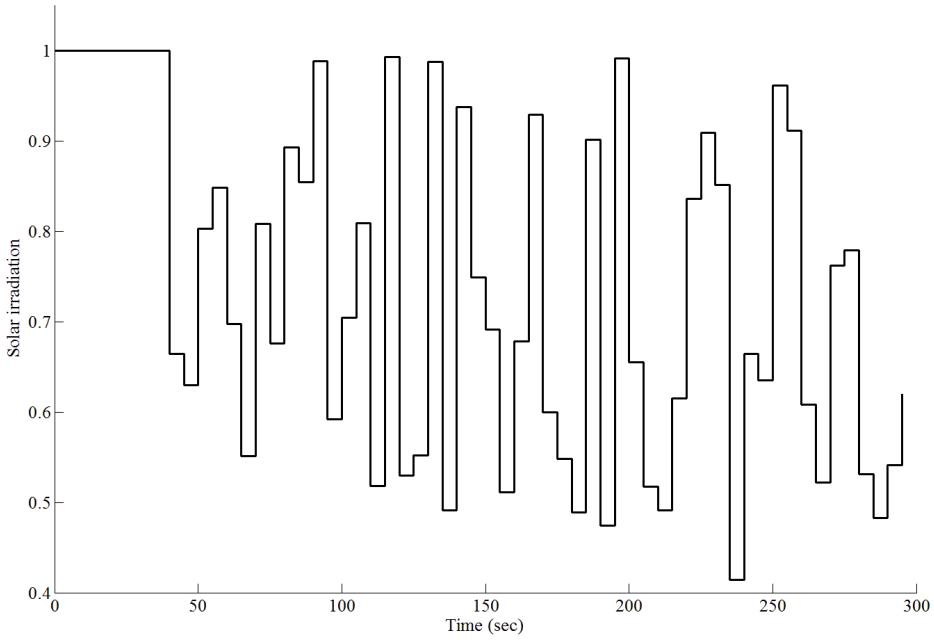

Figure 5.11 Solar irradiance as a random signal between 1 and 0.4 (p.u.)

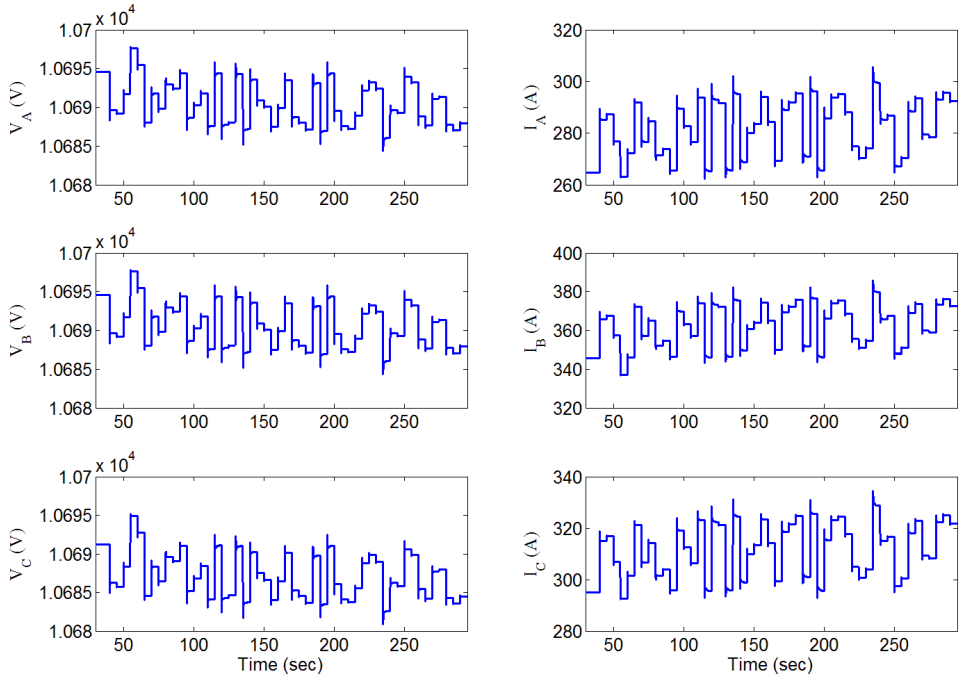

Figure 5.12 Voltages at the feeder head with solar irradiance varying as a random signal

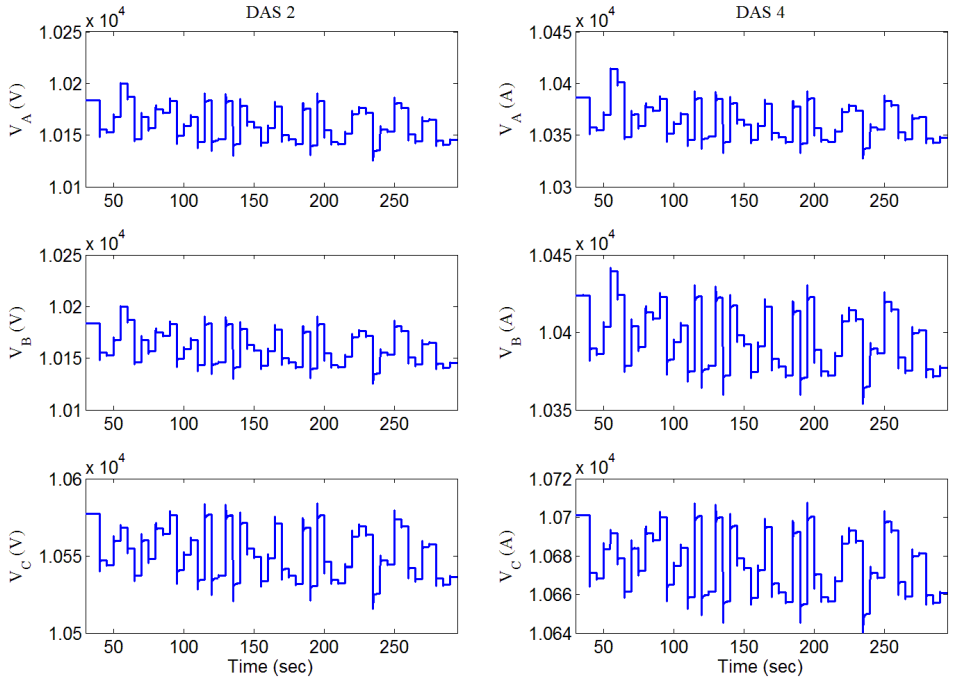

Figure 5.13 Voltages near the capacitor banks with the solar irradiance varying as a random signal

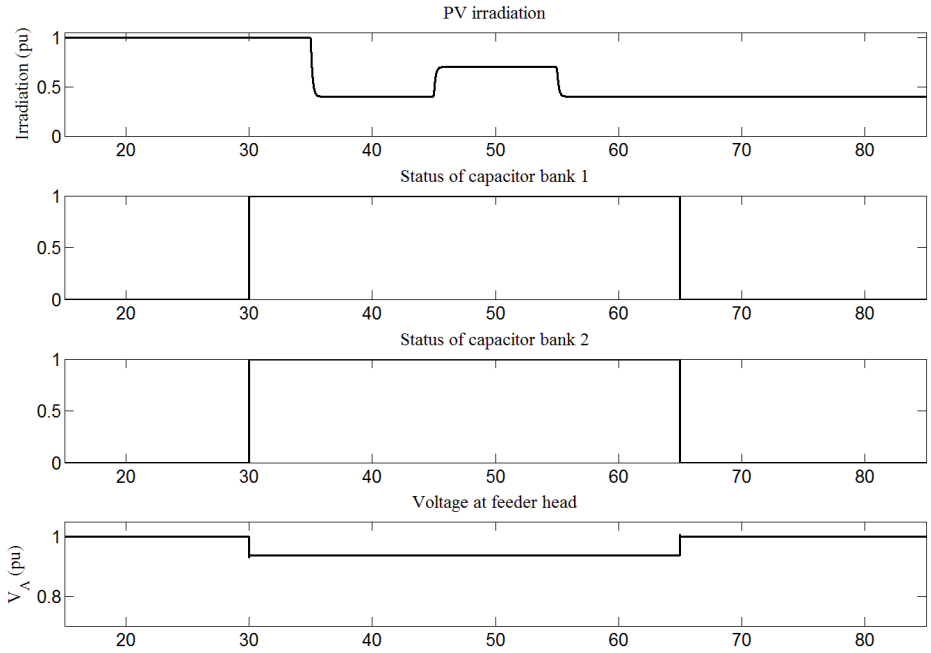

Figure 5.14 Effect on capacitor bank operation without voltage control feature of two three-phase PV generators

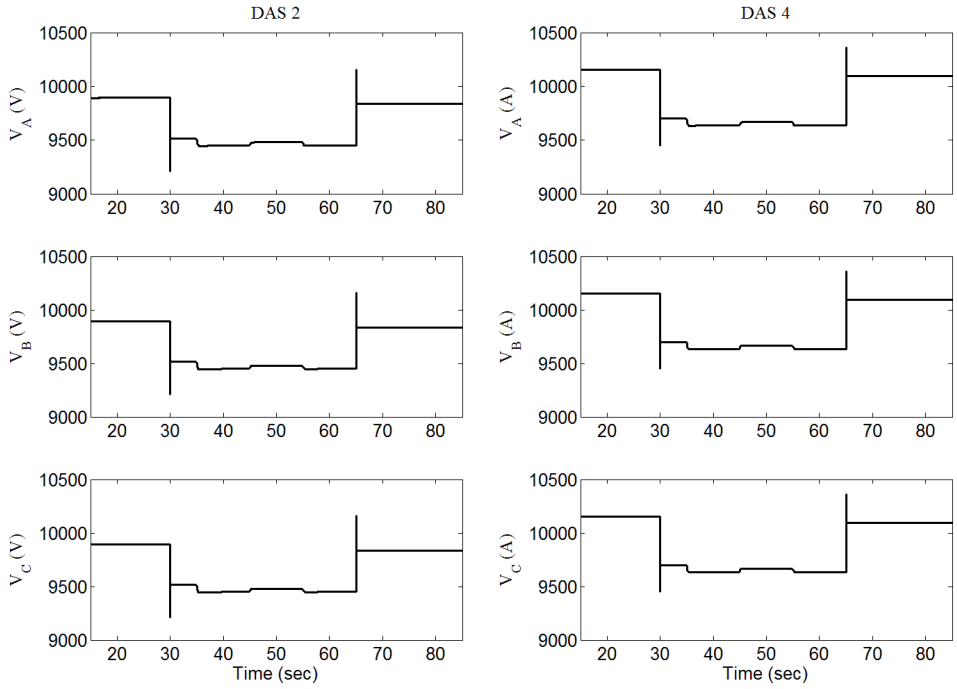

Figure 5.15 Effect on capacitor bank voltage without voltage control feature of two three-phase PV generators

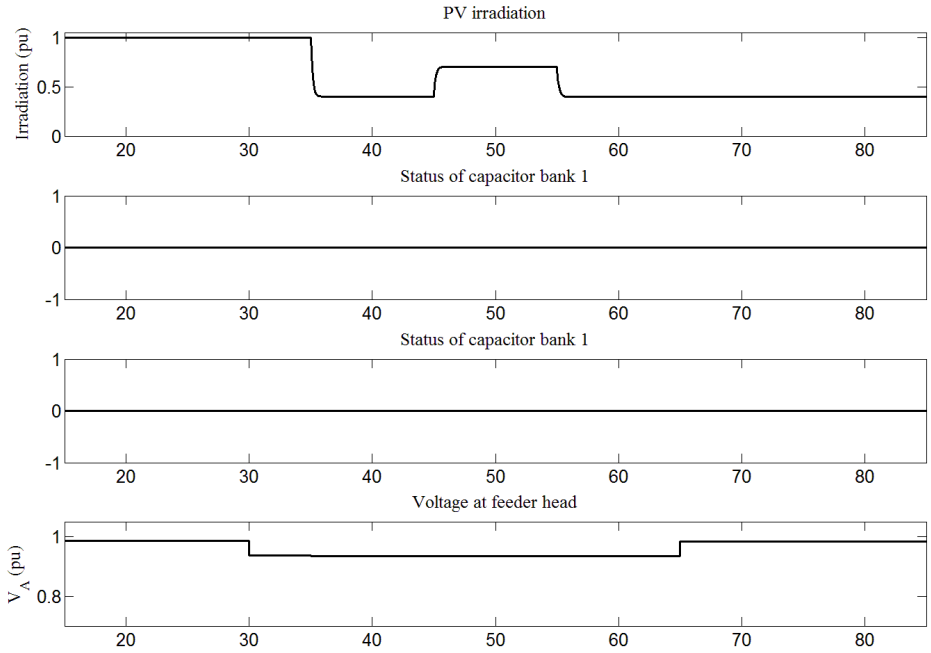

Figure 5.16 Effect on capacitor bank operation with voltage control feature of two three-phase PV generators

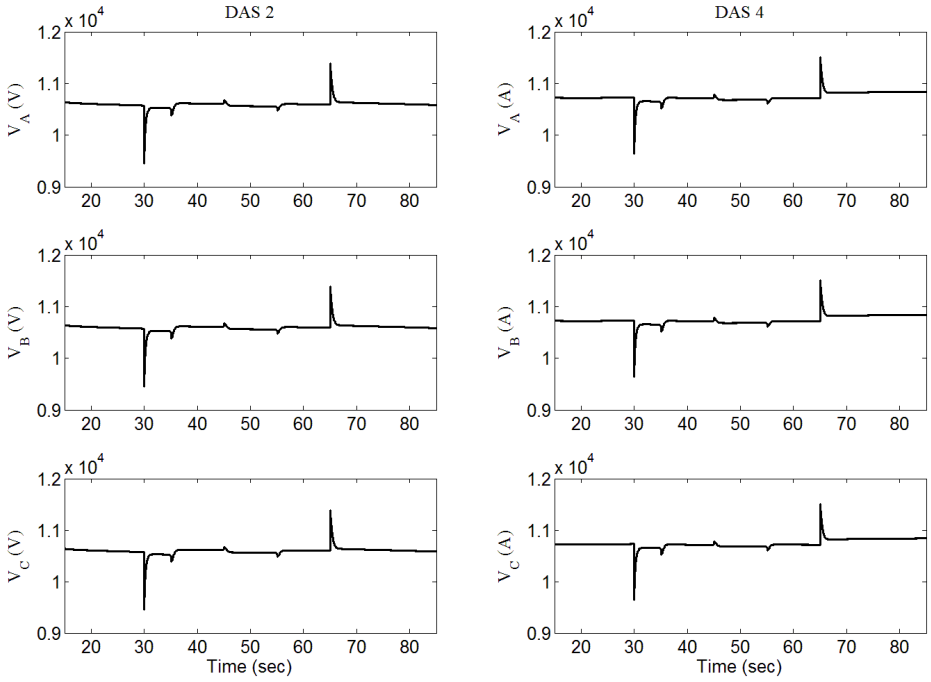

Figure 5.17 Effect on capacitor bank voltage with voltage control feature of two three-phase PV generators

6. Conclusions

This research work contributed to the development of models, algorithms and analytical features for distribution system analysis tools that will be essential for studying the impact of distributed PV generation, and eventually aiding in the design and operation of distribution systems with high penetration of PV. Following a careful gap analysis on the existing analytical tools, the research focused on three major areas: (1) development of automated procedures and algorithms for creating the complete feeder network and equipment model starting from a utilitys GIS database, and (2) development of network reduction techniques, and algorithms for automated implementation of the feeder model in transient analysis tools, and (3) development of suitable models, especially for PV power converters, and methods for dynamic analysis using the concept of dynamic or time-varying phasors implemented in conventional transient analysis tools.

The proposed techniques and the developed scripts were used to generate a detailed model of an actual feeder in Arizona where high penetration PV has been implemented. The feeder model is developed directly from extensive GIS database and is used to conduct time series analysis in OpenDSS for several case studies. The results for the quasi-static analysis matched well with the filed measurements made available from an extensive network of field data acquisition systems. The quasi-static analysis on the complete feeder model including detailed secondary model can be used to obtain the impact of different levels of PV penetration and for analyzing several what-if scenarios. The network reduction techniques based on graph search algorithms were applied on the same feeder model and the reduced network model was transferred to Simulink/SimPowerSystems using the developed automated methods. The developed models and algorithms can be used for dynamic analysis of realistic distribution feeders or larger distribution systems over long intervals of time. The details of control functions of the distributed PV inverters can be incorporated in this model, and the potential for control interactions can be studied. Several test cases for transient conditions corresponding to various cloud induced transients and load shedding were simulated and presented in this report.

In terms of future work, the dynamic phasor models of specific loads can be derived and used to perform a more accurate transient analysis. In the present study, the control characteristics of all the distributed PV inverters have been modeled to be identical. More accurate representation of the different control characteristics corresponding to different manufacturers will yield more accurate results and confidence in the analyses, especially for studies related to unintentional islanding protection and control interactions. On the same note, the developed models and techniques of dynamic phasor analysis are inherently well-suited for detailed study of microgrids in the grid-connected and islanded modes. In this work, the steady-state and quasi-static results have been validated by comparing with measured field data. Similarly, the future work may attempt validation of the dynamic

models and results of transient analysis through comparison with corresponding dynamic field measurements.

References

[1] B. P. Chuco, "Electrical software tools overview," Centro de Investigaciones Electricas Electronicas del Peru - CIEEP, Tech. Rep., June 2010.

[2] "High-penetration of photovoltaic generation study - Flagstaff community power," Arizona Public Service Company, Arizona State University, Tech. Rep., Sept. 19 2011.

[3] Y. Tang and R. Ayyanar, "Modeling secondary lines of Sandvig 04 feeder in CYMDIST," Arizona Public Service Company, Arizona State University, Tech. Rep., Nov. 11 2011.

[4] X. Mao and R. Ayyanar, "Average and phasor models of single phase PV generators for analysis and simulation of large power distribution systems," in *Twenty-fourth Annual IEEE Applied Power Electronics Conference and Exposition*, Feb. 2009, pp. 1964 –1970.

[5] T. Demiray, G. Andersson, and L. Busarello, "Evaluation study for the simulation of power system transients using dynamic phasor models," in *IEEE Transmission and Distribution Conference and Exposition*, 2008, pp. 1–6.

[6] G. Wester and R. Middlebrook, "Low-frequency characterization of switched dc-dc converters," *IEEE Transactions on Aerospace and Electronic Systems*, vol. AES-9, no. 3, pp. 376–385, 1973.

[7] V. Vorperian, "Simplified analysis of PWM converters using model of PWM switch. continuous conduction mode," *IEEE Transactions on Aerospace and Electronic Systems*, vol. 26, no. 3, pp. 490–496, 1990.

[8] ——, "Simplified analysis of PWM converters using model of PWM switch. ii. discontinuous conduction mode," *IEEE Transactions on Aerospace and Electronic Systems*, vol. 26, no. 3, pp. 497–505, 1990.

[9] S. Sanders and G. C. Verghese, "Synthesis of averaged circuit models for switched power converters," in *International symposium on Circuits and Systems*, 1990, pp. 679–683.

[10] Y. S. Lee, "A systematic and unified approach to modeling switches in switch-mode power supplies," *IEEE Transactions on Industrial Electronics*, vol. IE-32, no. 4, pp. 445–448, 1985.

[11] R. Tymerski, V. Vorperian, F. Lee, and W. Baumann, "Nonlinear modeling of the PWM switch," *IEEE Transactions on Power Electronics*, vol. 4, no. 2, pp. 225–233, 1989.

[12] R. D. Middlebrook and S. Cuk, "A general unified approach to modelling switching-converter power stages," in *Power Electronics Specialists Conference*, vol. 1, 1976, pp. 18–34.

[13] R. Brockett and J. Wood, "Electrical networks containing controlled switches," *NASA STI/Recon Technical Report*, vol. 75, 1974.

[14] S. Sanders, J. Noworolski, X. Liu, and G. C. Verghese, "Generalized averaging method for power conversion circuits," *IEEE Transactions on Power Electronics*, vol. 6, no. 2, pp. 251–259, 1991.

[15] V. Venkatasubramanian, H. Schattler, and J. Zaborszky, "Fast time-varying phasor

analysis in the balanced three-phase large electric power system," *IEEE Transactions on Automatic Control*, vol. 40, no. 11, pp. 1975 –1982, nov 1995.

[16] A. Stankovic and T. Aydin, "Analysis of asymmetrical faults in power systems using dynamic phasors," in *Power Engineering Society Summer Meeting*, vol. 3, 2000, pp. 1957 – 1963.

[17] A. Coronado-Mendoza, J. L. Bernal-Agustin, and J. A. Dominguez-Navarro, "Photovoltaic boost converter system with dynamic phasors modelling," *Electric Power Systems Research*, vol. 81, no. 9, pp. 1840 – 1848, 2011.

[18] A. Emadi, "Modeling and analysis of multiconverter DC power electronic systems using the generalized state-space averaging method," *IEEE Transactions on Industrial Electronics*, vol. 51, no. 3, pp. 661–668, 2004.

[19] R. Ashino, M. Nagase, and R. Vaillancourt, "Behind and beyond the MATLAB ODE suite," *Computers & Mathematics with Applications*, vol. 40, no. 4, pp. 491–512, 2000.

[20] L. Shampine and M. Reichelt, "The MATLAB ODE suite," *SIAM Journal on Scientific Computing*, vol. 18, no. 1, pp. 1–22, 1997.

[21] J. B. Ward, "Equivalent circuits for power-flow studies," *American Institute of Electrical Engineers, Transactions of the*, vol. 68, no. 1, pp. 373 –382, july 1949.

[22] J. Yang, G. Cheng, and Z. Xu, "Dynamic reduction of large power system in pss/e," in *Transmission and Distribution Conference and Exhibition: Asia and Pacific, 2005 IEEE/PES*, 2005, pp. 1 –4.

[23] H. Oh, "A new network reduction methodology for power system planning studies," *IEEE Transactions on Power Systems*, vol. 25, no. 2, pp. 677 –684, may 2010.

[24] C. Coulston and R. Weissbach, "Routing transmission lines via steiner trees," in *Power Engineering Society General Meeting, 2003, IEEE*, vol. 3, july 2003, p. 4 vol. 2666.

[25] A. Ishchenko, A. Jokic, J. Myrzik, and W. Kling, "Dynamic reduction of distribution networks with dispersed generation," in *International Conference on Future Power Systems*, nov. 2005, p. 7.

[26] T. L. Le, Q. T. Tran, O. Devaux, O. Chilard, and R. Caire, "Reduction and aggregation for critical and emergency operation of distribution network in presence of distributed generators," in *Electricity Distribution - Part 1, 2009. CIRED 2009. 20th International Conference and Exhibition on*, june 2009, pp. 1 –4.

[27] H. Oh, "Aggregation of buses for a network reduction," *Power Systems, IEEE Transactions on*, vol. 27, no. 2, pp. 705 –712, may 2012.

[28] S.-Y. Yun, C.-M. Chu, S.-C. Kwon, and I.-K. Song, "A reduction method of distribution network for smart distribution operation system," in *Integration of Renewables into the Distribution Grid, CIRED 2012 Workshop*, may 2012, pp. 1 –4.

[29] T. H. Cormen, C. E. Leiserson, R. L. Rivest, and C. Stein, *Introduction to algorithms*. MIT press, 2001.

[30] Y. Tang, X. Mao, and R. Ayyanar, "Distribution system modeling using CYMDIST for study of high penetration of distributed solar photovoltaics," in *North American Power*

Symposium (NAPS), 2012, sept. 2012, pp. 1 –6.

[31] J. Nesetril, E. Milkova, and H. Nesetrilova, "Otakar boravka on minimum spanning tree problem translation of both the 1926 papers, comments, history," *Discrete Mathematics*, vol. 233, pp. 3 – 36, 2001. [Online]. Available: http://www.sciencedirect.com/science/article/pii/S0012365X00002247

[32] M. Mares, "The saga of minimum spanning trees," *Computer Science Review*, vol. 2, no. 3, pp. 165 – 221, 2008. [Online]. Available: http://www.sciencedirect.com/science/article/pii/S1574013708000270

Part 2

The Modeling of Distributed Photovoltaic Generation for the Transient Stability Assessment of Power Grids

Authors

Tom Overbye
Rajesh Bhana, Ph.D. Student
University of Illinois at Urbana-Champaign

For information about Part 2, contact:

Thomas J. Overbye
Fox Family Professor of Electrical and Computer Engineering
University of Illinois at Urbana-Champaign
1406 W. Green St
Urbana, IL 61801
Tel: 217-333-4463
Fax: 217-333-1162
Email: Overbye@illinois.edu

Power Systems Engineering Research Center

The Power Systems Engineering Research Center (PSERC) is a multi-university Center conducting research on challenges facing the electric power industry and educating the next generation of power engineers. More information about PSERC can be found at the Center's website: http://www.PSERC.org.

For additional information, contact:

Power Systems Engineering Research Center
Arizona State University
527 Engineering Research Center
Tempe, Arizona 85287-5706
Phone: 480-965-1643
Fax: 480-965-0745

Notice Concerning Copyright Material

Table of Contents

1 Introduction 1
1.1 Background 1
1.2 Motivation 1
1.3 Related works in the area 2
1.4 Contribution and methodology 2
1.5 Report Structure 2
2 Transient Analysis Models 4
2.1 Distributed PV Transient Stability Models 4
2.1.1 Constant current 4
2.1.2 Constant power 4
2.1.3 PVD1 by the WECC REMTF 4
2.1.4 Type IV Wind Turbine 5
2.1.5 Emulation of a conventional generator (curtailing PV) 5
2.2 Load Transient Stability Models 6
2.2.1 Constant Power 6
2.2.2 Constant Impedance 6
2.2.3 ZIP 6
2.2.4 Induction Machine 6
2.2.5 CLOD 7
3 Study Systems 8
3.1 4-bus system 8
3.2 37-bus system 8
3.3 WECC system 9
4 Study Results 10
4.1 Comparison of PV models 10
4.2 Comparison of Load models 13
4.3 Effect of PV penetration 17
4.4 Locational effect of PV penetration 18
5 Conclusions and Future Work 25
References 27

List of Figures

Figure 3.1 The 4-bus system one line diagram 8

Figure 3.2 The 37-bus GSO system one line diagram 9

Figure 4.1 Generator speed for the 4-bus system with 5 MW loss of generation contingency for three different PV model types. 10

Figure 4.2 Generator speed for the 4-bus system with 10 MW loss of generation contingency for three different PV model types. 11

Figure 4.3 Generator speeds for the 37-bus system base case and 50% PV penetration using both constant power and conventional generator emulation models. 12

Figure 4.4 Distributed PV generator output for the 37 bus case where the distributed PV is modeled as 25 conventional generators. 12

Figure 4.5 Generator speed for the 4-bus system with 5 MW loss of generation contingency for four different load model types using a constant power PV model. 14

Figure 4.6 Generator speed for the 4-bus system with 5 MW loss of generation contingency for four different load model types using a WT4 PV model. 14

Figure 4.7 Generator speeds for the 37-bus system base case using both constant power and CLOD load models. 15

Figure 4.8 Generator speeds for the 37-bus system 50% PV (constant power model) case using both constant power and CLOD load models. 16

Figure 4.9 Generator speeds for the 37-bus system 50% PV (generator emulation model) case using both constant power and CLOD load models. 16

Figure 4.10 Generator speed of the 4-bus system for different levels of PV penetration. 17

Figure 4.11 Generator speeds of the 37-bus system for different levels of PV penetration..... 18

Figure 4.12 WECC system base case generator speeds. 19

Figure 4.13 WECC system generator speeds with generator inertia reduced to 50%. 19

Figure 4.14 WECC system generator speeds with generator inertia reduced to 25% in one region. 20

List of Tables

Table 4.1 Simulation result summary for faults and inertia changes in different regions of the WECC system 21

1 Introduction

This report details the modeling of distributed photovoltaic (PV) generation for the transient stability assessment of power grids. A number of distributed PV models and load models are detailed. The models are then applied in both small and large system simulations.

1.1 Background

The decrease in cost and the increase in efforts to combat climate change have resulted in a steady increase in PV installations for the generation of electricity in both interconnected and standalone power systems [1]. A major portion of these PV installations can be categorized as grid-connected distributed PV installations. Installations in this category are often associated with residential or commercial customers and generally have a peak real power capacity ranging from 1 kW to 5 MW [2].

This report focuses on the modeling of the behavior of distributed PV installations for simulation of the transient stability problem, which is the assessment of the short term (several to 30 seconds) angular and voltage stability of the power system following a disturbance [3]. At present, in North America, such distributed resources with an "aggregate capacity of 10 MVA or less at the point of common coupling" must follow the IEEE 1547 Standard [4]. This standard does not align completely with other international standards/guidelines, such as those in Germany [5], which encourage grid support through distributed resources. Thus, it is widely assumed that the IEEE 1547 Standard will be amended in the coming years to allow distributed resources to provide a higher level of grid support. As such, the distributed PV models presented in this report include grid support functionality not currently permitted in North America.

1.2 Motivation

Transient stability studies require models which correctly simulate the response of each of the systems components to changes in system conditions and thus correctly simulates the interaction between system components. As such, the growth of a new generation type necessitates an investigation into suitable transient models to evaluate system stability. Higher complexity models, with more dynamic states, increase the computational complexity of a simulation [6]. As a consequence, a balance between simulation accuracy and computational burden must be found.

Transient stability analysis is used in the planning, design and operation of power systems [3]. Simulation results are used to determine a course of action for the growth of a stable grid and also to inform the system regulators to determine the limits within which the system must operate. One example of regulated limits is the set of frequency response specifications prescribed by the North-American Electric Reliability Corporation in their Standard BAL-003-1 [7]. Such limits are set in an effort to maintain a level of system reliability and to protect system components.

Two relatively recent phenomena in power systems are the progressive decrease in both system inertia and governor response [8]. The reduction of governor response has many contributors, and renewable resources without frequency responsive capabilities can exacerbate the issue [9]. PV generation, together with the majority of wind turbine generators (Types III and IV) naturally provide no inertia to the system. In addition, the recent drop in natural gas prices in North America has led to the displacement of larger high-inertia coal units by smaller low-inertia gas turbines. These phenomena have some impact on the behavior of a power system. In particular, the rotor angle stability is likely to be affected. With the growth of distributed PV, there is a need for the accurate modeling of this resource under a variety of potential control schemes in the transient time frame.

1.3 Related works in the area

With the growth of PV generation, much effort has been made in the modeling of PV cells and PV inverters. Much of this work has been conducted by researchers with a focus power electronics [10] and, as a result, the corresponding simulations have generally been conducted using all 3-phases at the tens-of-microseconds level in order to capture power electronic switching frequencies of up to 100 kHz.

To make transient simulation computationally feasible for large systems, power system planners and operators typically conduct single-phase transient stability analysis with a time-step in the order of half a cycle (8.33 ms for a 60 Hz system) [11]. Other researchers, have worked to develop transient models suitable for large system analysis [12]. The Western Electricity Coordinating Council (WECC) Renewable Energy Modeling Task Force (REMTF) has worked on generic wind farm models along with models for both utility scale and distributed PV [13]. Additionally, some researchers have performed both small and large system studies of power systems with high-penetration PV [14], [15].

1.4 Contribution and methodology

This report describes a number of different distributed PV models that can be used for transient system analysis. The models, implemented in PowerWorld Simulator [16], are used on both small and large test systems with variations in PV penetration, location and control strategies. As multiple models are used, comparisons of the models can be made and insights are gained on both the effect of using different models and the system effects of high-penetration, distributed PV. The SimAuto application programming interface functionality of PowerWorld Simulator allows automated modification and simulation of the system cases and was used extensively.

1.5 Report structure

The remainder of this report is structured as follows. Section 2 begins with the description of the various distributed PV models and explains the communication/control functionality necessary for the models to be realistic. Section 2 also contains the descriptions of the load models that were used in simulation. In Section 3, the systems used in the simulations are described. The results and analysis of the system simulations

and are presented in Section 4. Finally, concluding remarks and avenues for future research are detailed in Section 5.

2 Transient Analysis Models

In this section, the various distributed PV and load models considered for the transient stability studies are described. The differences in both the physical and communication structures needed to implement different control schemes associated with the models are also discussed.

2.1 Distributed PV Transient Stability Models

Grid-connected PV systems generally consist of two major components. The PV modules/panels and the dc-ac inverter. A basic understanding of these components can be found in many textbooks [17]. In transient stability simulation, it is assumed that solar insolation levels will be (on average) constant in the timeframe of interest. Thus, the modeling focuses on the capability and response of the inverter. There are many ways to model the inverter in addition to the control systems employed over single or multiple PV installations, as described below.

2.1.1 Constant current

PV modules can be accurately modeled using the single-diode model which are affected by solar radiation and temperature [18]. The single-diode model consists of a current source in parallel with a diode, with additional series and parallel resistances. It is however, erroneous to approximate a distributed or utility scale PV source as a constant current power source. The power extracted from the module is inverted via power electronics with switching frequencies in the order of 100 kHz. Transient stability simulation is generally in the order of milliseconds, not microseconds. As such, the operation of the PV module is basically decoupled from voltage and frequency changes in the grid thus grid and a constant current source should not be used to model the system output. The constant current distributed PV model presented in Section 4.1 is simply presented as a comparison to other models and is not a recommended model.

2.1.2 Constant power

As described above, the power extracted by PV modules is considered effectively constant for single-phase equivalent, transient stability simulation. Thus, if a PV installation is connected to the grid and remains grid-connected throughout a transient stability contingency or event, the installation can be modeled as a constant power source. That is, the inverter operates in such a fashion that it maintains a constant real (and reactive, if desired) power output regardless of the voltage or frequency of the grid. Note that this model assumes no current saturation/limitation in the ac output of the inverters.

2.1.3 PVD1 by the WECC REMTF

The Distributed PV System Model PVD1 is a model developed by the WECC Renewable Energy Modeling Task-Force (REMTF) [19]. The model, currently in its second generation of development, includes active power control, reactive power control and protective functions.

The active power current for this model is current limited, with a high-frequency droop (governor) response function with deadband and droop gain set points. Similarly the reactive power current is settable with initial reactive power set by initial power flow and a droop for deviation of voltage at a specified bus. The protective functions trip off portions of the distributed PV above and below high and low voltage and frequency set points.

This model has significant functionality and versatility for modeling inverters of today and of the future. Automatic real power governor response and reactive power voltage control are realistic possibilities for PV inverters, albeit with significant signal propagation delays for the voltage control. The difficulty will be in determining the correct set points to emulate the aggregate distributed PV at a distribution bus.

At the time of this report, unfortunately, this model had not yet been implemented in the modeling software used for simulation. As a result, there are no simulation results for this model in this report. These simulations remain a future task for the researchers.

2.1.4 Type IV Wind Turbine

A model presently implemented in commercial simulation software is the Type IV wind generator model. This generic model is also being developed by the WECC REMTF, which includes collaborators from turbine manufacturing companies and commercial transient simulation software vendors. A Type IV wind turbine fully converts the ac output energy of the wind turbine generator to dc and then back to ac to match the grid voltage and frequency. The power electronics are therefore very similar to that of PV generators in that it decouples the initial conversion to electrical through the dc link. The full description of the second generation WECC generic WT4 model is detailed in [20].

If PV inverters are to have common/standard settings and/or advanced communication structures, such as those suggested in various smart grid infrastructure plans [21], the aggregate response of distributed PV at a feeder could mimic that of a WT4 wind generator. As such a WT4 transient stability generator model can be used to model distributed PV.

2.1.5 Emulation of a conventional generator (curtailing PV)

Although there is great incentive to do so, PV modules do not necessarily have to operate at their maximum power yielding point. It is possible for their voltage/current controllers to be set so as to extract a lower than maximum power level or, put another way, curtail their output. As a result, given the speed of their power electronics, PV operation is able to mimic that of a conventional generator. If such operation was to be employed, it is more likely that it would be employed at utility scale installations. However, given very fast smart grid communication, it is feasible that this conventional generator emulation could be performed by aggregate distributed PV. The distributed PV can therefore be modeled as a conventional generator, using established conventional generator models.

The level of PV curtailment relates to the level of real power reserve provided by the PV. Accordingly, when using a conventional generator model to model PV, the post-simulation inertial response of the generator must be verified to ensure that the real power output did not exceed the total available PV power level. In current situations, where renewable energy yield is generally small in comparison to conventional generation, it does not make sense to curtail PV. The lost revenue due to lower energy yield outweighs the revenue received to provide 'spinning reserve'. However, given extremely high PV penetration scenarios and the right ancillary service market structure, it is possible that PV curtailment will be necessary for the safe and reliable operation of the grid.

2.2 Load Transient Stability Models

In the course of exploring the differences between the various PV models, it became apparent to the researchers that the effect of using different load models was quite significant. Other researchers have highlighted the need for better dynamic load modeling [22]. The various load models used for the simulations in this report are described below. Determination of appropriate load model parameters is an area in which much research has been completed, though further research is needed [23].

2.2.1 Constant Power

Stability studies are often conducted with constant power loads. This can prove to yield the wrong results as many loads respond to changes in system voltage and frequency. More and more loads are connected through power electronics, e.g., machine drives. Such loads can be modeled as constant power loads. Other loads should be modeled using a more complex model.

2.2.2 Constant Impedance

Incandescent lighting and electric heating are examples of loads that are accurately modeled by constant impedance models. Once again, this model type is good for some loads but not necessarily accurate when modeling an aggregate load.

2.2.3 ZIP

A zip load model portions the load into three real power and three reactive power components. The three types are constant impedance, constant current and constant power. Accordingly, the model requires six parameters to be set. Power electronics are an example of a load that can contain a constant current portion in addition to constant power and impedance portions.

2.2.4 Induction Machine

Induction machines respond to changes in system frequency and this response is not captured in ZIP models, which are simply a function of voltage magnitude. There are various transient stability induction machine models with different levels of complexity [24]. This additional complexity can add significantly to simulation computation time for large systems with many induction machine models.

2.2.5 CLOD

The CLOD model is a composite aggregate load model that combines the models of a both a large and a small induction motor, discharge lighting, constant power, and branch distribution impedance. Though the parameters of each load type cannot be adjusted, the proportion of each category can be adjusted. As such, a large array of load types can be modeled without too many user-specified parameters.

3 Study Systems

In this section, the study systems and the transient contingencies are described. The systems studied vary from the very small to the very large.

3.1 4-bus system

The one line diagram of a 4-bus system is presented in Figure 3.1. In this system, a distributed PV model is added to the lone load bus and supplies approximately 50% of the total real power load. The main contingency investigated is the loss of a 5 MW generator (approximately 5% of the system generation) at Bus 2. The bus 1 slack generator is modeled with a GENSAL machine model, IEEEX1 exciter model, and a TGOV1 governor model. Each line has a 0.2 p.u. reactance.

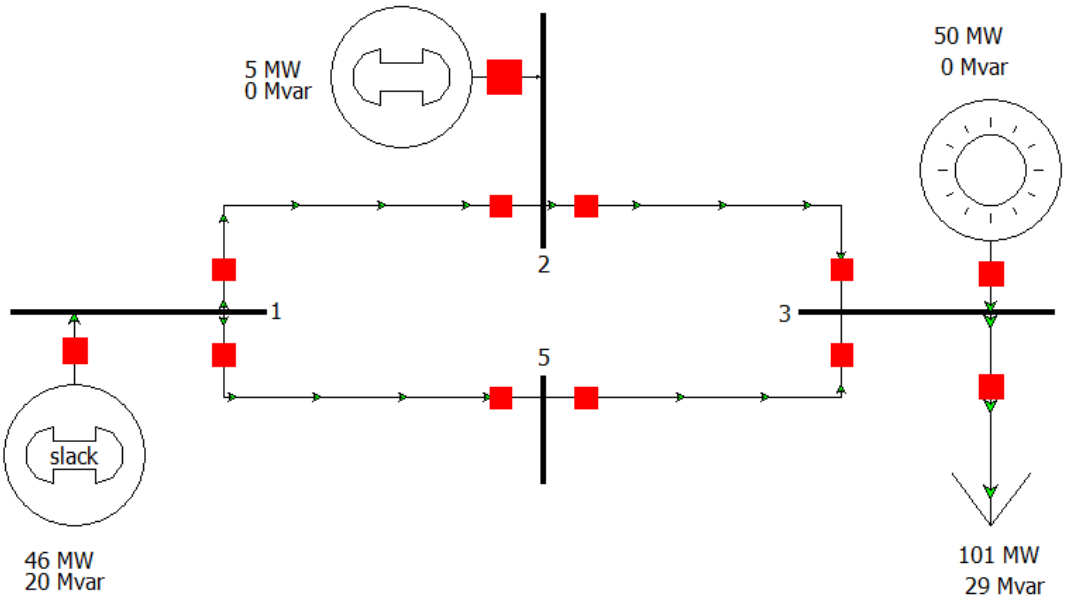

Figure 3.1 The 4-bus system one line diagram

3.2 37-bus system

Figure 3.2 depicts a one line diagram for a 37 bus system. This 9-generator, 25-load system was developed by the authors of [11] and is available online [16]. In the reference case, the 9 conventional generators output a total of 800 MW and the contingency normally investigated is the tripping of the 75 MW generator.

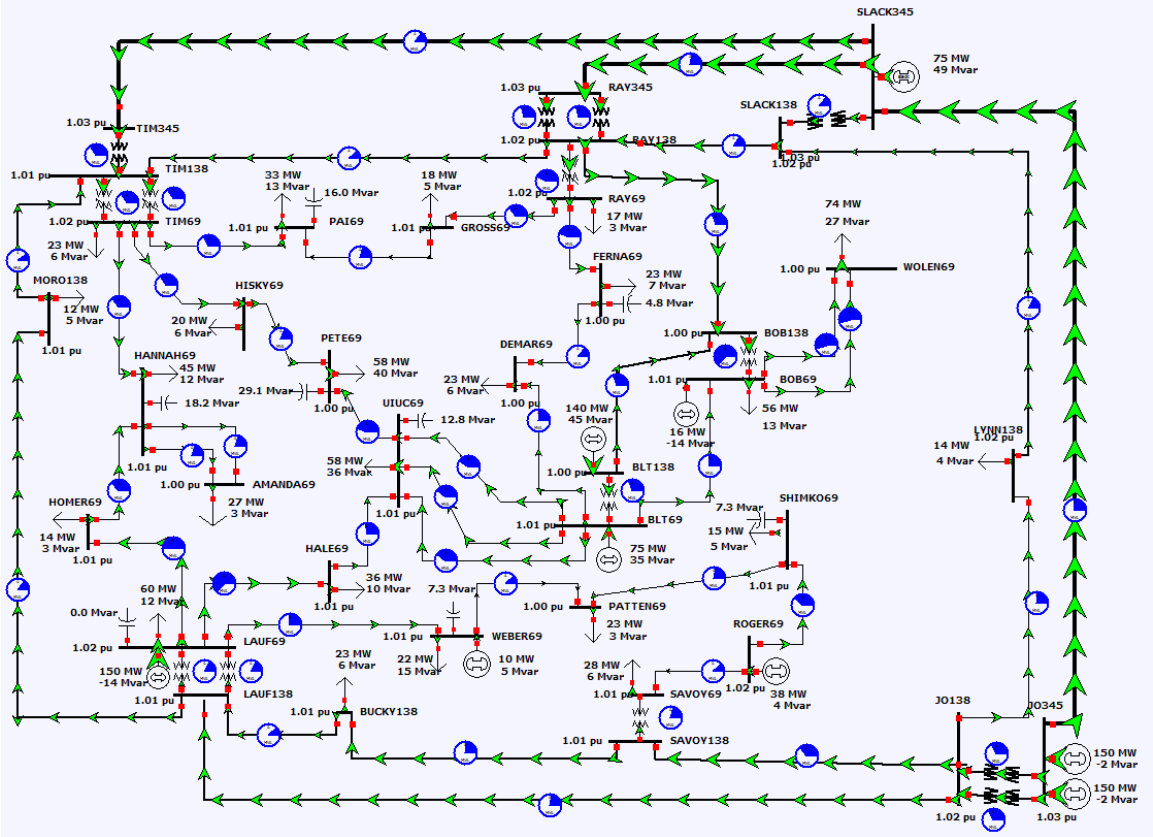

Figure 3.2 The 37-bus GSO system one line diagram

3.3 WECC system

The WECC system model is a 16,000-bus, 3,000-generator, 8,000-load model of the Western Interconnect of North America. A large variety of machine, exciter and governor models are utilized. The main contingency investigated is the simultaneous tripping of two large generators in the same region.

4 Study Results

A number of simulations were run to explore the differences in both the distributed PV models and system configurations. In this section, the simulation results are presented and compared. The time domain simulations focus on the effect of PV on the speed of the generators, with the contingency investigated usually being a loss of generation.

4.1 Comparison of PV models

The different PV models were compared on both the 4-bus and 37-bus systems. The post-contingency 4-bus system has a single post-fault conventional generator. Figure 4.1 depicts the rotor angle response of this generator to a 5% loss of generation for three different wind model types. In these simulations, the same CLOD load model as utilized in Section 4.2 (ahead) is used. The reader should note that the constant current model is not recommended for use as a valid model, as discussed in Section 2.1.1. In this case, the distributed PV generation supplies over 50% of the post-contingency load.

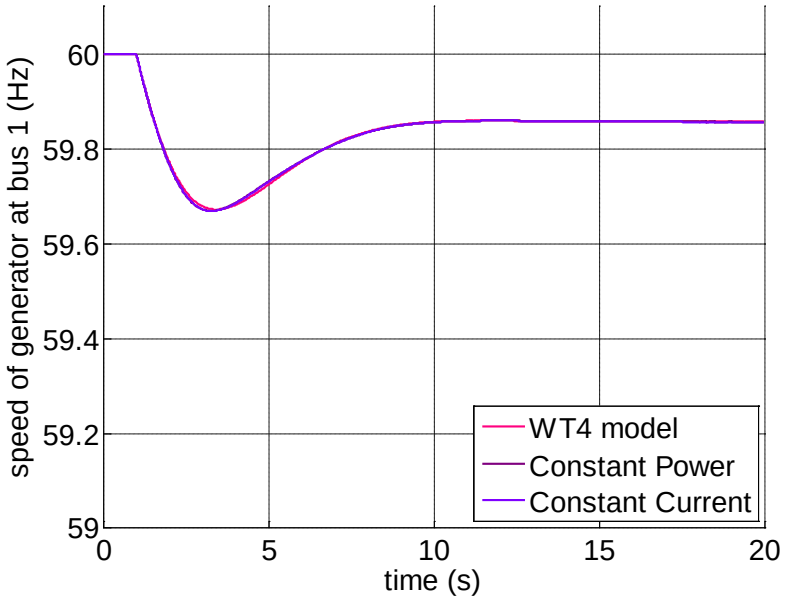

Figure 4.1 Generator speed for the 4-bus system with 5 MW loss of generation contingency for three different PV model types.

All three of the PV models respond in an almost identical fashion. The similarity in the response for the three model types indicates that the more complex components of the more complex WT4 model are only marginally affected by this contingency. The contingency was modified to a 10 MW (approximately 10%) loss of generation. The simulation results are presented in Figure 4.2. Once again, the results for the three model types are close to identical.

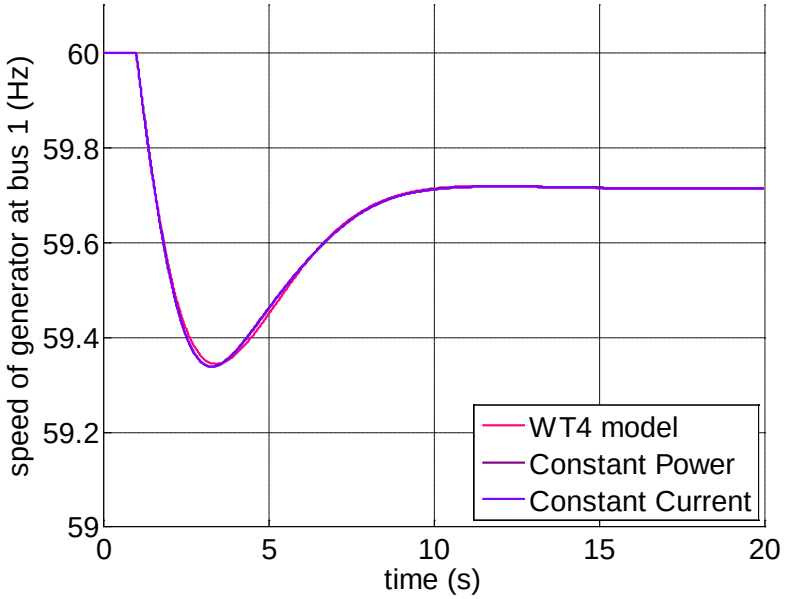

Figure 4.2 Generator speed for the 4-bus system with 10 MW loss of generation contingency for three different PV model types.

Simulation results for the 37-bus system is presented in Figure 4.3. First, a base case simulation was performed with the contingency being the loss of a 75 MW generator (9% of the total system generation). Next, three of the nine generators (the lone generator at bus 44 and both generators at bus 28) were then displaced by distributed PV spread evenly across the 25 load buses. On the modified system, 55% of the load is served by the distributed PV. Two PV models are compared: the constant power model and the conventional generator emulation model. For the conventional generator emulation model, in an effort to 'replace' the displaced generators, the conventional generator emulation model consists of a GENROU machine, HYGOV governor and IEEET1exciter. The total system inertia contribution of the PV generators was made equal to that previously contributed by the displaced generators.

The results clearly show that the generators in this system swing together and are strongly tied. The 55% constant power PV penetration results in a detriment to the performance of the system with respect to frequency response. The maximum deviation from standard frequency is much higher than the base case and the settling frequency is significantly lower. Further investigation into the effects of PV penetration is presented in Section 0.

The case with distributed PV emulating conventional generation shows a response similar to that of the base case. However, in order to achieve this response the total PV available must be greater than 55%.

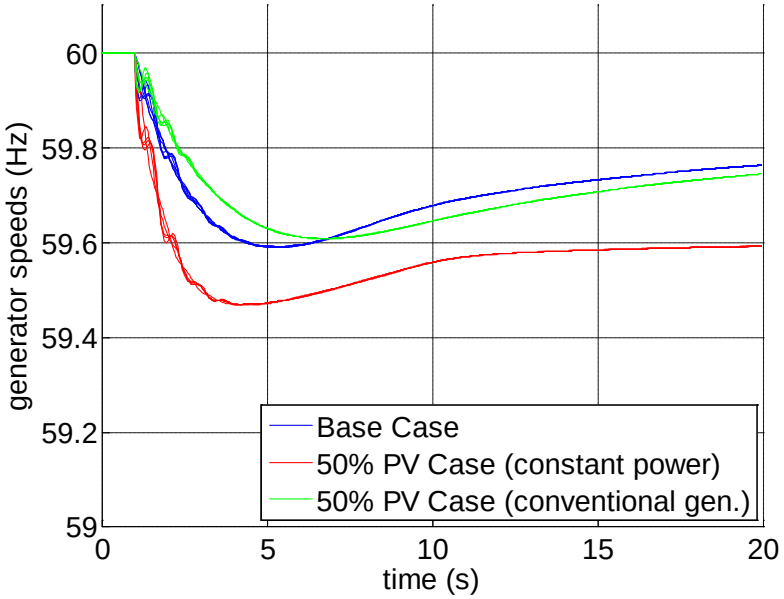

Figure 4.3 Generator speeds for the 37-bus system base case and 50% PV penetration using both constant power and conventional generator emulation models.

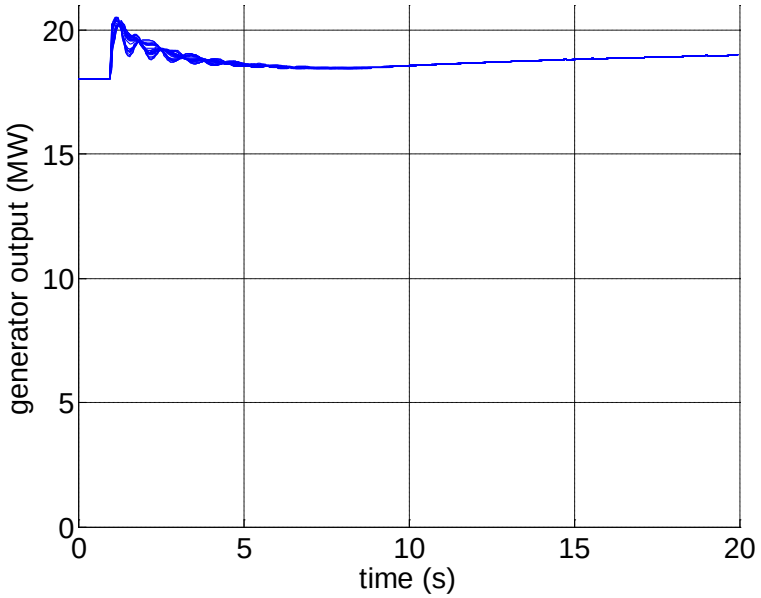

Figure 4.4 Distributed PV generator output for the 37 bus case where the distributed PV is modeled as 25 conventional generators.

The real power output for the 25 distributed PV generators emulating conventional generators is presented in Figure 4.4 with each PV generator initially provided 18 MW (the same as in the constant power model case). However, during the event, the power

output of the distributed generation increases to as much as 20.53 MW for a generator. For this to be possible, the PV must have been operating with a curtailment of approximately 13 percent. The economic driver for curtailment could be associated with excess PV availability and/or the need to keep conventional generators on at the minimum output levels. To achieve this, an ancillary service market could be in place whereby offering the aggregated distributed PV as instantaneous spinning reserve could reap higher benefits to that of supplying energy in certain situations. Unfortunately, using the conventional generator models does not allow the investigation of the effect of the PV generation saturating. New models with available power saturation are needed for those simulations.

In summary, with regard to rotor angle stability, the basic constant power model and the more complex WT4 equivalent model have shown to provide almost identical results. If distributed PV is to be curtailed and used as ‘spinning reserve’, the transient model used would need to capture this performance.

4.2 Comparison of Load models

Load models were also compared on both the 4-bus and 37-bus systems. The load models compared were constant power, constant impedance, a ZIP (33% Z, 33% I, 33% P) model and the CLOD model with default parameters (25% large motor, 25% small motor, 20% discharge lighting and the remainder at constant power).

The four models were used in the simulation of the 4-bus system contingency of a 5MW loss in generation. Both the constant power and WT4 PV models were used and the results are presented in Figure 4.5 and Figure 4.6, respectively. In both cases, using the constant power, constant impedance, and the ZIP models results in almost identical generator speed response. The use of the CLOD model, however, results in a response with a lower maximum frequency deviation. It is clear that the frequency dependent load model gives a significantly different response.

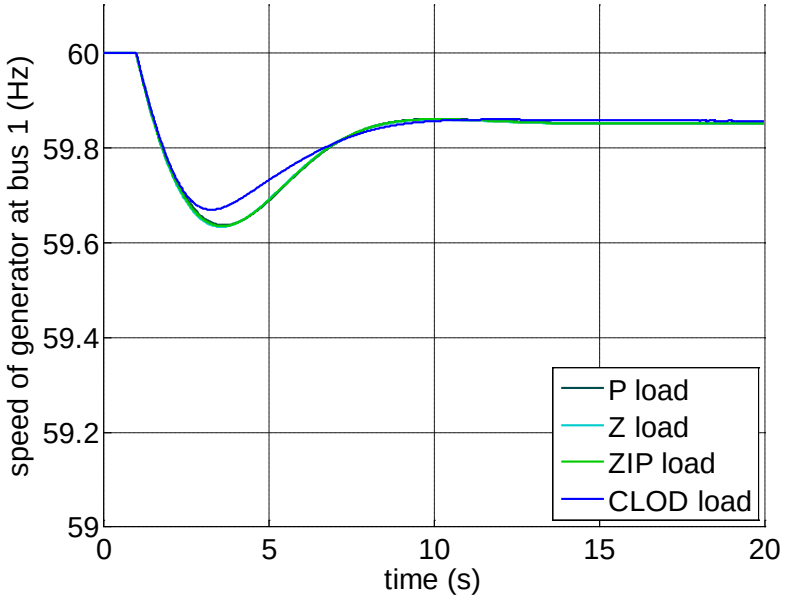

Figure 4.5 Generator speed for the 4-bus system with 5 MW loss of generation contingency for four different load model types using a constant power PV model.

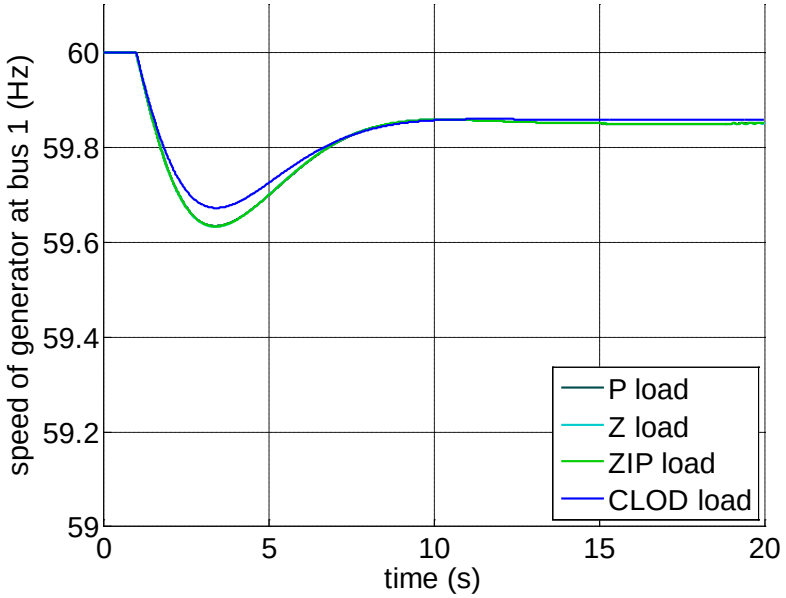

Figure 4.6 Generator speed for the 4-bus system with 5 MW loss of generation contingency for four different load model types using a WT4 PV model.

The constant power and CLOD models were also tested on the 37-bus system. The results for the same three cases as presented in Figure 4.3 comparing the two different load models are presented in Figure 4.7, Figure 4.8, and Figure 4.9. In these three cases, it is

clear that the different model results in significantly different responses. However, it should be noticed that contrary to the high-PV penetration cases presented in Figure 4.5, Figure 4.6, Figure 4.8, and Figure 4.9 the no-PV base case presented in Figure 4.7 shows a larger deviation with the CLOD model than that of the constant power load. As a result, we can conclude that the assumption that the system will have superior performance when using the more detailed CLOD model is false and thus, the importance of more accurate load models is highlighted: one cannot say the frequency performance with the CLOD load model is always superior to that of the constant power load model.

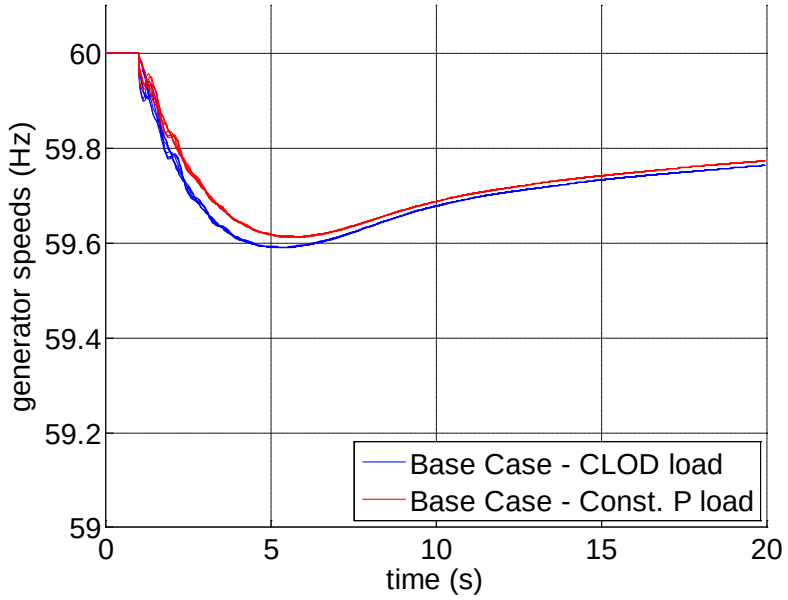

Figure 4.7 Generator speeds for the 37-bus system base case using both constant power and CLOD load models.

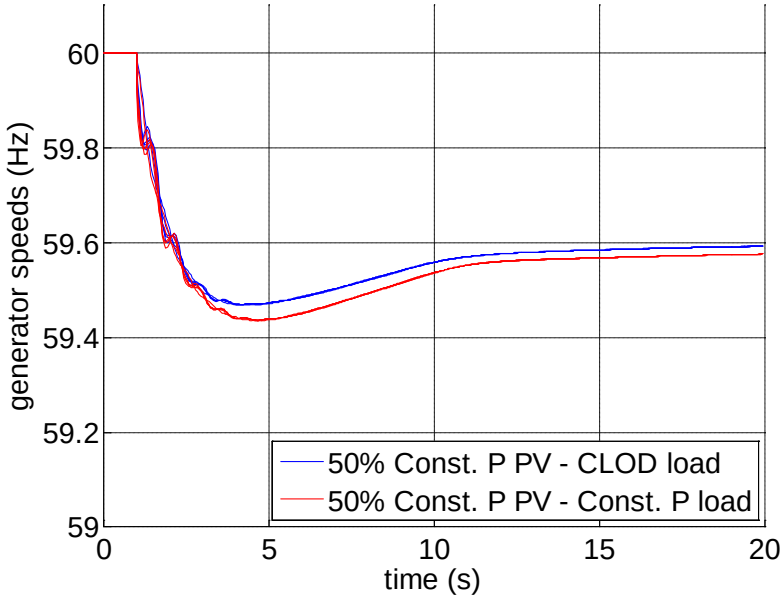

Figure 4.8 Generator speeds for the 37-bus system 50% PV (constant power model) case using both constant power and CLOD load models.

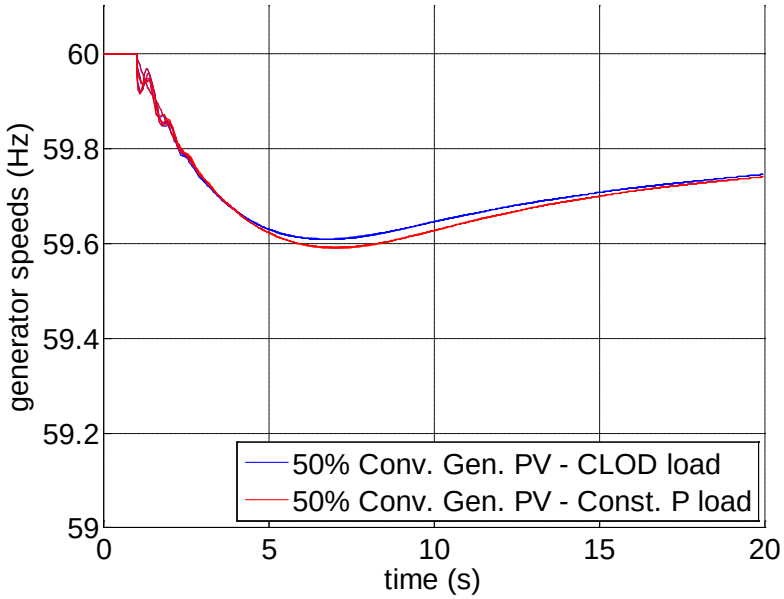

Figure 4.9 Generator speeds for the 37-bus system 50% PV (generator emulation model) case using both constant power and CLOD load models.

In summary, with regard to rotor angle stability, the difference between the basic (constant power, constant impedance and ZIP) models and the more complex (CLOD) frequency dependent models is fairly significant. Far more significant than that of using a more complex distributed PV model. As such, if compromises are to be made to reduce

the complexity of simulation. More complex load models may take precedence over more complicated distributed PV models.

4.3 Effect of PV penetration

Inspection of Figure 4.3 clearly reveals that increased PV penetration results in the inferior inertial response of a system to loss of generation (assuming the PV resources have not been curtailed). This is an obvious result given that PV generation is inherently without inertia, as discussed in Section 1.2. An investigation of the decrease in inertia was conducted on the 4-bus system. Using a constant power PV model and the CLOD load model, the PV penetration was increased from 0% to approximately 90 percent. At the same time, the inertia of the conventional generator was decreased linearly from 10 p.u. to 1 p.u. in order to simulate the drop in the inertial response across a larger system. The results from this analysis are presented in Figure 4.10, with a green trace corresponding to 50% PV penetration. The results show the obvious degradation in inertial response due to increased PV. Somewhat surprisingly, the results also show a faster recovery for the high PV scenario.

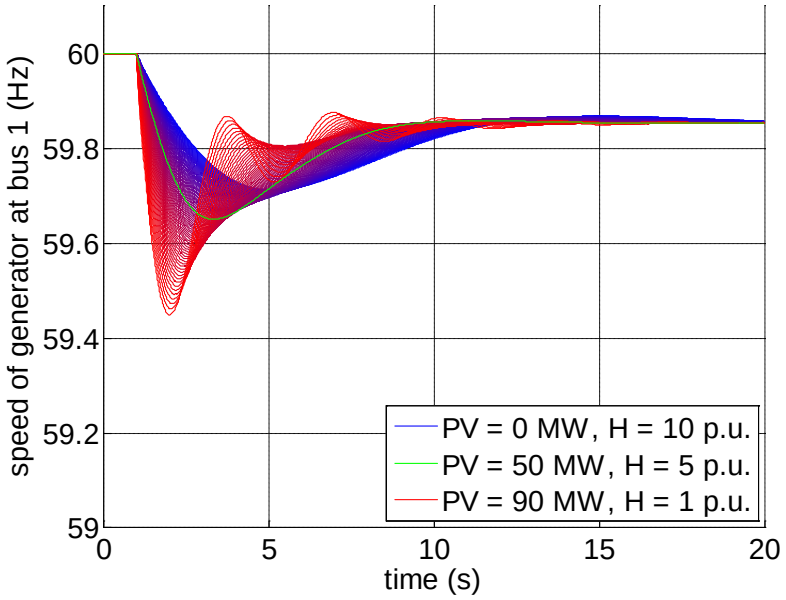

Figure 4.10 Generator speed of the 4-bus system for different levels of PV penetration.

The 37-bus case was also simulated to investigate the effect of PV penetration. However, in this case, no changes were made to the inertial constants. Generators, by decreasing size, were gradually displaced by the distributed PV, which were modeled by constant power sources. The results, presented in Figure 4.11, do not show the faster recovery for the high PV scenario.

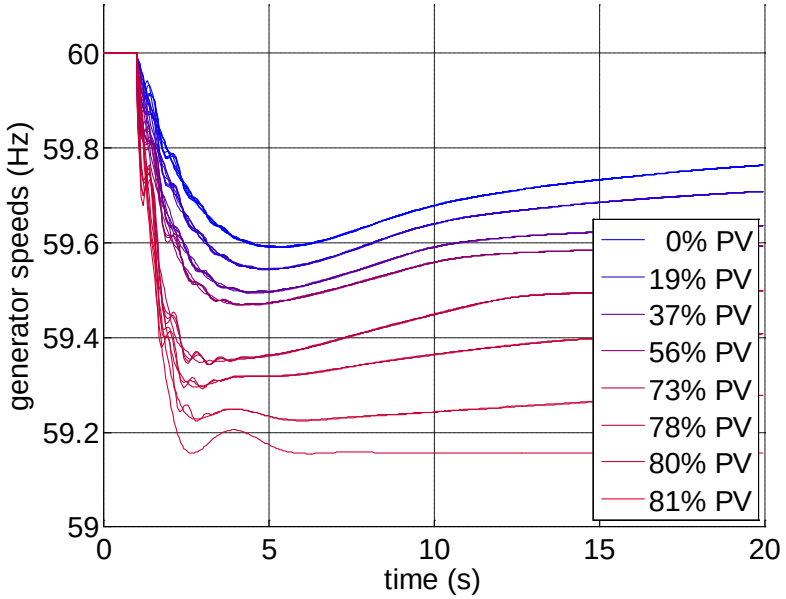

Figure 4.11 Generator speeds of the 37-bus system for different levels of PV penetration.

In summary, with regard to rotor angle stability, the performance of a system generally degrades with an increase in PV penetration. That being said, PV generation is immune to rotor angle instability and thus the argument to allow operation with larger deviation from nominal frequency remains valid in high PV scenarios.

4.4 Locational effect of PV penetration

The 37-bus case results show that the system and, more specifically, the generators are strongly connected and swing together in a single area. Larger systems with multiple areas should also be considered when investigating PV penetration. The WECC system is an example of a very large system with many areas and some weak ties. In addition, some regions of the WECC system have considerably greater potential when it comes to PV energy yield, e.g., Nevada. Other studies have shown the effect of increased wind penetration on large systems [25]. As Type III and IV wind turbines have no inertia, their effect on rotor angle stability is expected to be similar to that of PV.

Simulations were performed on the WECC system using a large two generator trip contingency. The load model used was predominantly one with a 20% induction machine portion. The base case simulation result is presented in Figure 4.12. In Figure 4.13, the results for the system are presented for the case with the generator inertial constants for all the generators reduced to 50% of their original values. The maximum frequency deviation increases for many of the generators, however the magnitude of post fault oscillations are similar and, in the case of some generators, reduced.

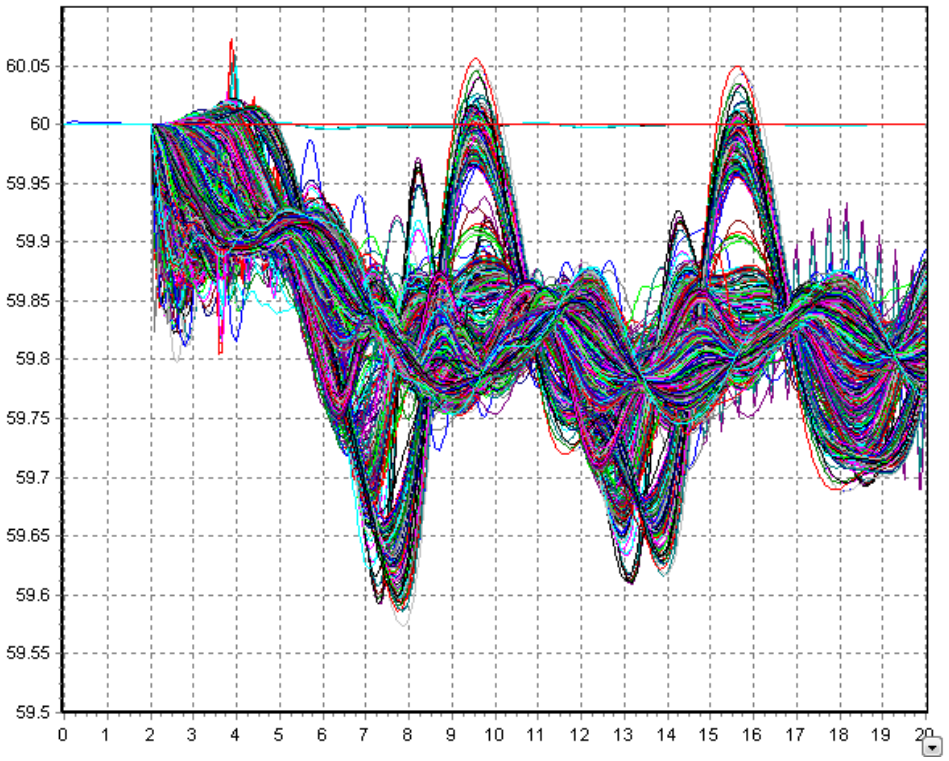

Figure 4.12 WECC system base case generator speeds for a fault in region 1.

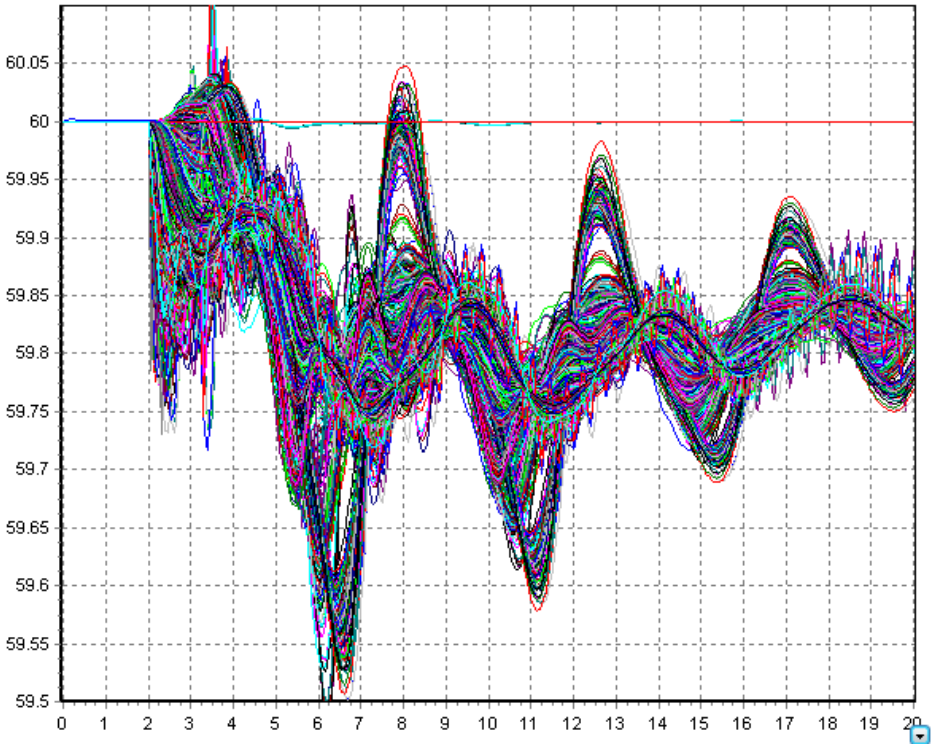

Figure 4.13 WECC system generator speeds for the fault in region 1 with generator inertia reduced to 50% across the entire system.

Another case was created to investigate the effect of decreased inertia in one region. The generator inertia values in a region previously accounting for 23% of the total system inertia, were reduced to 25% of their initial values. As a result the total system inertia dropped to 83%. The results of the simulation of this case are presented in Figure 4.14. These results show instabilities in a number of generators. The results also show a significantly inferior inertial response to that of the 50% inertia case presented in Figure 4.13.

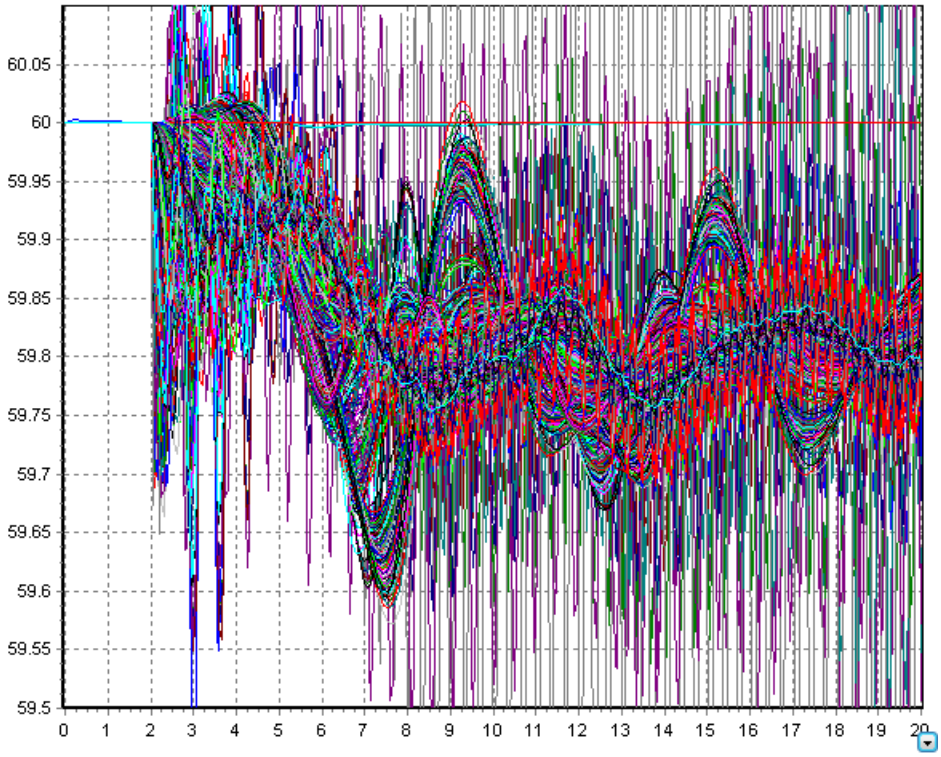

Figure 4.14 WECC system generator speeds for the fault in region 1 with generator inertia reduced to 25% in region 1.

The results in Figure 4.14 highlight the fact that unstable operating scenarios can arise when PV generation displaces conventional generation in one region. The generators across two weakly connected areas can swing against one another and if one area does not have sufficient inertia, rotor angle stability may occur. In addition, if an area of a system has a high level of PV, the flow of power in the system can be dramatically different, depending on the time of day, level of insolation or pattern of load. Such differences may result in a system moving from a secure state to a vulnerable state.

Further studies were performed to investigate the effects of faults in 3 different regions. In each case, the contingency analyzed was the simultaneous tripping of two of the largest generators in the region. For each of the three faults, simulations were performed at the base case, for changes in inertia across the entire system, and then for changes in inertia in each of the three regions. A summary of the simulation results is presented in Table 4.1.

Table 4.1 Simulation result summary for faults and inertia changes in different regions of the WECC system.

Modified region	Modified inertia	System inertia	Fault region/size		
			1 2820 MW	2 1424 MW	3 2150 MW
-	-	100%	S	S	S
Entire system	75%	75%	S	S	S
	50%	51%	S	S(M)	S
	25%	26%	U	U	U
1	75%	94%	S	S	S
	50%	89%	S	S	S
	25%	83%	U	U	U
2	75%	93%	S(M)	S	S
	50%	87%	U	S(M)	S
	25%	80%	U	U	U
3	75%	93%	S	S	S
	50%	87%	S	S	S
	25%	80%	U	U	U

S = stable, U = unstable, (M) = marginal

The results indicate that a drop in inertia to 25% of base case levels in any region results in an unstable response to a major fault. For an instability to occur, it does not necessarily take the largest fault. The loss of generation simulated for the region 2 fault is approximately half of that simulated for region 1. Despite that, the region 2 fault with a decrease to 50% of the inertia in region 2, results in a marginally stable result and the further drop to 25% of the base case level results in complete instability, as presented in Figure 4.15 and Figure 4.16, respectively.

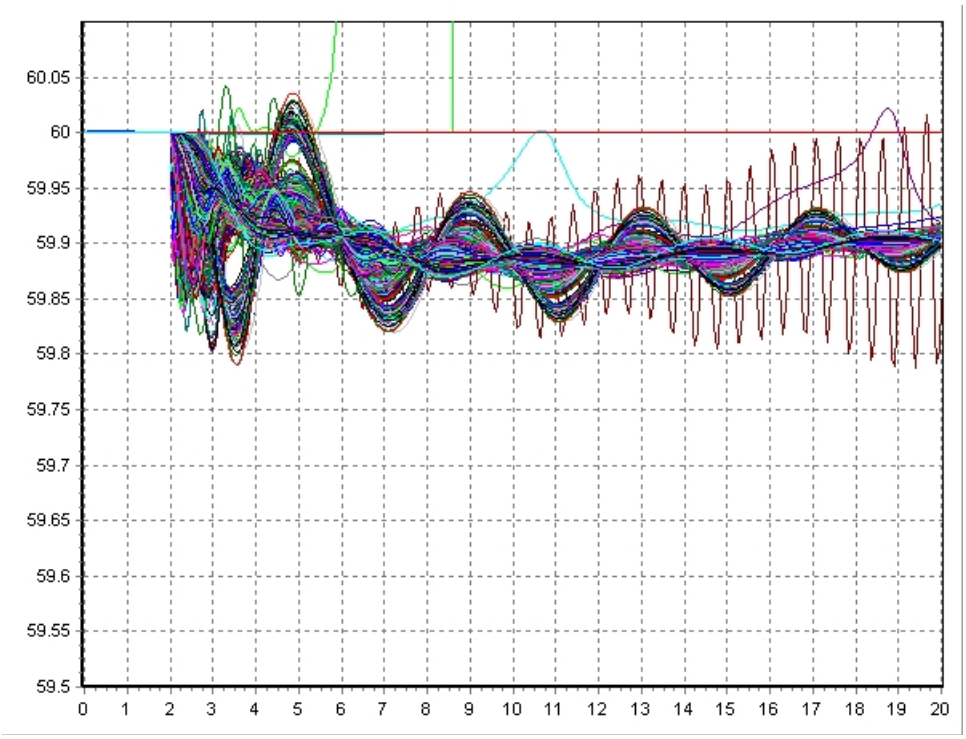

Figure 4.15 WECC system generator speeds for the fault in region 2 with generator inertia reduced to 50% in region 2.

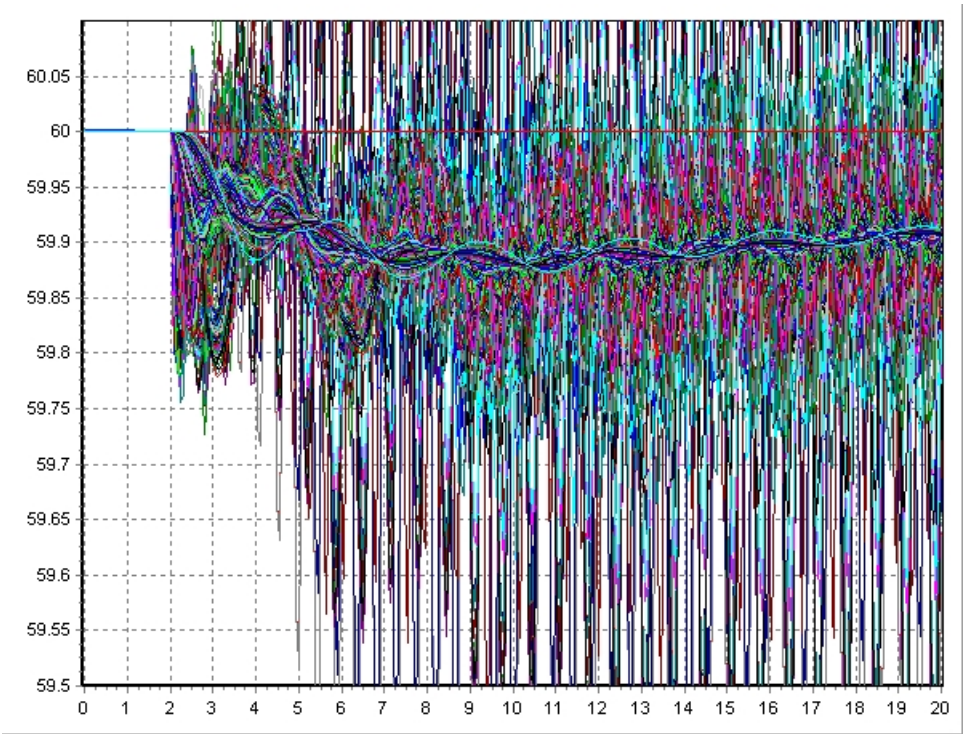

Figure 4.16 WECC system generator speeds for the fault in region 2 with generator inertia reduced to 25% in region 2.

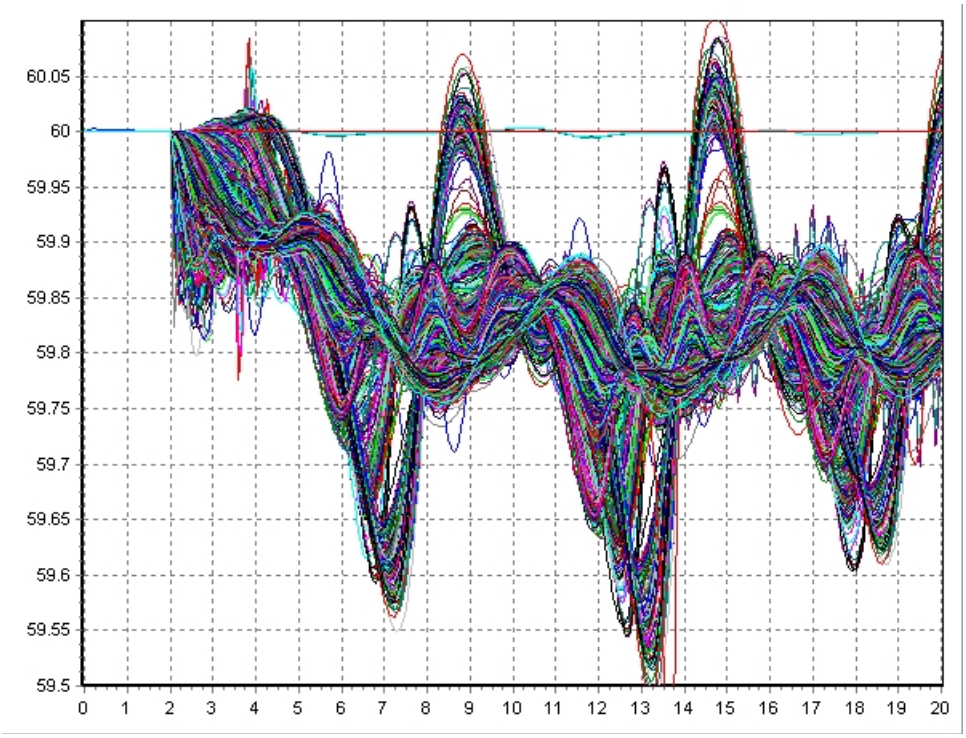

Figure 4.17 WECC system generator speeds for the fault in region 1 with generator inertia reduced to 75% in region 2.

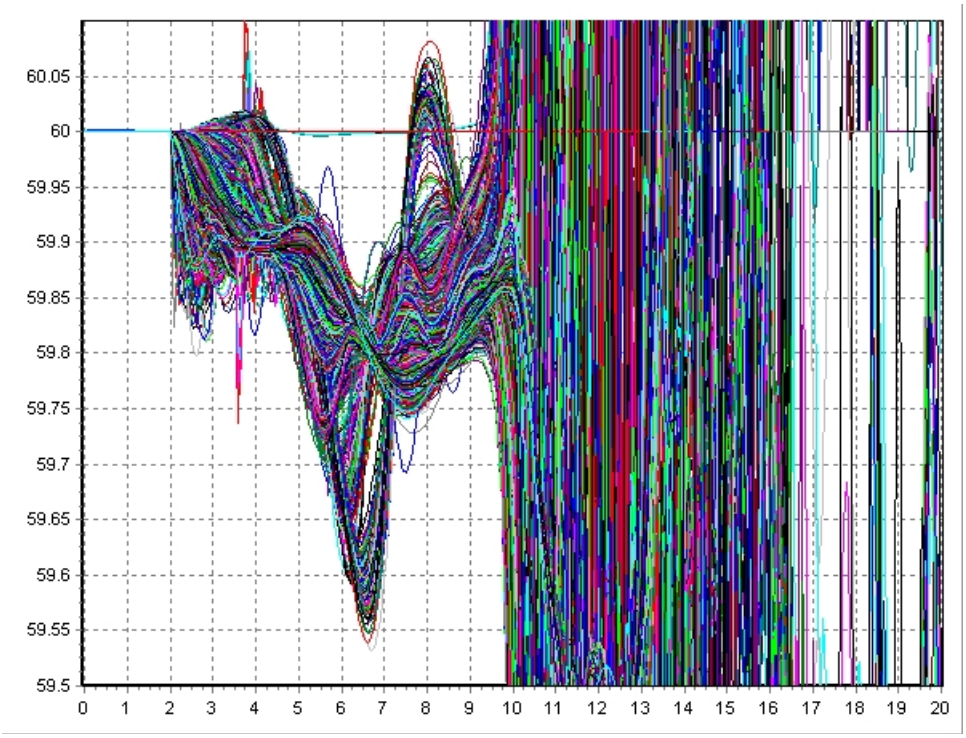

Figure 4.18 WECC system generator speeds for the fault in region 1 with generator inertia reduced to 75% in region 2.

The results also indicate that the location of the fault relative to the region of inertia change does not necessarily increase or decrease the chances of instability. For example, the fault in region 1 results in a stable results when the region 2 inertia is dropped to 75% but an instability results when dropped further to 50%, as presented in Figure 4.17 and Figure 4.18, respectively. This is an interesting result as the region 1 fault, with 50% inertia in region one itself does not result in an instability, as presented in Figure 4.19. Of all the simulations performed, the region 1 fault, with 50% inertia in region 2 is the simulation with the highest total system inertia (87%) that results in an unstable response.

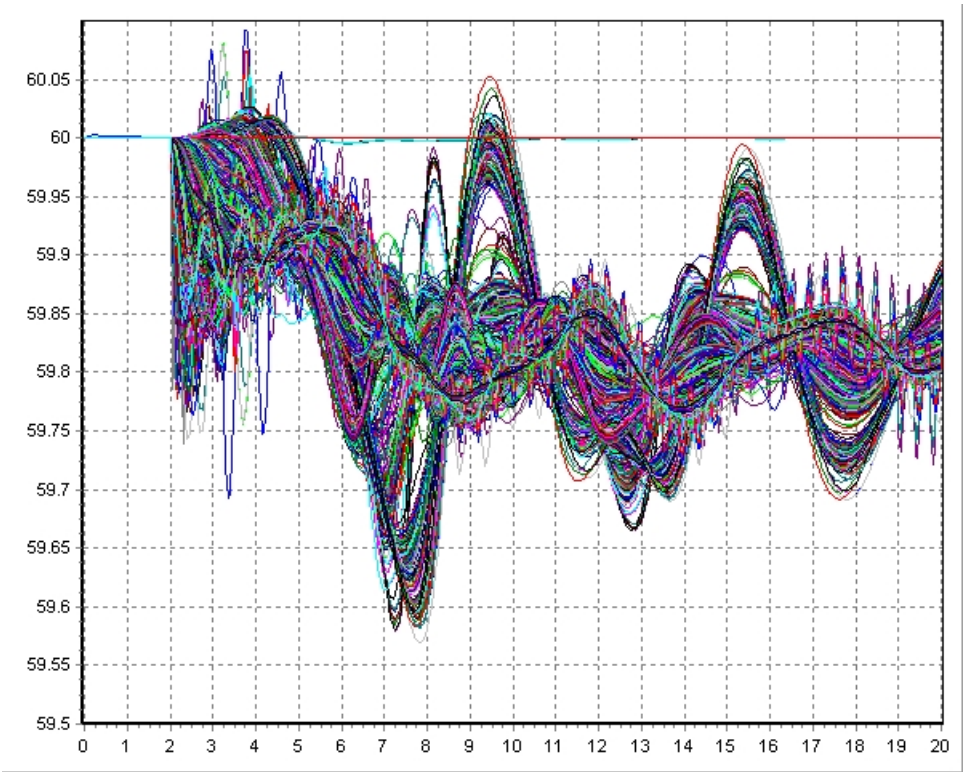

Figure 4.19 WECC system generator speeds for the fault in region 1 with generator inertia reduced to 50% in region 1.

In summary, with regard to rotor angle stability, it is not only important to consider the total system inertia. The location of the inertia in multi-area systems is also of great importance. Distributed PV will likely grow in regions where the resource is most available and or the subsidies/policies make it economic. When it does grow in these regions, it will be important to assess the changes in system response and, when necessary, adjust control accordingly.

5 Conclusions and Future Work

This report focuses on the modeling of distributed PV generation for transient stability analysis with a focus on the effects of distributed PV on conventional generator speeds. The results presented in Section 4 discuss not only the models used, but also the effect of PV penetration.

The PV models investigated respond in different ways to changes in system voltage in frequency and this is almost completely defined by the control strategy used by the PV installations. As a result, some models give almost identical results when used in simulation. More complex models should be employed when considering the use of PV as 'spinning reserve'. The fast response of the generators to frequency is of great interest. Future research will involve the investigation of the effects of the abrupt, non-linear current limiting of inverters when PV is used as 'spinning reserve'. Possible models include the PVD1 or a modified conventional generator model. Of great assistance would be real world data from installations over a large footprint to validate these models.

Different load models were also presented in this report. The simulation results suggest that more complex load models can significantly change simulation results, more so than complex PV models. Accordingly, there is an argument for including the distributed PV model within a complex load model. If this was done, however, simulation would need to consider the variability of distributed PV and run simulations with different levels of available distributed PV generation.

The analysis of increasing PV penetration shows the effect of the loss of inertia and reserve capability. Though it should be reiterated that PV generation is immune to rotor angle instability and thus the argument to allow system operation with larger deviation from nominal frequency remains valid for systems with low levels of conventional generation.

Simulation shows that the location of the PV generation can also play a major part in multi-area systems with weak inter-area ties, suggesting a possible need for a locational inertia requirement. Further to this, given the variability between peak and off-peak (zero) PV output, investigation into the use of adaptive power system stabilizing methods will be conducted. Such methods are generally not employed at present, but the changes in power flow brought about by variable renewable generation may eventually warrant its widespread use.

The large system (WECC) analysis in this report was conducted by adjusting generator inertia levels. An extension of this analysis will be to perform a unit-commitment and optimal power flow analysis to displace conventional generators with distributed PV, while maintaining a feasible power flow. This would allow the use of the various distributed PV models in simulation. The results of that analysis could be used to validate the results presented in this report.

The models and techniques presented in this report allow system planners to determine the effect of distributed PV on their systems. It is unlikely that power systems will make dramatic switches to different resources resulting in an abrupt loss of system security. Instead, power systems tend to grow in size and change incrementally. Planning decisions are made based on predictions of load growth and generation resource mix, amongst other considerations. Having the right tools will allow planners to make educated decisions on investment and topology as well as on changes to system control strategies.

References

[1] Solar Energy Industries Association. (2013, June) Solar Energy Facts: Q1 2013. [Online]. http://www.seia.org/sites/default/files/Q1%202013%20SMI%20Fact%20Sheetv3.pdf

[2] National Renewable Energy Laboratory. The Open PV Project. [Online]. https://openpv.nrel.gov/

[3] P. Kundur, *Power System Stability and Control*. New York: McGraw-Hill, 1993.

[4] IEEE Standards Coordinating Committee , "1547-2003 - IEEE Standard for Interconnecting Distributed Resources With Electric Power Systems," New York City, 2003.

[5] BDEW, "Guideline for generating plants' connection to and parallel operation with the medium-voltage network," Berlin, 2008.

[6] P.W. Sauer and M.A. Pai, *Power System Dynamics and Stability*. New Jersey: Prentice-Hall, 1998.

[7] NERC, "Reliability Standards for the Bulk Electric Systems of North America," Atlanta, 2013.

[8] J.W. Ingleson and E. Allen, "Tracking the Eastern Interconnection Frequency Governing Characteristic," in *IEEE Power and Energy Society General Meeting*, Minneapolis, MN, 2010.

[9] E. Ela and C. Clark. (2013, May) Second Workshop on Active Power Control From Wind Power - Welcome. [Online]. http://www.nrel.gov/electricity/transmission/pdfs/wind_workshop2_01ela.pdf

[10] P.P. Dash and M. Kazerani, "Dynamic Modeling and Performance Analysis of a Grid-Connected Current-Source Inverter-Based Photovoltaic System," *IEEE Transactions on Sustainable Energy*, vol. 2, no. 4, pp. 443-450, 2011.

[11] J.D. Glover et al., *Power System Analysis and Design, 5th Ed.*: Global Engineering, 2012.

[12] Y.T. Tan et al., "A Model of PV Generation Suitable for Stability Analysis," *IEEE Transactions on Energy Conversion*, vol. 19, no. 4, pp. 748-755, 2004.

[13] A. Ellis. (2013, June) Western Electricity Coordinating Council Renewable Energy Modeling Task Force Wind/PV Modeling Update. [Online]. http://www.wecc.biz/committees/StandingCommittees/PCC/TSS/MVWG/20130618/Lists/Presentations/1/Ellis%20-%20REMTF%20Report%20-%20June2013%20-

%20share.pdf

[14] B. Tamimi et al., "System Stability Impact of Large-Scale and Distributed Solar Photovoltaic Generation: The Case of Ontario, Canada," *IEEE Transactions on Sustainable Energy*, vol. 4, no. 3, pp. 680-688, 2013.

[15] S. Eftekharnejad et al., "Impact of Increased Penetration of Photovoltic Generation on Power Systems," *IEEE Transactions on Power Systems*, vol. 28, no. 2, pp. 893-901, May 2013.

[16] PowerWorld Corporation. (2013, July) Simulator Overview. [Online]. http://www.powerworld.com/products/simulator/overview

[17] G.M. Masters, "Renewable and Efficient Electric Power Systems," in *Renewable and Efficient Electric Power Systems*. Hoboken, NJ: John WIley & Sons, 2004, pp. 385-595.

[18] M. Villalva et al., "Comprehensive approach to modeling and simulatoin of photovoltaic arrays," *IEEE Transactions on Power Systems*, vol. 24, no. 5, pp. 1198-1208, May 2009.

[19] WECC Renewable Energy Modeling Task Force, "Generic," Western Electricity Coordinating Council, Salt Lake City, UT, 2012.

[20] P. Pourbeik, "Proposed Changes to the WECC WT4 Generic Model for Type 4 Wind Turbine Generators," Electric Power Research Institute, Knoxville, TN, 2013.

[21] A.P.S. Meliopoulos et al., "Smart Grid Technologies for Autonomous Operation and Control," *IEEE Transactions on Smart Grid*, vol. 2, no. 1, pp. 1-10, March 2011.

[22] A. Ellis et al., "Dynamic Load Models: Where are we?," in *IEEE PES Transmission and Distribution Conference and Exhibition*, Dallas, TX, 2006, pp. 1320-1324.

[23] S. Guo and T.J. Overbye, "Parameter Estimation of a Complex Load Model Using Phasor Measurements," in *Power and Energy Conference at Illinois*, Champaign, IL, 2012, pp. 1-6.

[24] Siemens Energy, Inc., "PSS E 33.0 Program Application Guide Volume 2," Siemens Power Technologies International, Schenectady, NY, 2011.

[25] Lawrence Berkeley National Laboratory, "Dynamic Simulation Studies of the Frequency Response of the Three U.S. Interconnections with Increased Wind Generation," LBNL, Berkeley, CA, 2010.